UNIVERSITY OF MINNESOTA
ST. ANTHONY FALLS LABORATORY
Engineering, Environmental and Geophysical Fluid Dynamics

Project Report No. 448

Inflow Dynamics And Potential Water Quality Improvement in Lake McCarrons

by

Deborah E. West-Mack and Heinz G. Stefan

Prepared for

METROPOLITAN COUNCIL ENVIRONMENTAL SERVICES (MCES)
St. Paul, Minnesota

September 2000
Minneapolis, Minnesota

Prepared for: MCES
Last Revised: 9/15/2000
Disk Locators: PR448cov.doc; PR448 McCarrons.doc;
(Zip Disk #9/Stefan Reports\West

ABSTRACT

This report describes the results of a study on (a) mediation of inflow water temperatures in the wetland of Lake McCarrons, (b) summer stratification dynamics of Lake McCarrons, (c) changes in intrusion depths of inflows to Lake McCarrons caused by the wetland. Water temperature mediation by the wetland was assessed by application of theoretical/model results and by analysis of field temperature data collected in 1999. It was found that the mediation is very strong and produces up to 5°C (mean monthly) warming. To determine summer temperature stratification dynamics, two thermister chains were placed in the lake. They recorded 10-minute average temperatures for seven months at up to 12 depths. The stratification characteristics, including a 2 to 3 m surface mixed layer in midsummer, have been well documented. Plunging of the inflow was verified in a field study. Intrusion depths are reduced by 1 to 2 m due to the warming of the inflow from the watershed in the wetland.

This report also outlines several phosphorus and lake surface mixed layer management techniques to reduce primary productivity of phytoplankton in Lake McCarrons, and how these alternative methods can be tested by numerical model simulation. The actual simulation results and recommendations are presented in another report.

ACKNOWLEDGEMENT

The study described in this report was conducted with financial support from the Metropolitan Council Environmental Services, St. Paul, Minnesota. The water temperature data acquisition systems were designed and built under the guidance of Chris Ellis of St. Anthony Falls Laboratory. The systems were operated by Karen Jensen of MCES. Historical data were provided by Gary Oberts and Karen Jensen of MCES. Technical assistance in the preparation of this report was given by Omid Mohseni and Travis Bogan. The report was formatted and edited by Pat Swanson.

TABLE OF CONTENTS

LIST OF FIGURES

I. BACKGROUND

Lake McCarrons in Roseville, Minnesota, displays signs of anthropogenic eutrophication. To increase its summer transparency, different approaches/actions have been considered. A wetland system designed to remove phosphorus from the watershed surface runoff into the lake was installed and went into operation in 1985. Its performance has been described in reports by Oberts and Osgood (1988) and the Metropolitan Council Environmental Services (MCES, 1997). Other reduction techniques for primary productivity can be considered. There is also some question about the effect that the wetland system has had on inflow water temperatures. By exposing the tributary water to the atmosphere, a wetland may cause a warming of the tributary water, which is then more likely to enter the surface mixed-layer of a stratified lake in summer. In the surface mixed layer, light can be plentiful, and the phosphorus in the inflow may stimulate increased algae growth.

The Executive Summary of the MCES (1997) report ends with this statement:

> "Because of the amount of polluting material discharged into the lake over the past decades, lake improvement will be difficult and expensive. The MWTS has been helpful over the past 12 years in reducing net inputs to the lake, but this study has shown that the system is decreasing the effectiveness and may be directing inflow to a limited volume of the lake above the thermocline. Possible approaches to lake improvement include chemical treatment of the lake and/or inflows; rerouting inflow below the thermocline; whole or partial lake mixing; and attention to the management changes noted above for the MWTS to improve performance."

In this report we shall address some of these issues.

II. PURPOSE/OBJECTIVE

The objective of this study is twofold. The first is to better understand and explain the wetland effect on the inflow intrusion dynamics of Lake McCarrons. The second is to explore alternative methods to increase the lake's summer transparency.

To meet the first objective, historical water temperature profiles have to be assembled, new data have to be collected, and both have to be interpreted in terms of inflow to a temperature stratified lake environment. Of particular concern are the effects of the constructed wetland on inflow intrusion dynamics to the lake. To what depth does the inflow from the wetland intrude into the lake? How has the wetland changed that instrusion depth? What is the effect of the change on inflow nutrient distribution in the lake?

To meet the second objective, it is necessary to make numerical dynamic model simulations of water quality profiles for Lake McCarrons under hydrologic and weather conditions observed during past open water periods. The model has to be process oriented so that the effect of different management strategies can and will be simulated to determine what strategies for the improvement of lake transparency and reduction of plant growth have a chance of being effective. Strategies that may be considered are:

1. Phosphorus reduction

Specific lake management/improvement techniques to be considered are: Routing of the tributary inflow through the lake by a pipeline, reduction of phosphorus inflow from the residential areas surrounding the lake, sealing of lake sediments to reduce phosphorus release from the lake sediments, aeration of the lake hypolimnion to alter anoxic summer conditions to reduce phosphorus release from the sediments, phosphorus reduction in the inflow by chemical precipitation, and flushing of phosphorus out of the lake in spring.

2. Mixing

Increasing the surface mixed depth by artificial mixing during the summer stratification period reduces the exposure of algae to light and therefore reduces the standing crop (*chla* concentration). Mixing can be hydraulic jet mixing or air bubble mixing. Mixing to depths of 6-10m below the surface can be considered.

III. SITE DESCRIPTION

1. Lake Setting (from MCES, 1997)

"Lake McCarrons (Fig. III-1) and its 821 acre (332 ha) contributing watershed (excluding the lake) lie within the City of Roseville in Ramsey County, Minnesota. The lake itself has a surface area of about 81 acres (32.9 hectares) and has mean and maximum depths of 7.7 and 17.3 meters (25.0 and 57.0 feet), respectively. The resulting water volume of the lake is 2.52 x 10^6 m^3. Lake McCarrons is classified ecologically by the Minnesota Department of Natural Resources (MDNR) as a roughfish-gamefish lake.

The primary lake uses include swimming at the county beach, pleasure boating (small boats), and fishing. The lake's size normally restricts the use of larger or faster boats. The lake is eutrophic with abundant densities of macrophyte growth around its shore (to a maximum depth of 3.2 m [10.5 feet]) and occasional algal blooms. The lake is strongly dimictic and the hypolimnion becomes anoxic early in the summer and, depending on the extent of the fall overturn, may remain anoxic through the winter. These anoxic conditions have in fact resulted in some partial winterkills on the lake in past years."

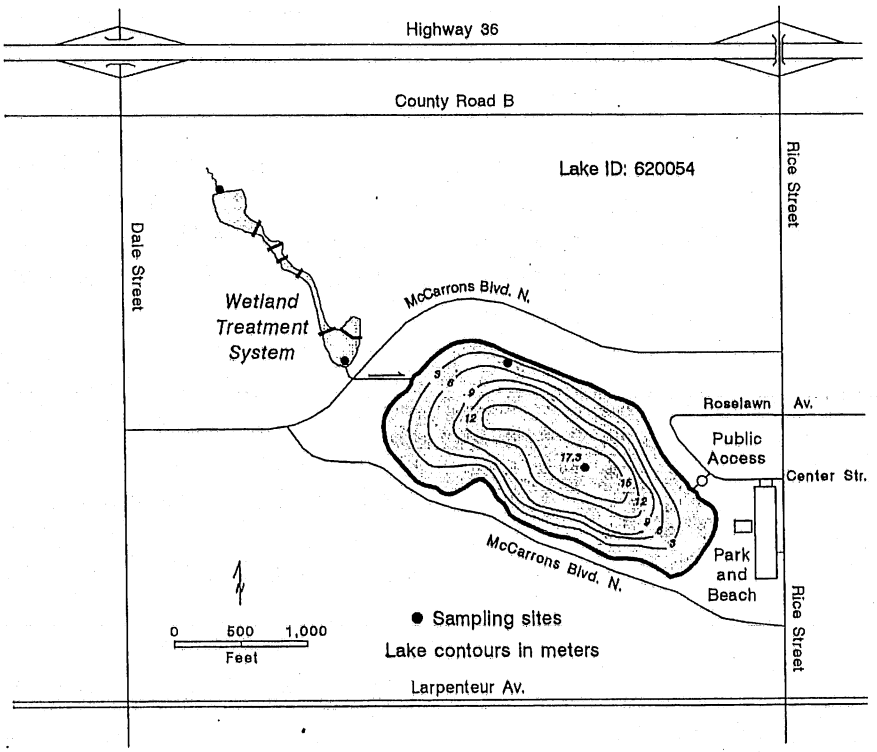

Figure III.1. Lake McCarrons location map.

2. Historical Data

Lake McCarrons has been the subject of intensive limnological measurements by the Metropolitan Council for many years. Data in the USEPA STORET database indicate that the lake stratifies strongly in summer. With a surface area of 0.33 km^2 and a maximum depth of 17.3 m (Oberts and Osgood, 1988), the lake geometry ratio $A_s^{0.25}/H_{max}$ is 1.38 $m^{-0.5}$, which is clearly in the range of seasonally stratified lakes. The seasonal thermocline (Fig. III-2) is usually near the 4 m depth as indicated by the historical data plots in Appendix A. These plots were obtained by retrieving the data in the STORET system and applying linear interpolation in depth and time. The plots show a very consistent pattern of temperature stratification year after year. The hypolimnetic waters are typically very cold (4-6°C) year-round.

The seasonal variations of Secchi depth, phosphorus, nitrogen, and chlorophyll-a near the surface of Lake McCarrons have been shown by Oberts and Osgood (1988). Osgood (1989) states that "Lake McCarrons' water quality does not appear to have changed this decade, despite intensive watershed management. In fact, the lake's phosphorus concentration was actually lowest when external loadings were highest. This unexpected observation has not been satisfactorily explained (Oberts and Osgood, 1988)." The historical water quality information for the 1980's was updated for the 1990s (Metropolitan Council Environmental Services, 1997). In that MCES (1997) report the performance of the McCarrons Wetland Treatment System (MWTS) is evaluated and data from the 1990s and trends on Lake McCarrons water quality are provided. A review of McCarrons Lake water quality in the context of other Metropolitan area lakes was given by Osdgood (1988) and by Jensen (1998).

The MCES (1997) report gives a limnological assessment of Lake McCarrons that shows an upward trend in TP, from 34 to 60 mg/l; a slight downward trend in Secchi depth readings from 2.2 to 1.9 m; and a constant mean summer *Chla* concentration (20 mg/l) over the period 1984 to 1996. A summary of selected summer water quality means for Lake McCarrons surface waters is given in Table III-1.

In addition to the nutrient concentrations and Secchi depths, DO levels were also measured during the summers of 1984-1991, and 1993-1996. Concentrations ranged from less than 5.0 to more than 10.0 mg/l in the lake's surface waters, and annually indicated anoxia (> 2.0 mg/l) in the lakes hypolimnion throughout the summer and winter months. Because the lake is so strongly stratified during the summer months, the hypolimnion (and resulting anoxic conditions) in mid-summer generally extended from 4.0 meters to 17.0 meters.

The Executive Summary of the MCES (1997) report summarizes the recent water quality of Lake McCarrons as follows:

> "Lake McCarons is eutrophic with abundant densities of macrophyte growth around its shore and occasional dense algal blooms. The lake is strongly stratified, and becomes anoxic early in the summer, at times

remaining so throughout the following winter. The Metropolitan Council has sampled the water quality of Lake McCarrons since 1984. An intensive study was done concurrently with the 1995-1996 MWTS sampling.

Data collected on the lake indicate slight degradation in water quality, indicated by increasing phosphorus and decreasing transparency. Chlorophyll-a levels have remained fairly constant. Year-to-year variability in precipitation and temperature could account for some of this appearance of degradation. Very high levels of TP in the hypolimnion become available to the entire lake at fall and spring overturn.

Spring and early summer phytoplankton populations are small, consisting of a mixture of green algae, diatoms and dinoflagellates. Blue-green algae dominates from mid-summer through the winter. Zooplankton grazing on algae would likely be enhanced by introducing oxygen into the hypolimnion. Macrophyte occurrence has remained fairly stable since 1983. There is no evidence that the distribution or species composition of the lake's macrophyte community are related to nutrient concentrations in the water. Lake McCarrons has an abundant panfish population. Bass, muskellunge (Tiger), walleye pike, and northern pike have all been caught in the lake recently.

Runoff and water quality entering the lake were directly monitored for about 90% of the watershed draining to the lake via the MWTS. During this period of study, approximately 45% of the lake's TP load came in the summer, 35% in the spring and snowmelt, and 15% in the autumn. The lake's summertime phosphorus concentrations appear to be insensitive to inputs of phosphorus prior to mid-May, when the lake is not stratified. Inputs become far more important after stratification in the late spring. To achieve a desirable summertime mean TP of 30-35 µg/l, a 50-60% reduction in the lake's current summertime epilimnetic load is needed. The lake continues to degrade, possibly the result of warming the inflow as noted previously. Yearly precipitation and air temperature variation could also be responsible for lake quality variation because of water temperature and dilution dynamics in the epilimnion."

"Temperature data collected during part of the study at both an inflow site and the outflow to the lake show that water is warmed as it moves through the MWTS. During warm months, this results in outflow into the reduced volume of the lake above the thermocline. This appears to contribute to the continuing degradation of the lake's quality even though the MWTS reduces some pollutant input."

The first objective of this study is related to this concern--It is to assess the degree of warming that the watershed runoff experiences in the wetland system (MWTS) in summer, and to examine by how much the inflow dynamics into the stratified Lake McCarrons are changed by this warming.

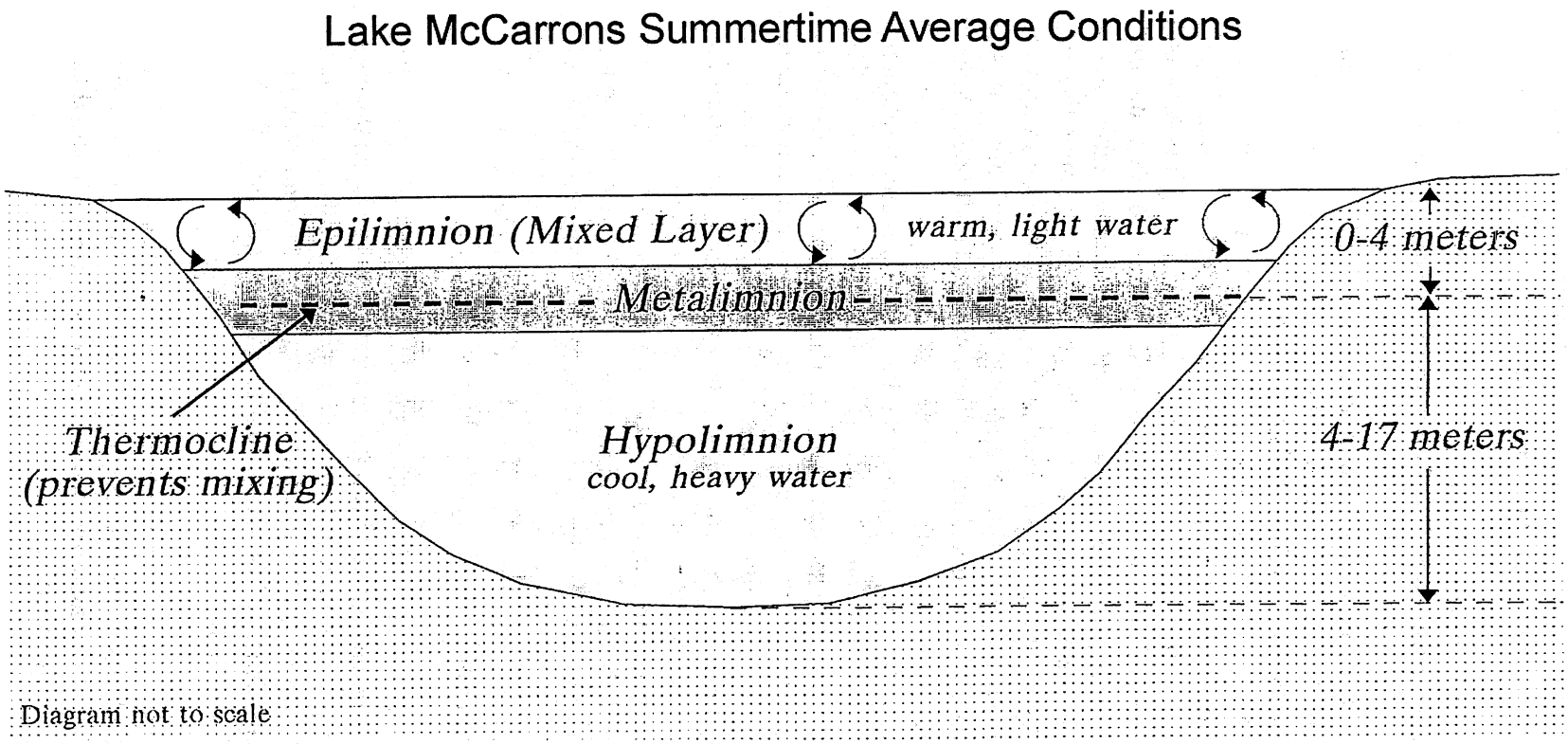

Figure III-2. Lake McCarrons generalized ecosystem.
(from MCES, 1997)

Table III-1. Summary of Selected Summer Quality Means for Lake McCarrons Surface Waters (from MCES, 1997)

Year	Total Phosphorus (µg/l)	n	Chlorophyll-a (µg/l)	n	Secchi transparency (m)	n	Kjeldahl Nitrogen (mg/l)	n
1984	38	10	20	10	2.3	10	1.08	10
1985	34	15	16	15	2.1	15	0.97	15
1986	28	11	14	11	2.8	11	0.82	11
1987	46	11	26	11	1.8	11	1.11	11
1988	61	11	30	11	1.4	11	1.38	11
1989	34	11	17	11	1.8	11	1.01	11
1990			18	10	3.1	10	1.10	10
1991	47	11	30	11	1.5	11	1.22	11
1992								
1993	35	10	15	10	2.1	10	0.90	10
1994	36	10	13	10	2.3	10	0.90	10
1995	69	11	28	11	1.8	11	1.41	11
1996	78	10	16	10	1.7	10	1.28	10
Mean	46.0	11	20.3	12	2.1	12	1.10	12

n=number of monitoring events

IV. INFLOW DYNAMICS

1. Concept

Inflows from tributaries enter lakes or reservoirs near the water surface and may progress into a lake as overflows, interflows or underflows. Which of these three occurs depends on the density of the inflowing water relative to the density of the water encountered at different depths of a lake. Minute differences in densities cause buoyancy effects (upward or downward) that may send an inflow to the bottom of a lake or reservoir or keep it floating across the surface of a lake. In the case of interflows, the inflow plunges at first but then enters the metalimnion of a lake.

Density of Minnesota lake water is usually controlled by water temperature; only in very exceptional cases do dissolved salts or inorganic suspended sediments make a significant contribution to the buoyancy. Water temperature in tributaries to Minnesota lakes in summer may fluctuate by several degrees during a day (Sinokrot and Stefan, 1993), and may therefore be warmer or cooler than a lakes epilimnion (surface layer). If the tributary is shaded by trees or is fed by seepage or groundwater, the inflow water will most likely be cooler than the lake surface and will plunge below the surface of a lake after entering a lake.

In the case of Lake McCarrons, the situation is complicated by the presence of a wetland between the tributary and the lake. Wetlands are known to modify water temperatures by added (longer) exposure of the tributary water to atmospheric heating and cooling. Some water temperature recordings by MCES at the outflow of the wetland gave a preliminary idea of the degree of temperature modulation in the wetland in 1998, but the relationship to lake temperatures could not be well established because of a lack of lake temperature data. To obtain a clearer picture, thermister chains were installed in Lake McCarrons in the spring of 1999 and operated until fall of 1999.

2. Water temperature data collection in 1999

Water temperatures were recorded at 1 minute intervals and averaged over 10 minutes at four stations, one at the inflow to the MWTS, one at the outflow from the MWTS, one in the littoral waters of the lake, and one near the deepest point of the lake (Figure III-1). At the two lake stations (rafts) thermister chains linked to dataloggers were installed. The thermister spacing with depth is given in Table IV-1 and the starting date of thermister operation in Table IV-2. The YSI thermisters were surface coated and had time constants of about 1 minute.

The entire field installation was built, installed and operated by Karen Jensen assisted by Randy Ahern of MCES and Deborah West of SAFL. Guidance was provided by Dr. Christopher Ellis of the St. Anthony Falls Laboratory, University of Minnesota,

and the authors. The data were processed by the senior author and Dr. Omid Mohseni of SAFL.

3. Data interpretation

Water temperatures recorded at the outflow of the wetland in 1995 and 1996 are reproduced in Appendix B. Those measured in 1999 are plotted in Figure IV-1 and show variations at three different timescales: (a) seasonal warming until about the end of July and cooling thereafter, (b) warming or cooling in response to weather systems passing through the region at a timescale ranging from several days to weeks, and (c) diurnal warming and cooling at a 24-hour timescale. Water temperature excursions at the seasonal time scale are 0 to 29°C; at the daily to weekly scale water temperature variations are up to 10°C and diurnal water temperature fluctuations in the wetland outflow are often between 2° and 4°C. Outflow from the wetland becomes inflow to the lake. Outflow from the wetland into the lake is often cooler than the lake surface temperature and will therefore tend to sink below the water surface in the lake. The questions are (a) To what depth will the inflow plunge and intrude into the lake after it has entered the lake? and (b) Would this depth be substantially different if the inflow did not have to pass through a wetland?

Table IV-1. Vertical location of thermistors in Lake McCarrons - Summer 1999.

Probe Number	Center Raft	Littoral Raft
1	0.1 m	0.1 m
2	1.1 m	0.3 m
3	2.0 m	0.6 m
4	3.0 m	0.8 m
5	4.0 m	1.1 m
6	5.1 m	1.6 m
7	6.1 m	2.1 m
8	7.1 m	2.6 m
9	9.1 m	3.0 m
10	11.1 m	3.1 m
11	14.6 m	air temperature
12	17 m	wind speed

Table IV-2. Start and end dates for the operation of thermistor chains in Lake McCarrons - Summer 1999.

Location	Start Date	End Date
Center Raft	4-29-99	10-25-99
Littoral Raft	4-29-99	9-26-99
Wetlands Outflow	3-26-99	10-18-99
Wetlands Inflow	3-30-99	10-18-99

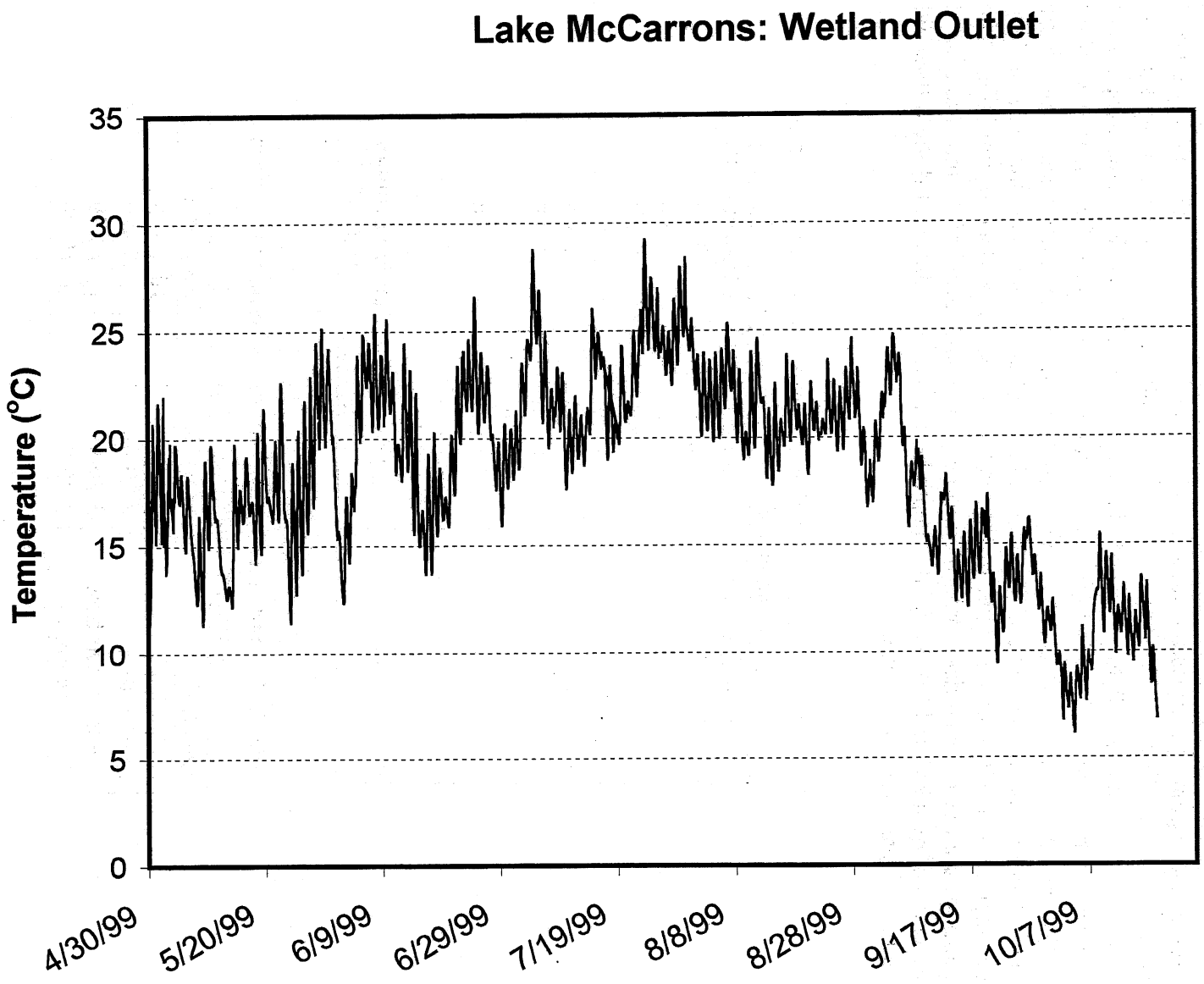

Figure IV-1. Lake McCarrons wetland outflow temperatures in 1999.

To answer the first question, water temperatures recorded in the littoral waters of the lake and in the wetland outflow were plotted simultaneously against time (Fig. IV-2). The plot shows that at times the wetland outflow is as warm as the littoral surface water of the lake and will therefore tend to "float" to the surface of the lake. This effect is seen to be particularly pronounced in warm periods of May and June It can also be seen that at other times the wetland outflow is considerably (5°C) colder than the littoral water indicating that the inflowing water will sink (plunge) and tend to follow along the lake bottom to a greater depth. These intrusions occur during many time periods throughout the year and always towards the end of periods of colder weather, i.e. cooling of water. The reason, of course, is that water in the shallow wetland cools faster than the deeper lake waters. To what maximum depths the outflow from the wetland may sink in the lake can be seen in Figure IV-3. In spring, the maximum potential depth of penetration is about 5 m; from the beginning of July to the middle of August, it is about 4 m; and after September 1, it increases from 5 m to 9 m depth. In summary, the maximum potential depths to which the wetland outflow will tend to sink can be read from Figure IV-3 and is in the range from 4 m in July to 9 m in October. Maximum potential plunging depths will be attained at the end of cooling periods due to cooler weather. At the end of warming periods, wetland outflows can attain water temperatures found in the upper 2 m of the lake. During those phases the wetland outflow will tend to 'float' into the lake and become part of the lake epilimnion. As warming and cooling periods alternate at timescales of day to weeks, so does the inflow change from plunging to floating at the end of those periods.

To answer the second question, i.e. if the watershed inflow to Lake McCarrons would behave substantially differently if it did not have to pass through a wetland, the following data interpretation procedure was used. The water temperature data recorded at the center raft were interpolated to give a graph of isotherms versus depth and time, a format frequently used in limnology. Isotherms were plotted in bands instead of lines. On this plot the depth corresponding to the temperature of the inflow was marked as a black line (Fig. IV-4). If water density is only related to water temperature (not dissolved or suspended material)--as is safe to assume for Lake McCarrons--the plot in Fig. IV-4 indicates to what maximum potential depth in the lake the inflow would go to find water of equal density. Figure IV-4 assumes that there is no dilution of the inflow by entrainment of ambient water. If a 1:1 dilution with surface water is applied to the inflow, the plots in Fig. IV-5 are obtained.

If no wetland existed, the inflow to the lake would have the inflow temperature of the tributary, not the wetland outflow temperature. The intrusion depths into the lake for this situation are shown in Figs. IV-6 and IV-7. They are deeper than in Figs. IV-4 and IV-5 and are below the surface mixed layer. With or without dilution, the inflow intrusion depths into the lake are different before and after the wetland. Before the onset of a strong stratification (about June 15) the difference is most substantial. After that, the average intrusion depths differ by only about 1 m. Even then the wetland outflow does enter the surface mixed layer (sometimes only during daytime), whereas the tributary inflow without wetland goes into the metalimnion.

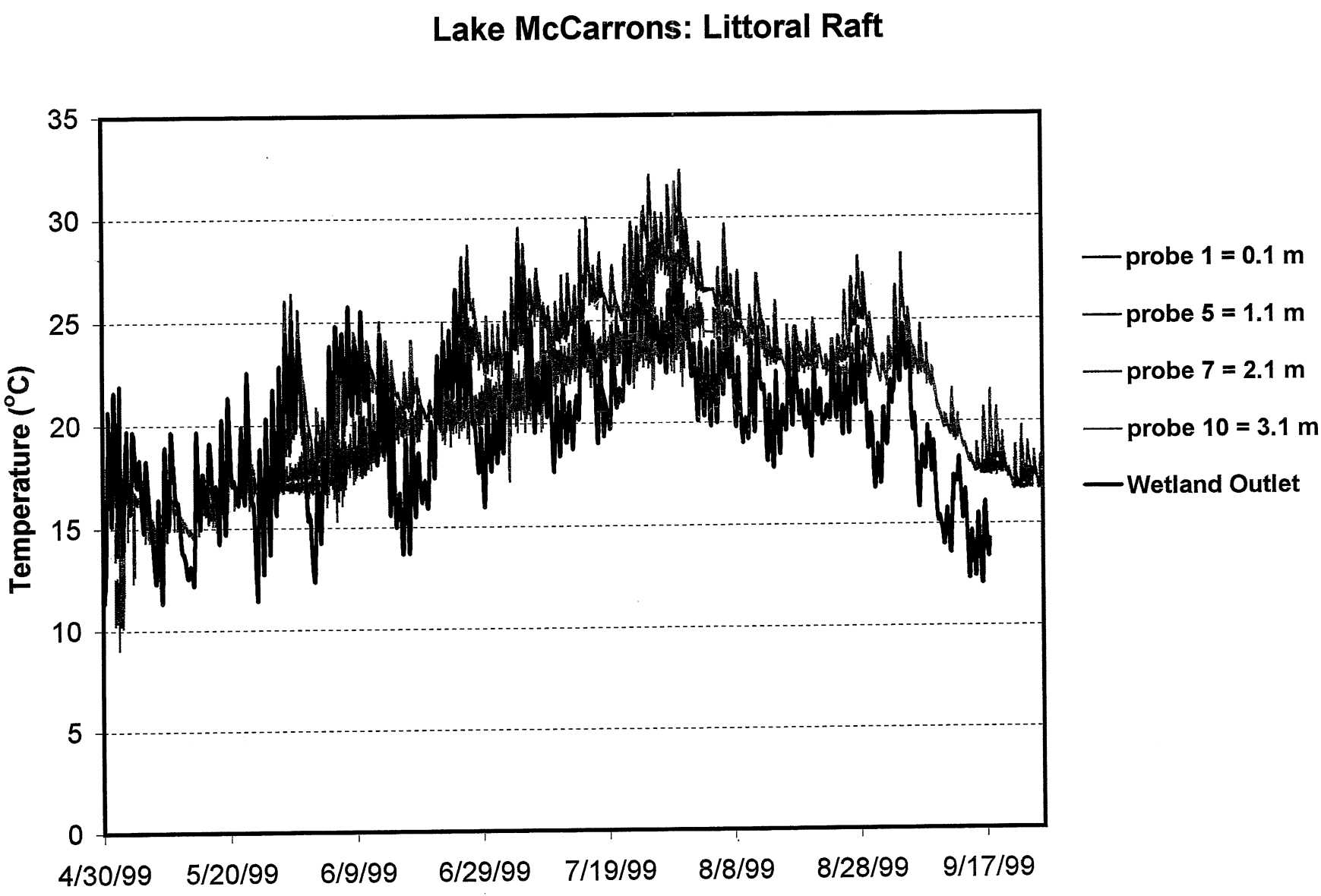

Figure IV-2. Lake McCarrons wetland outflow temperatures in relation to littoral lake temperatures in 1999.

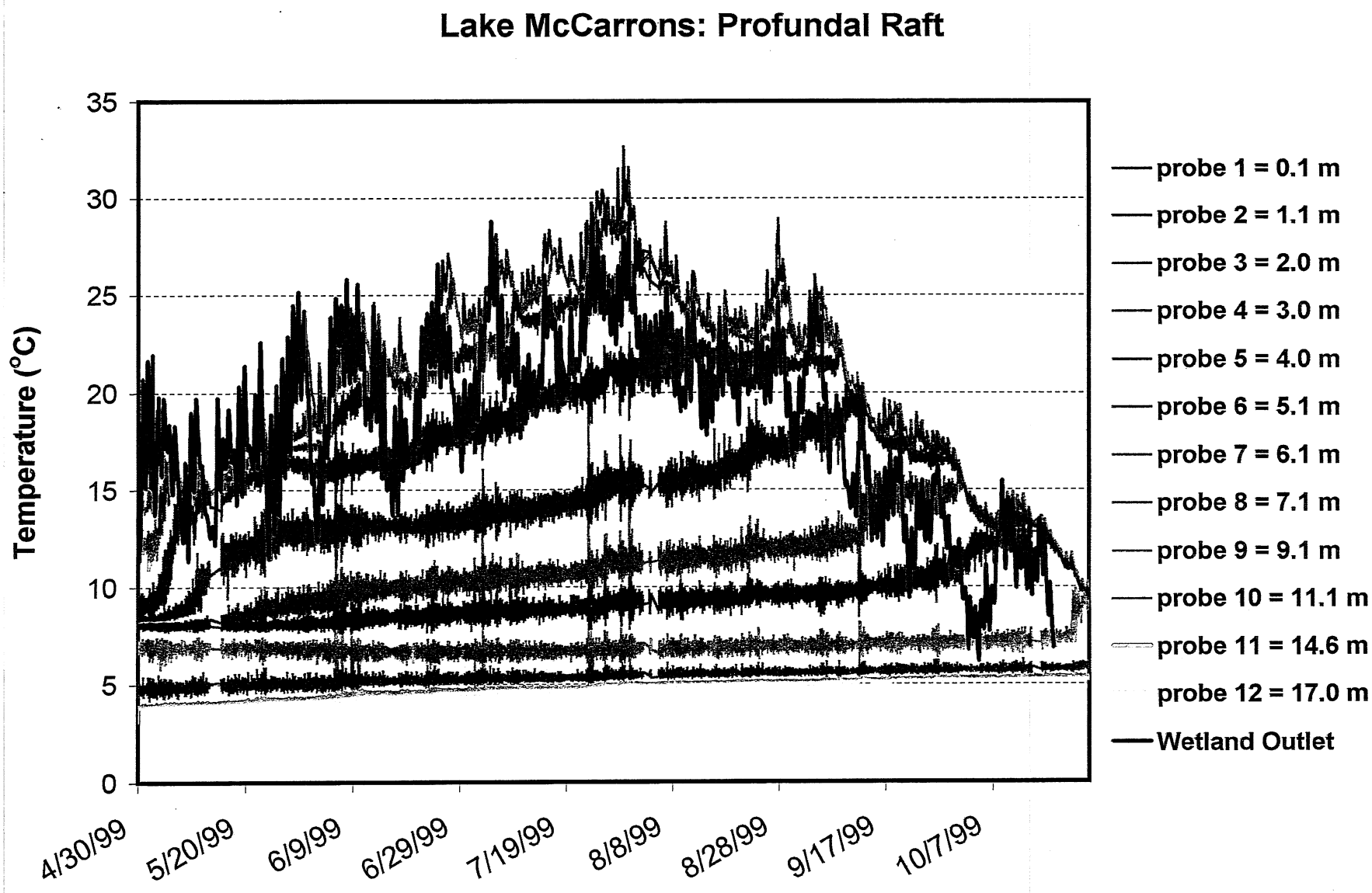

Figure IV-3. Lake McCarrons wetland outflow temperature in relation to Lake McCarrons temperature stratification in 1999.

Phosphorus contained in the inflow will be carried to the depths shown by the black lines in Figs. IV-4 to IV-7. On some days it will reach the surface mixed layer and thus become available to algae. Without warming in the wetland the inflow would fertilize the metalimnion where phytoplankton growth would be mostly light-limited.

4. Dye study of inflow intrusion

To prove that a cooler inflow to the lake actually plunges, a dye study was conducted. Rhodamine WT dye was added to the inflow and its path in the lake was followed for some distance and time. It was found that the dyed inflowing water followed the bottom of the lake. Higher dye concentrations were measured in water samples from the lake bottom than in samples from the water surface. This confirms the formation of a sinking (plunging) inflow.

The procedure and the results of the dye study are described in detail in Appendix C.

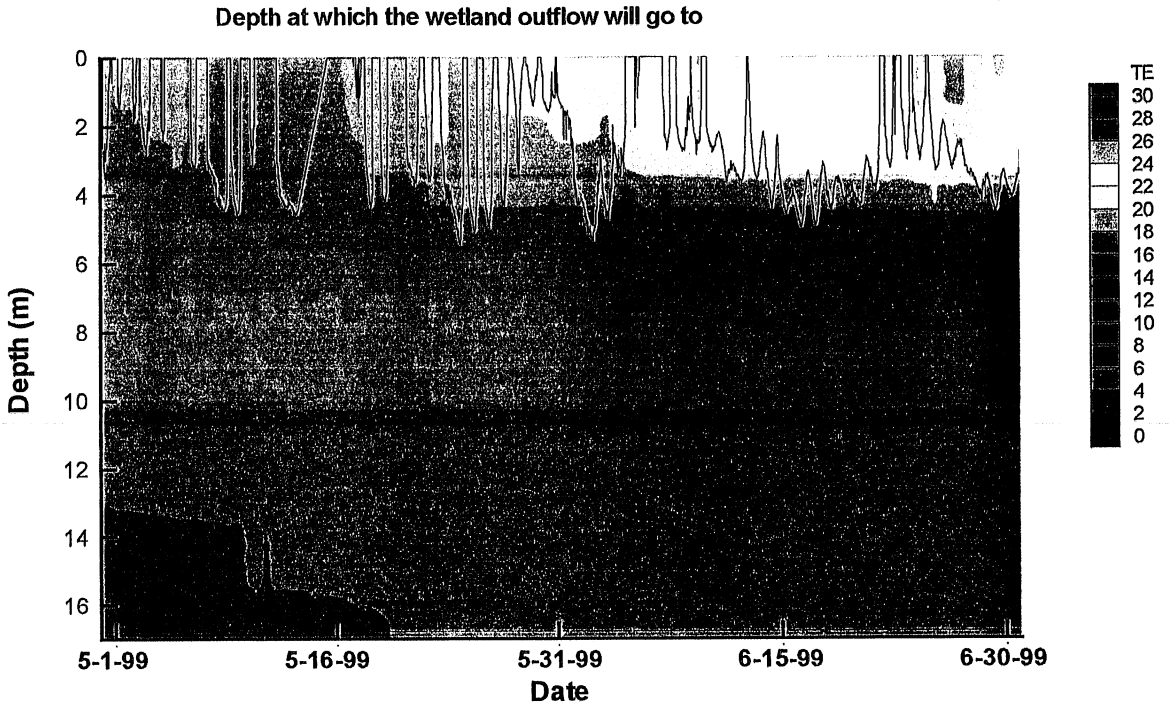

Figure IV-4. Intrusion depths of wetland outflows in Lake McCarrons (undiluted).

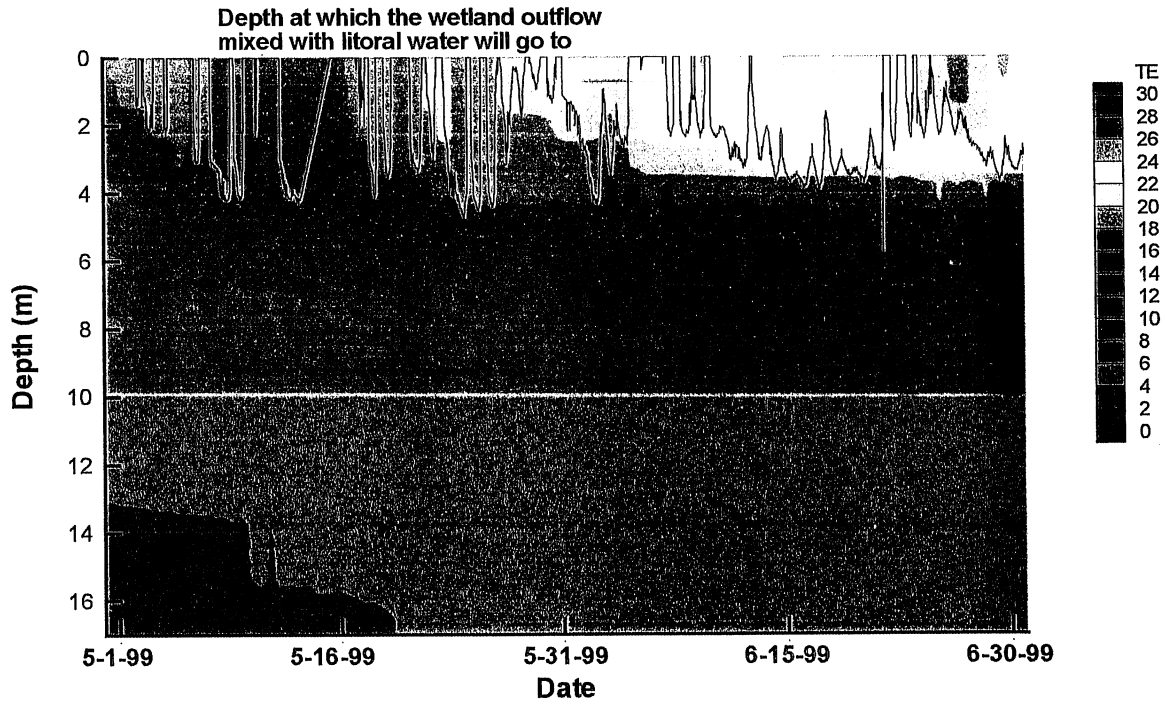

Figure IV-5 Intrusion depths of wetland outflows in Lake McCarrons (1:1 dilution with surface waters).

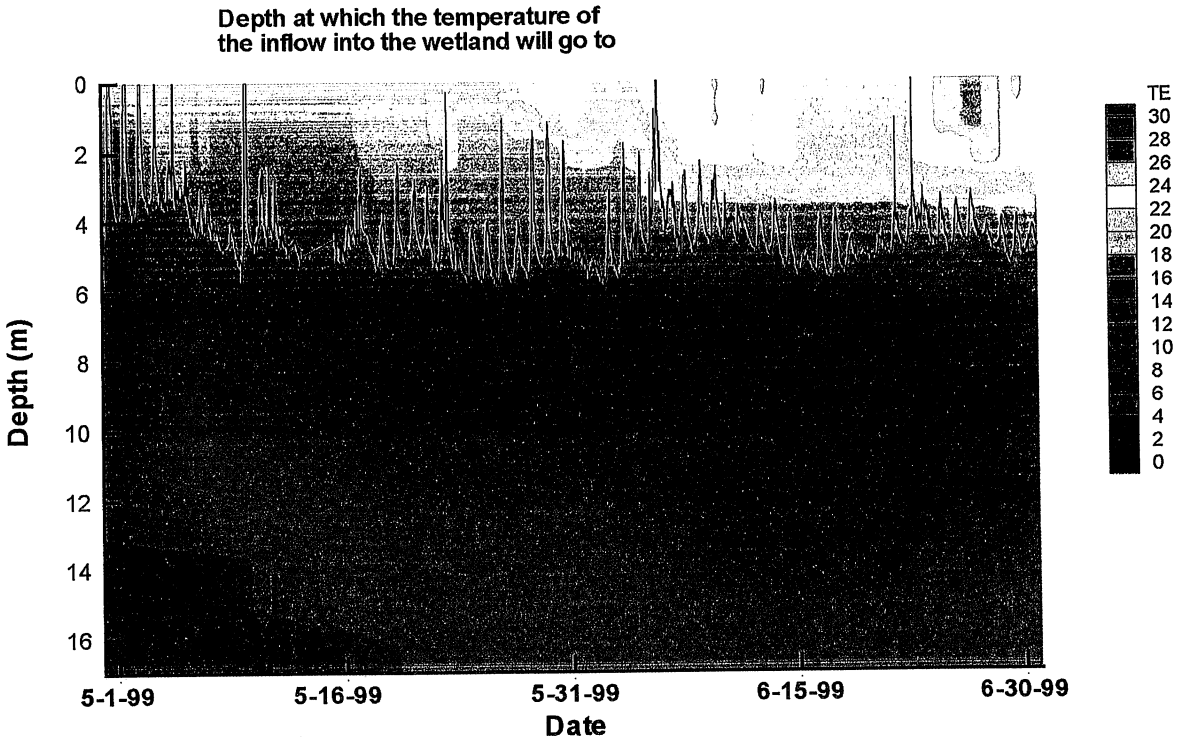

Figure IV-6. Intrusion depths of watershed runoff without wetland mediation in Lake McCarrons (undiluted).

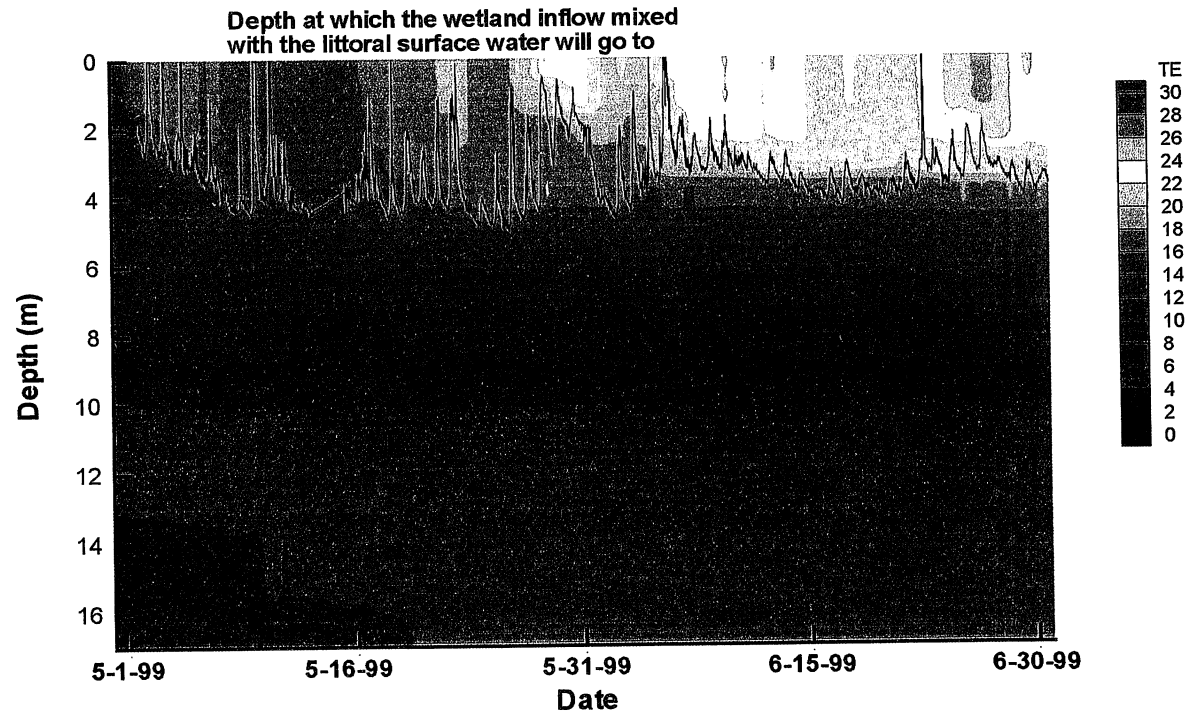

Figure IV-7. Intrusion depths of watershed runoff in Lake McCarrons (1:1 dilution with surface waters).

V. WATER TEMPERATURE MEDIATION BY THE WETLAND

1. Theoretical Temperature Mediation

Thermal mediation is a process through which shallow littoral regions such as wetlands can control the initial fate of tributary nutrient and contaminant fluxes within a lake or reservoir. As the lake inflow traverses these systems, the water temperature is modified through atmospheric heat exchange. The change in temperature can affect the intrusion depth, and thus impact the lake water quality.

According to Andradottir and Nepf (2000), the steady response of the wetland (Figs. V-1 and V-2) is governed by four non-dimensional parameters:

$r = \bar{t}/\bar{t}_{heat} = KWL/Q_r$	Thermal capacity.
$E^*=D_x/uL$	Dispersion number (or inverse Peclet number)
$\alpha^* = \alpha \cdot \bar{t} = \Delta Q/Q_r$	Non-dimensional lateral exchange coefficient.
$w = W_c/W$	Width ratio.

"The thermal capacity, r, reflects the heat/cooling potential of the system. It is defined as the ratio between the residence time, $\bar{t} = (A_c + A_d)L/Q_r$ (see Figure V-3), and nominal thermal inertia, $\bar{t}_{heat} = H/K$ where H is the average wetland depth. Notice that although both $\bar{t}$ and $\bar{t}_{heat}$ are functions of depth, the thermal capacity $r = \bar{t}/\bar{t}_{heat}$ is not. The three remaining parameters, E*, α^* and w, define the hydraulic or circulation regime within the wetland, and control the shape of the residence time distribution RTD (see figure V-2). The dispersion number, E*, describes the relative importance of longitudinal dispersion and advection. The lateral exchange coefficient, α^*, represents the fractional water exchange between the flow and dead-zone (*i.e.* $\Delta Q/Q_r$) and describes the relative importance of lateral exchange and advection. The width ratio, w, describes the size of the flow zone relative to the total wetland. If the wetland has uniform water depth, *i.e.* $H = H_c = H_d$, then $w = W_c/W$."

"In general, increasing the longitudinal dispersion, E*, reduces the degree of thermal mediation within the system. A more detailed description of this dependence is given by Jirka and Watanabe (1980). Instead, for simplicity, we assume E*=0 and use this sub-case to explore the remaining governing parameters and their effect on wetland thermal mediation. This simplification does not strictly limit the model, as short-circuiting, shear flow dispersion and plug flow can be represented with E*=0 (Andradottir and Nepf, 2000) and the general trends described apply for E*≠0 as well."

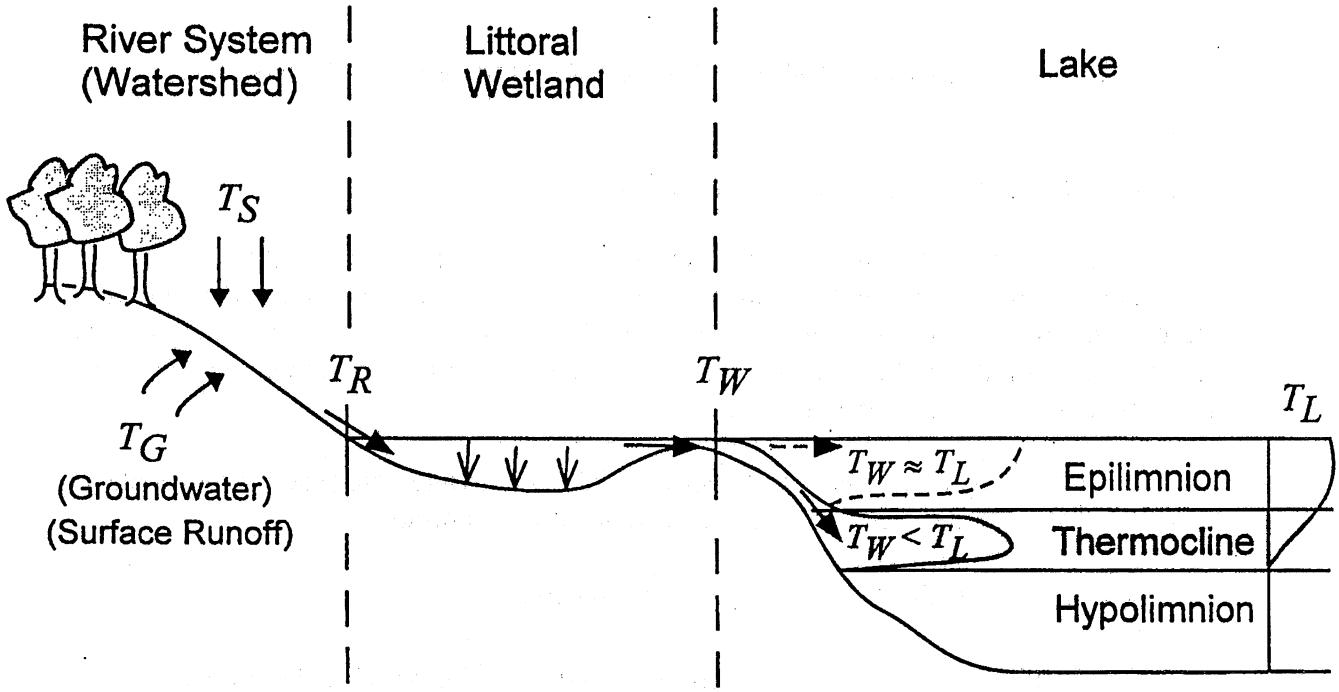

Figure V-1 Water temperature mediation in littoral wetlands as transition zones between uplands and deep aquatic systems. If thermal mediation occurs within the wetland, i.e. $T_W \neq T_R$, the lake intrusion dynamics may be altered. Specifically if $T_W \approx T_L$, then surface intrusions occur, whereas if $T_W < T_L$ a plunging inflow occurs (from Andradottir and Nepf, 2000).

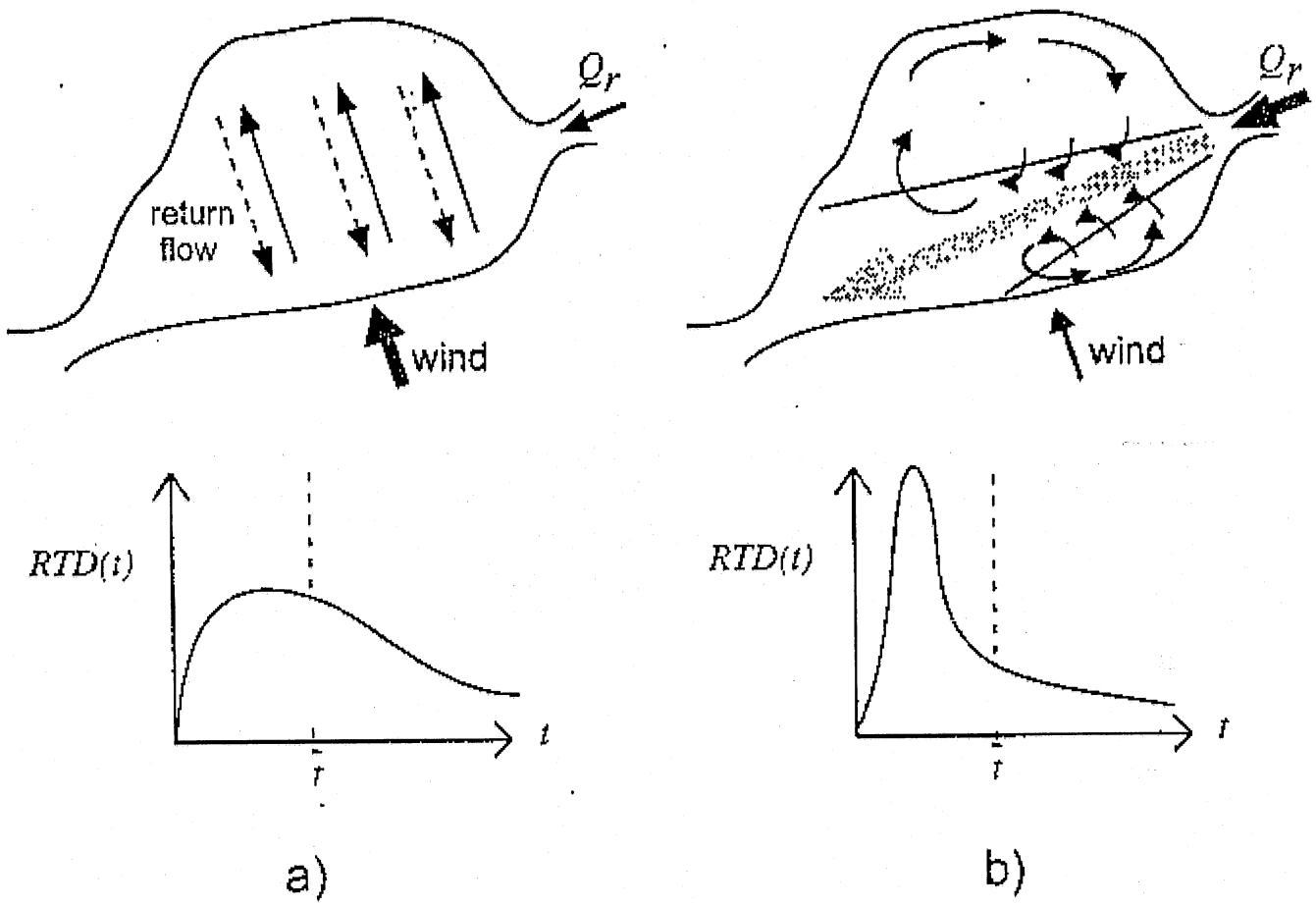

Figure V-2 Schematic of circulation regimes and residence time distributions (RTD) in free water surface wetlands. a) Wind-dominated circulation with a wind-driven surface drift (solid arrows) and a sub-surface return flow (dashed arrows). The wetland is well mixed, producing a RTD with a large variance around the mean nominal residence time, $\bar{t}$. b) River-dominated circulation with a distinct flow region (shaded). Short-circuiting occurs, producing a skewed RTD with much of the flow exiting the wetland in less time than $\bar{t}$ (from Andradottir and Nepf, 2000).

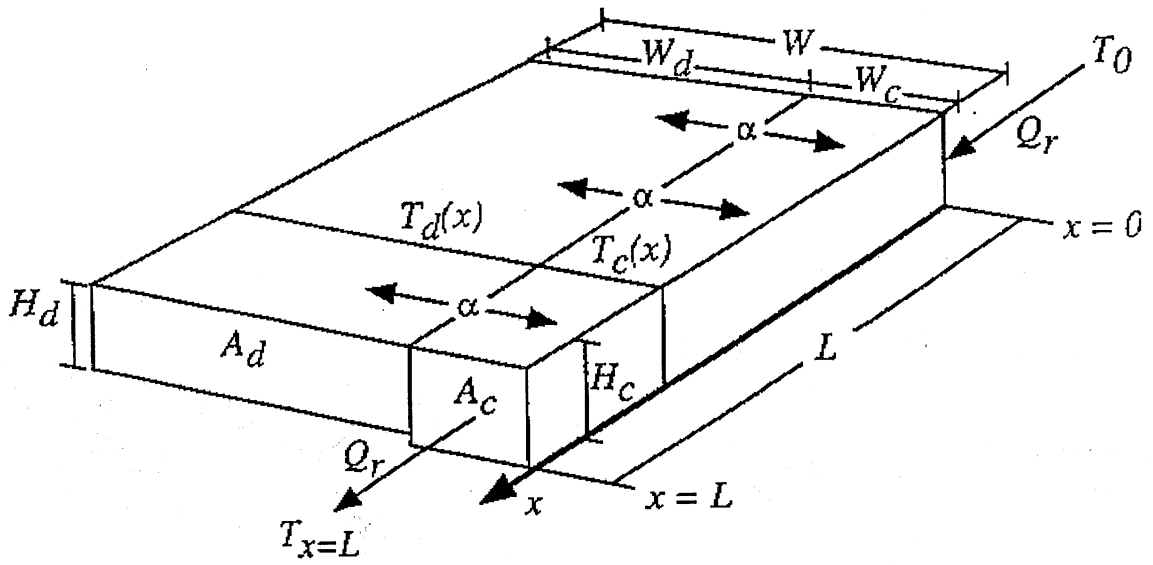

Figure V-3 Schematic of the dead-zone model. The wetland is divided into a channel or flow zone (shaded) and stationary dead-zone. These two zones communicate with one another through spatially uniform lateral water exchange, a[s^{-1}]. Thermal mediation within the wetland is reflected in $T_{x=L} \neq T_0$ (from Andradottir and Nepf, 2000).

"The dependence of the steady solution of the heat transport equation through the wetland on the parameters, r, α^*, and w is illustrated in Figure V-4 for E*=0. The degree of thermal mediation is given by the ratio $(T_{x=L}-T_0)/(T_E-T_0)$, which represents the actual change in temperature between the inlet and outlet of the wetland, T_{x+L}-T, relative to the maximum potential change, T_E-T_0, which would occur if thermal equilibrium with the atmosphere were reached. As shown on Figure V-4, the thermal capacity, r, controls the degree of thermal mediation provided by a wetland. For $r << 1$, the residence time limits the heat capture and no thermal mediation occurs, *i.e.* $T_{x=L}=T_0$. For $r >> 1$, however, the residence time is not limiting, and the outflow temperature reaches equilibrium with atmospheric conditions, *i.e.* $(T_{x=L}-T_0)/(T_E-T_0)=1$. The rate with respect to r at which the thermal mediation curves approach equilibrium is described as the thermal efficiency and depends on the hydraulic parameters a* and w. The most efficient flow regime is plug flow (dot-dashed line on Figure V-4), which is equivalent to $a^* \rightarrow \infty$ given E* = 0. A large dead-zone (small w) and a small exchange flow (small α^*) both reduce the effective thermal capacity of the wetland. Such systems have low thermal efficiency, *i.e.* produce less thermal mediation at any value of r (Fig. V-4)."

The Andradottir and Nepf (2000) model was applied to the MWTS as follows.

1. Thermal Capacity

Nominal thermal capacity = $r = t/t_{heat}$

Nominal residence time = $t = V/Q_r$

where

V = volume of wetland

Q_r= flow rate through wetland.

Nominal thermal inertia (or timescale of heat transfer) = $t_{heat} = H/K$

where

H = average wetland depth

K = rate of surface heating and cooling.

The surface heat transfer coefficient, K, represents the rate of surface heating and cooling, and varies temporarily with meteorological conditions (in particular wind speed) and surface water temperature. This coefficient generally lies between 0.4 - 1.0 m/day for low winds (< 2 m/s), increasing to 0.8 - 2.0 m/day for high winds (8 m/s) (Ryan et al., 1974).

Average windspeed in Minneapolis/St. Paul ~ 10 mph ~ 4.5 m/s. This gives K ~ 1.2 m/day.

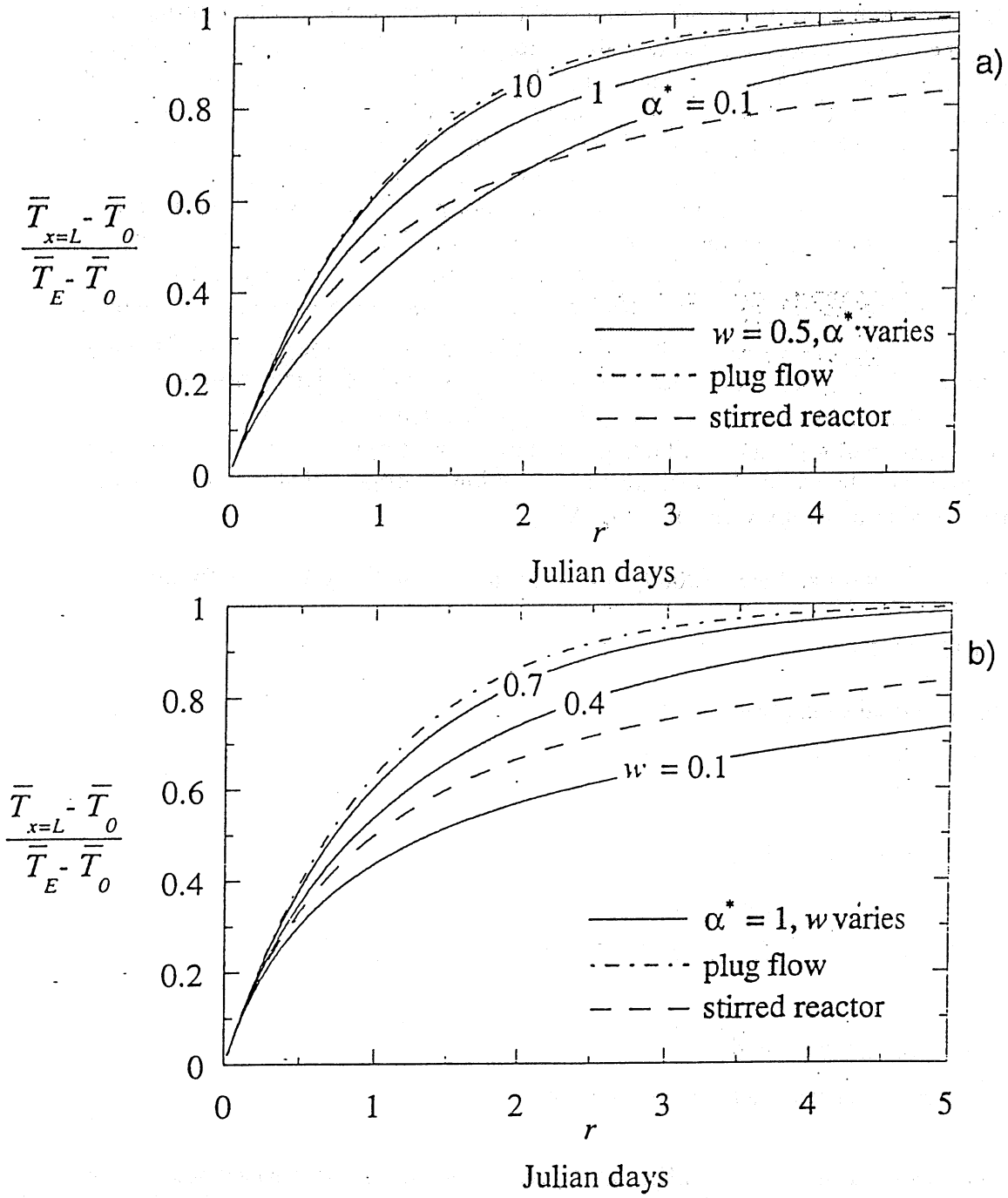

Figure V-4 Steady dead-zone model results (solid lines) as a function of thermal capacity r for E*=0. a) Variable α* with ω=0.5, and b) variable ω with α*=1. Stirred reactor solution (dashed line) and plug flow solution (dot-dashed line) are drawn for comparison. Increasing α* and/or ω improves the thermal efficiency, i.e. more thermal mediation $\left(\overline{T}_{x=L}-\overline{T}_0\right)/\left(\overline{T}_E-\overline{T}_0\right)$ is achieved at a given r (from Andradottir and Nepf, 2000).

The ratio = H/K is the timescale of heat transfer and represents the thermal inertia of the water column, which is a measure of how rapidly the system responds to changes in atmospheric forcing and how much heat it stores. Shallow wetland systems with low thermal inertia can more readily track changing atmospheric conditions, but store less heat than deep systems, *i.e.* as $H \rightarrow 0$, then $t_{heat} \rightarrow 0$ and $T \rightarrow T_E$.

Average volume, surface area, and depth of the wetland are V = 15.4 acre-feet, A = 8.5 acres and H = 1.8 feet, respectively. (See Appendix D for supporting data)

Average wetland flow rate at Site A (MCES, 1997) during dry weather in the summer of 1995/1996 is $Q_r \approx 1$ acre ft/day.

Average Values

Residence time $\quad t = \frac{15.4}{1.0} = 15.4$ days

Thermal response time $\quad t_{heat} = \frac{1.8}{1.2} = 1.5$ days

Thermal capacity $\quad r = \frac{15.4}{1.5} = 10.3$

Extreme Values

$t = \frac{15.4}{27} = 0.57$ days for 2.7 inches daily precipitation

$t = \frac{15.4}{0.2} = 77$ days for base flow

$t_{heat} = \frac{1.8}{0.4} = 4.5$ for a calm day and $\frac{1.8}{2.0} = 0.9$ for a windy day

High Estimate

$r = \frac{77}{0.9} = 86$ for a windy baseflow day

Low Estimate

$r = \frac{0.57}{4.5} = 0.13$ for a major rainfall event

2. Dispersion number

Dispersion number $E = \frac{D_x}{uL}$

where $\quad D_x$ = longitudinal dispersion coefficient in wetland flow

u = mean flow velocity through the wetland (in the flow zone only)
L = length of the wetland

Assumed: $E = 0$

3. Lateral Exchange

Non-dimensional lateral exchange coefficient $\alpha^* = \Delta Q / Q_r$

where ΔQ = total lateral exchange rate
Q_r = total flow rate through the wetland

Assumed: $\alpha^* = 0.5$

4. Width Ratio

Width ratio $w = W_c/W$

where W_c = width of the flow-through zone of the wetland
W = total width of the wetland

Estimated: W = 0.5 (see Appendix C)

For *dry weather conditions*, with an average r value of 10.3 and $\alpha^* = 0.5$ and w = 0.5, it can be concluded from Fig. V-4 that the Lake McCarrons wetland causes complete water temperature mediation, *i.e.* the effluent temperatures from the wetland will be close to the long-term (15 day) average equilibrium temperature imposed by the weather.

For *minor storm events*, the wetland will cause a water temperature mediation by at least 30% of the difference between inflow temperature and equilibrium temperature imposed by the long-term (15 day) average weather. Only for *very major storm events* will the residence time in the wetland be so short that the water temperature mediation will be insignificant.

To investigate the *daily fluctuations* in water temperature, Andradottir and Nepf (1999) used a periodic forcing function in the heat transport equation. The periodic solution has the same basic form as the steady solution. The important difference between the periodic and steady solutions arises from the additional dependence on the timescale ratio

$$\frac{H_c}{H} t_{heat} / P$$

which compares the thermal inertia of the channel,

$$t_{heat,ch} = \frac{H_c}{H} t_{heat} = \frac{H_c}{K}$$

to the period of the forcing, P. For periodic variations in the weather, the dimensionless parameter is t_{heat}/P for a constant depth wetland. This timescale ratio controls the degree to which the periodic heat capture of a wetland is limited by the thermal inertia of the flow zone, $t_{heat,ch}$. This dependence is illustrated on Figure V-5, which displays the periodic thermal mediation with respect to r for different value of $t_{heat,ch}/P$.

The periodic thermal mediation for $r >> 1$ is solely determined by $t_{heat,ch}/P$. When $t_{heat,ch}/P$ is large, the wetland is unable to track the atmospheric forcing because the forcing varies more rapidly than the wetland can respond.

For a diurnal fluctuation of weather P = 1 day. Hence t_{heat}/P becomes

$t_{heat}/P = 1.5$	for average weather conditions
$t_{heat}/P = 4.5$	for calm weather conditions
$t_{yeat}/P = 0.9$	for windy weather conditions.

On a calm day the daily amplitude of the wetland effluent temperature according to Fig. V-5 should be less than 10% of the weather imposed amplitude of the water equilibrium temperature. On a windy day it should be less than 20% and in the average with $t_{heat} \cong$ 1.5 days, about 15%. The daily equilibrium temperature amplitude is typically on the order $\Delta T_E = H_S/(K\rho c_p)$ where

H_S = total daily solar radiation
K = surface heat transfer velocity
ρc_p= specific heat.

In July H_S varies from about 780 cal $cm^{-2}d^{-1}$ on a clear day to 120 cal $cm^{-2}d^{-1}$ on a very overcast day. With K=1.2 m/d (range 0.4 m/d to 2 m/d), the value of $K\rho c_p$=120 $cal^{-2}d^{-1}$ (range 40 to 200). Hence, the daily equilibrium temperature excursion on a clear day in July should be on the order of 6.5°C (range 3.9 to 19.5°C). On an overcast day, it should be about 1°C (range 0.6 to 3°C). With mediation in the wetland, the daily water temperature amplitude in the wetland outflow is reduced to 20% of ΔT_E, hence water temperatures should fluctuate on the average by about 1.4°C and by 4°C at the most. Actual measurements of wetland effluent temperatures (MCES, 1997), some of which are reproduced in Appendix B, and in the next section show larger diurnal amplitudes than would be expected from this theory.

In summary, the theoretical analysis suggests that the MWTS can provide significant thermal mediation. During non-storm conditions, the addition of the wetland prolongs the time for heating/cooling, reducing the seasonal temperature differences between the wetland outflow and the lake. This makes the intrusion depth more sensitive to diurnal and synoptic meteorological fluctuations. Specifically in summer, the wetland can sufficiently raise the temperature of the lake inflow to produce a surface intrusion during the day, causing more born nutrients and contaminants to enter directly into the epilimnion where they can potentially enhance eutrophication. This scenario was

observed at Lake McCarrons (Oberts, 1988; Metropolitan Council, 1997). The analysis in this chapter show that the MTWS can provide significant mediation of the tributary inflow temperature, except for very major storm events.

2. Measured Temperature Mediation

Water temperatures recorded at the inflow to the wetland (Site D) and at the outflow from the wetland (Site A in the 1997 MCES report) at 10 minute intervals are plotted in Fig. V-6. With exception of early spring and late fall, inflow to the wetland is usually several degrees C cooler than the outflow, i.e. substantial heating occurs in the wetland.

The temperature differential between outflow from the wetland and inflow to the wetland is illustrated clearly in Fig. V-7. During the summer months (May to August) the inflow warms on the average by 4 to 5°C. In early spring (March) and fall (October) the inflow and outflow have about equal temperatures.

The diurnal amplitudes of inflow and outflow temperatures show a strong seasonal trend from high values in spring (April) to low values in fall (Figure V-8). The diurnal amplitudes of the outflow from the wetland are about 1°C smaller than those of the inflow throughout the observation period. If a damping factor is calculated for the entire weland as the ratio

$$\delta = \frac{\Delta T_{outlet}}{\Delta T_{inlet}}$$

where ΔT designates the difference between the daily maximum and minimum water temperatures, its mean value is found to be about δ=0.8.

The observed strong heating of the water in the wetland during the summer agrees qualitatively with the theoretical projections outlined in the previous section. The observed diurnal fluctuations in outflow water temperatures are higher than would be expected from the theory.

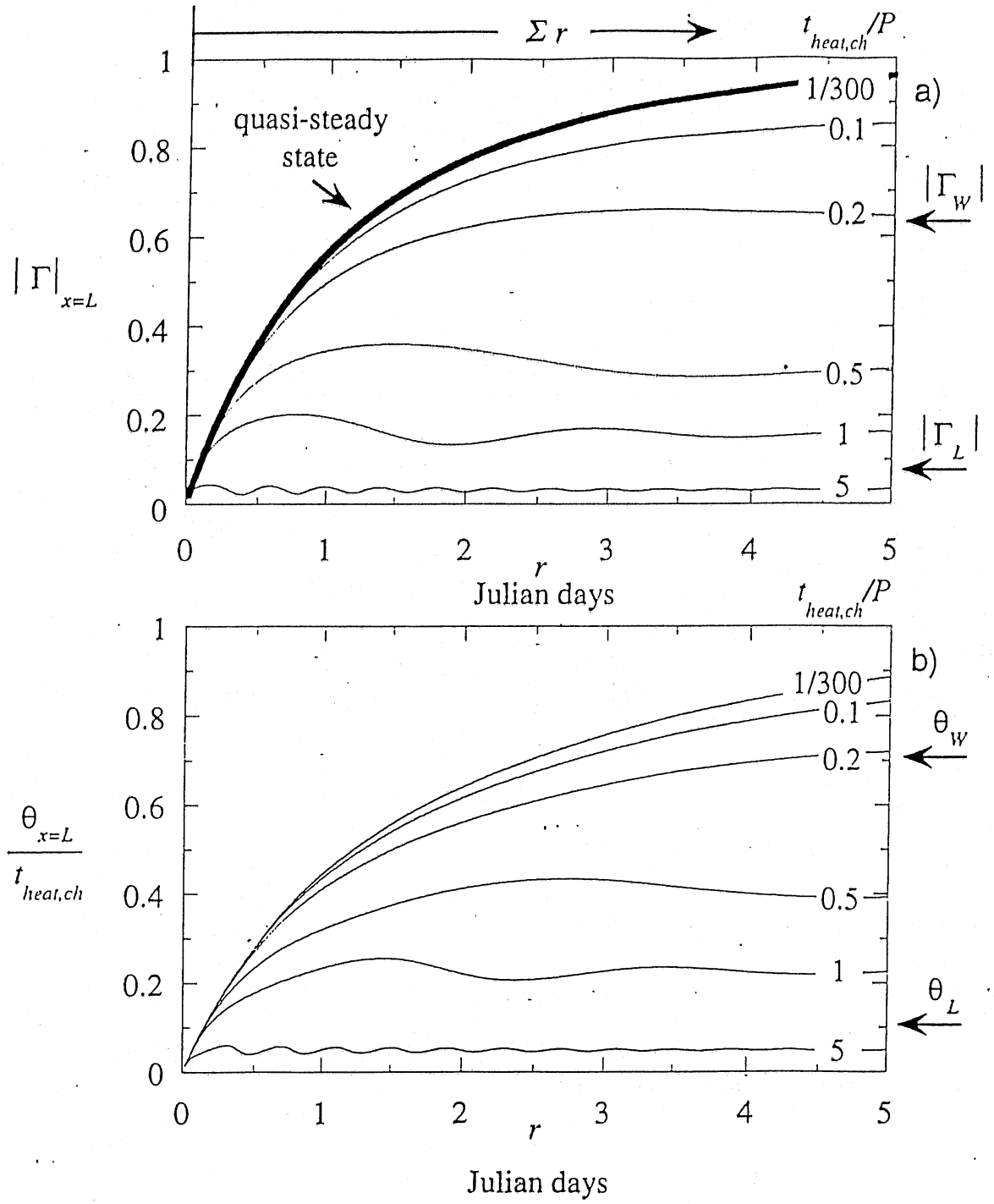

Figure V-5. Periodic dead-zone model results as a function of r and $t_{heat,ch}/P$ for E*=0, A*=1 and ω=0.5. For simplicity, inflow temperatures are assumed to be constant, i.e. Γ_0=0. a) Amplitude $|\Gamma|_{x=L}$, and b) non-dimensionalized phaselag between the outlet and equilibrium temperature $\theta_{x=L}/t_{heat,ch}$. The periodic thermal response becomes more damped as $t_{heat,ch}/P$ increases. As a result a 1 m deep wetland, $|\Gamma_w|$ and θ_w, heats and cools more rapidly than a 10 m deep lake $|\Gamma_L|$ and θ_L, in response to synoptic (shown) and diurnal heating cycles (from Andradottir and Nepf, 2000).

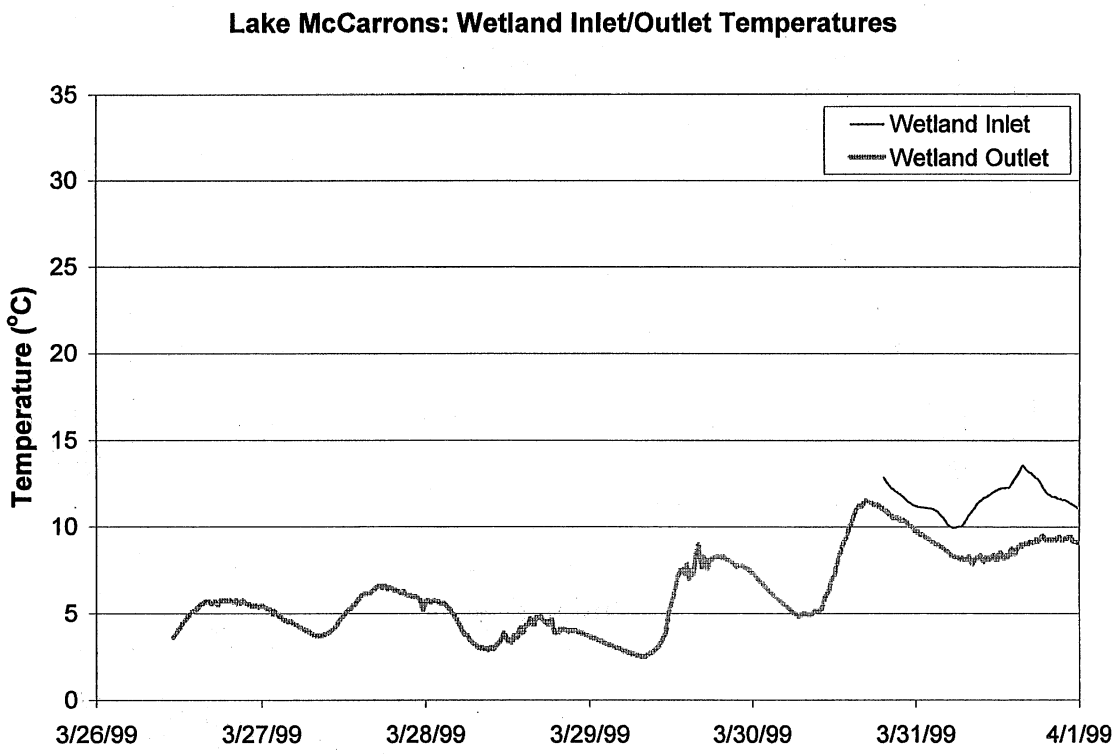

Figure V-6. Water temperatures recorded (10-min averages) at the inlet and the outlet of the Lake McCarrons wetland

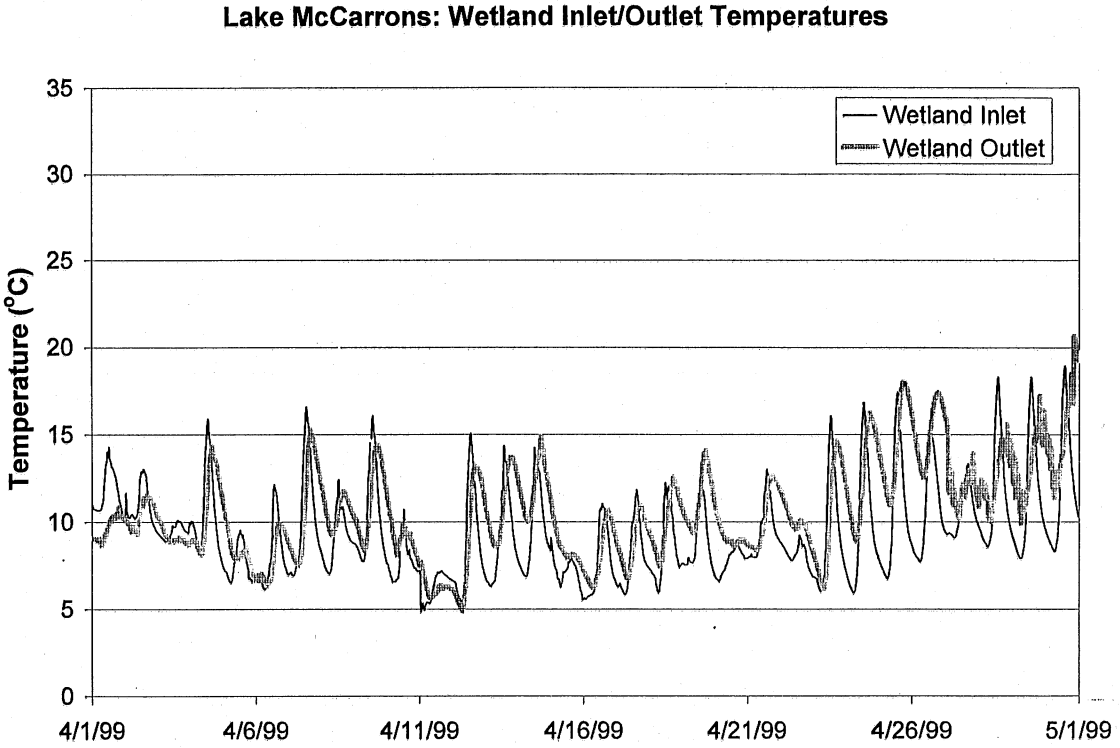

Figure V-6. (Cont'd) Water temperatures recorded (10-min averages) at the inlet and the outlet of the Lake McCarrons wetland

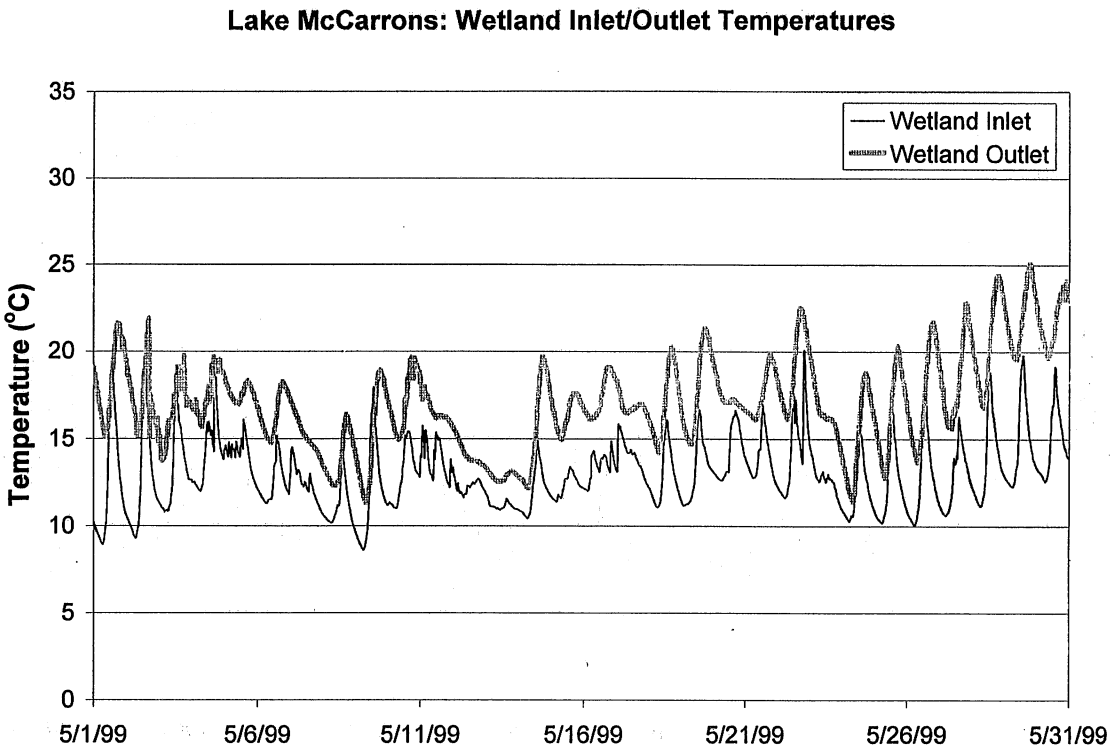

Figure V-6. (Cont'd) Water temperatures recorded (10-min averages) at the inlet and the outlet of the Lake McCarrons wetland

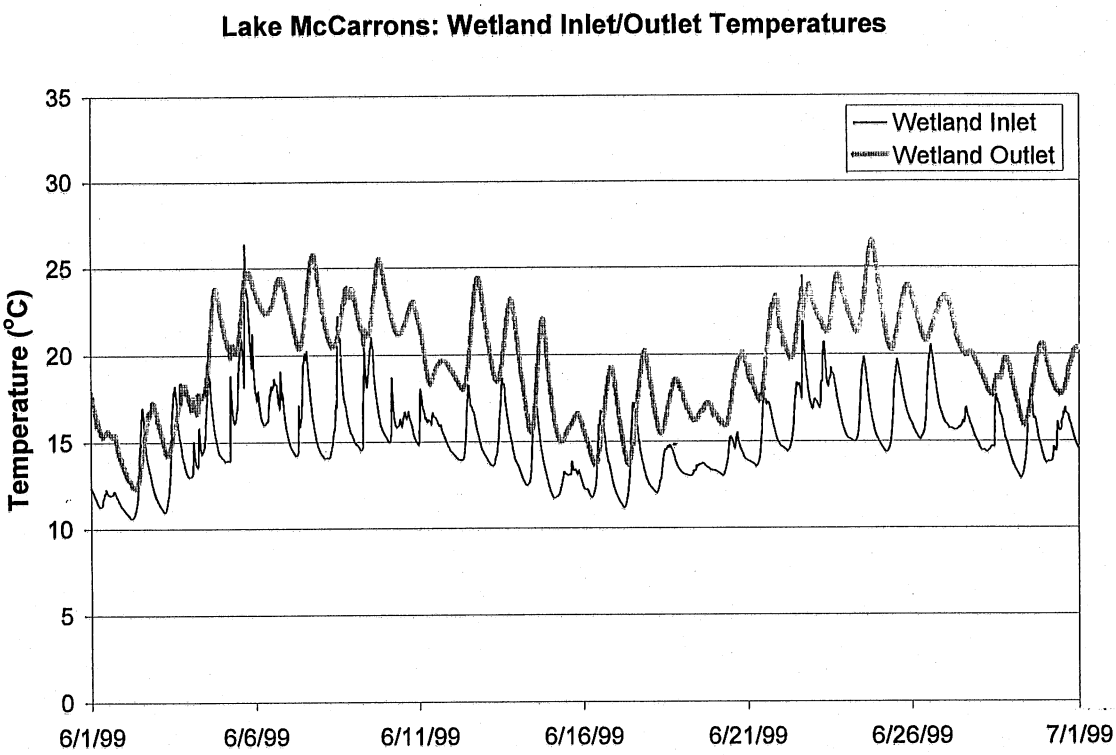

Figure V-6. (Cont'd) Water temperatures recorded (10-min averages) at the inlet and the outlet of the Lake McCarrons wetland

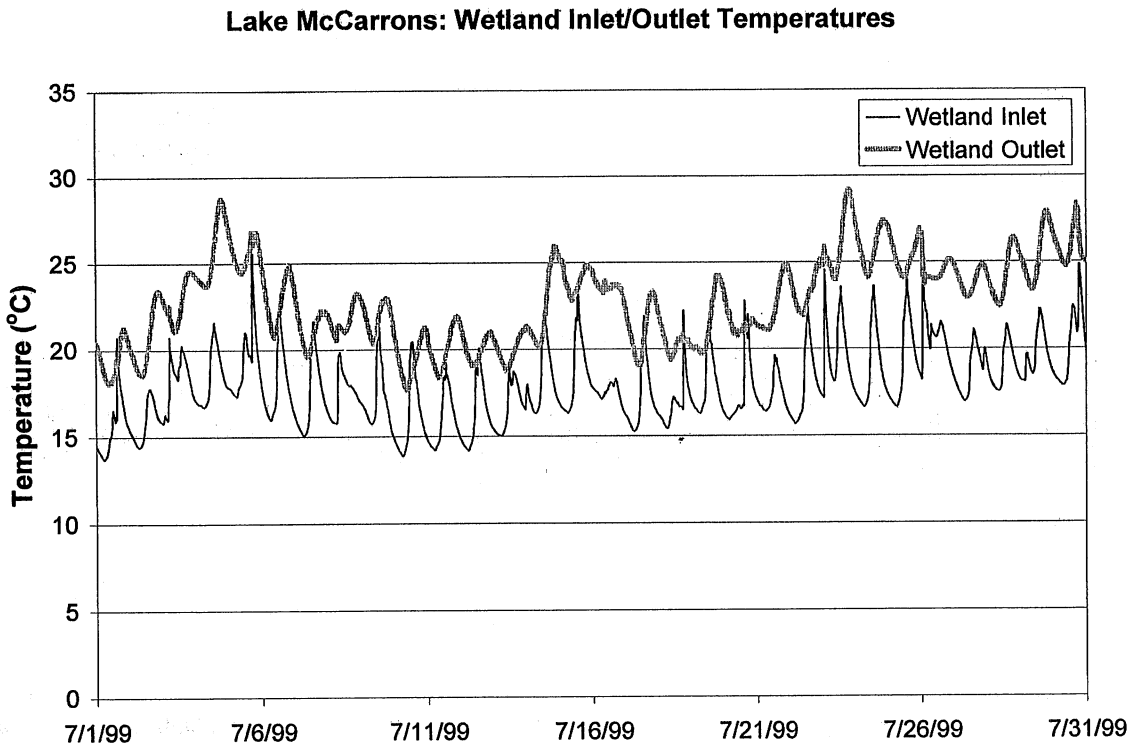

Figure V-6. (Cont'd) Water temperatures recorded (10-min averages) at the inlet and the outlet of the Lake McCarrons wetland

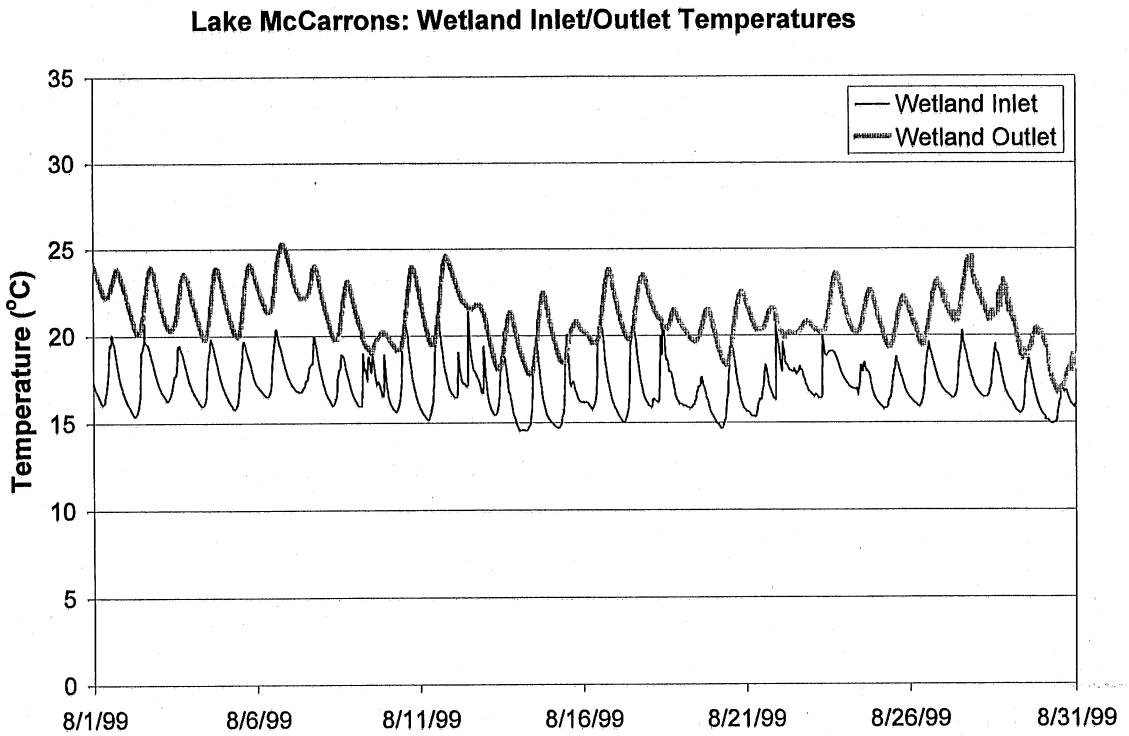

Figure V-6. (Cont'd) Water temperatures recorded (10-min averages) at the inlet and the outlet of the Lake McCarrons wetland

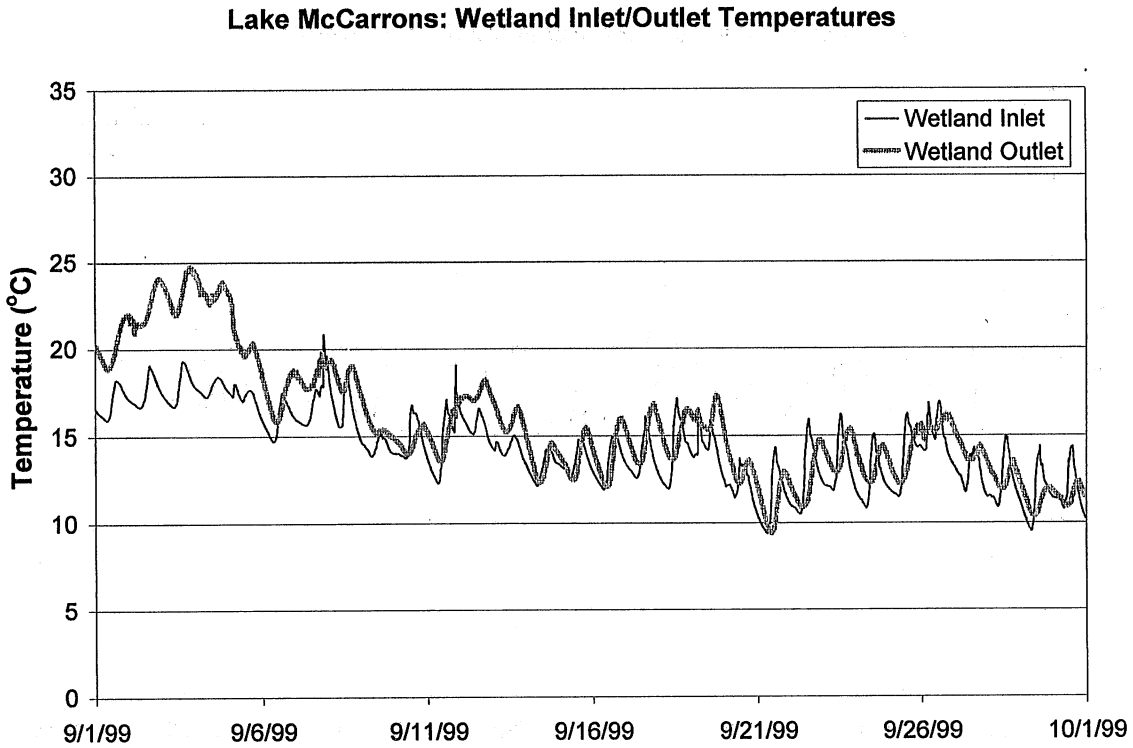

Figure V-6. (Cont'd) Water temperatures recorded (10-min averages) at the inlet and the outlet of the Lake McCarrons wetland

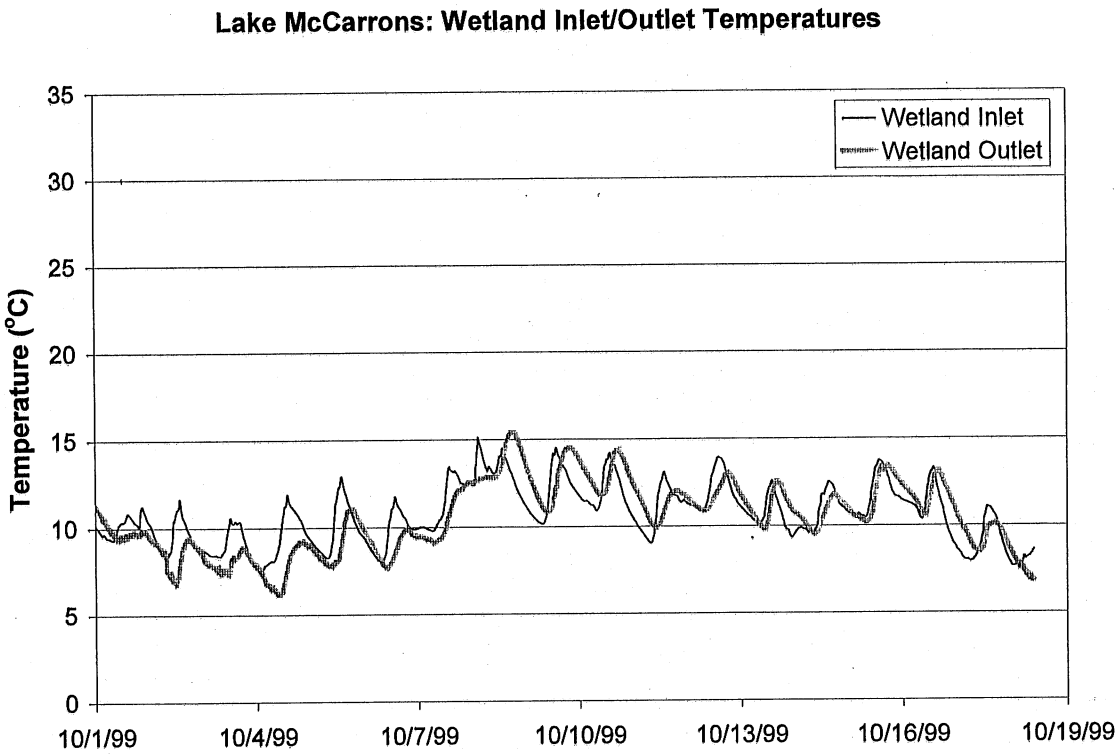

Figure V-6. (Cont'd) Water temperatures recorded (10-min averages) at the inlet and the outlet of the Lake McCarrons wetland

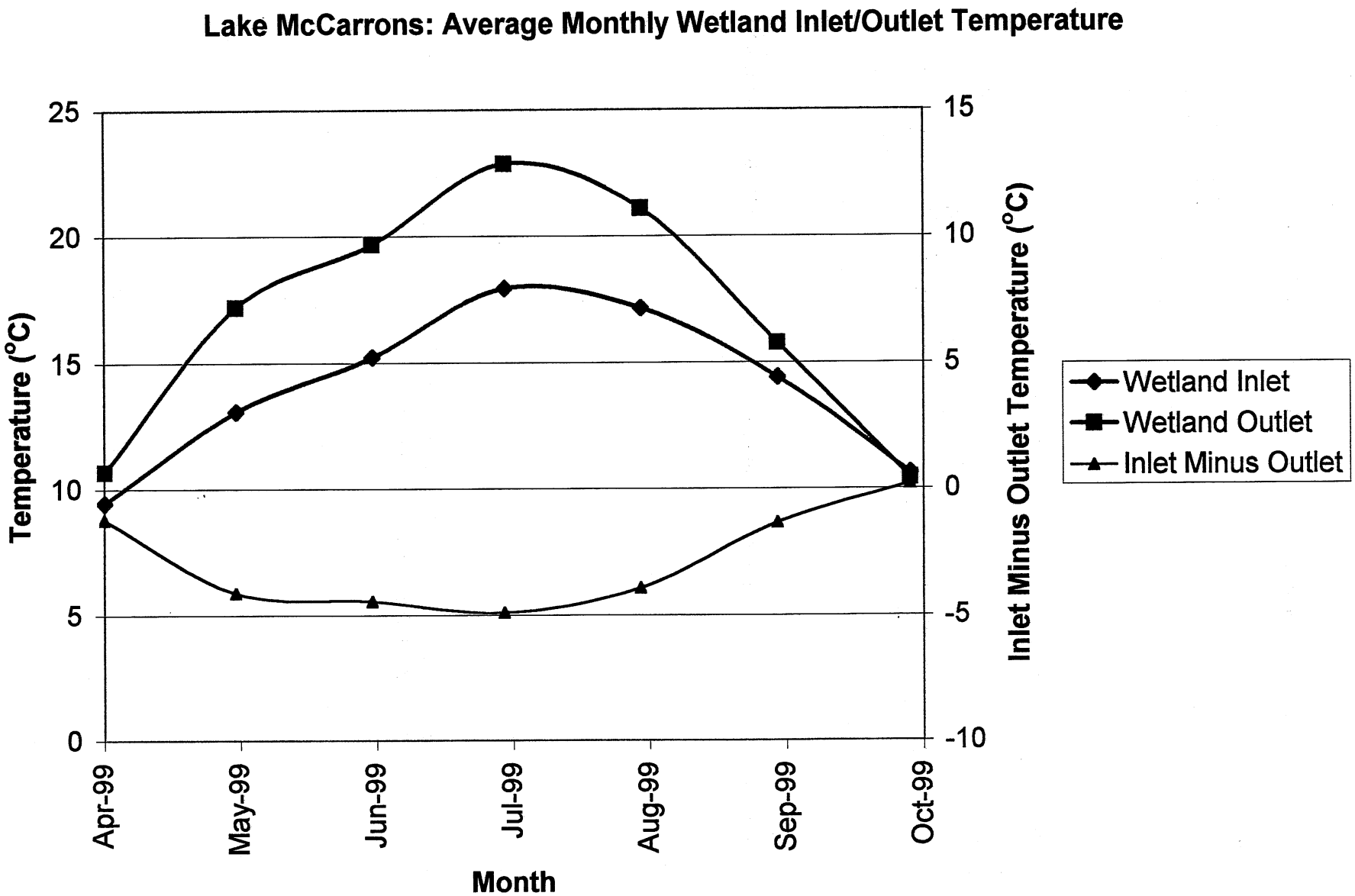

Figure V-7. Monthly average water temperature at the inlet and the outlet of the lake McCarrons wetland.

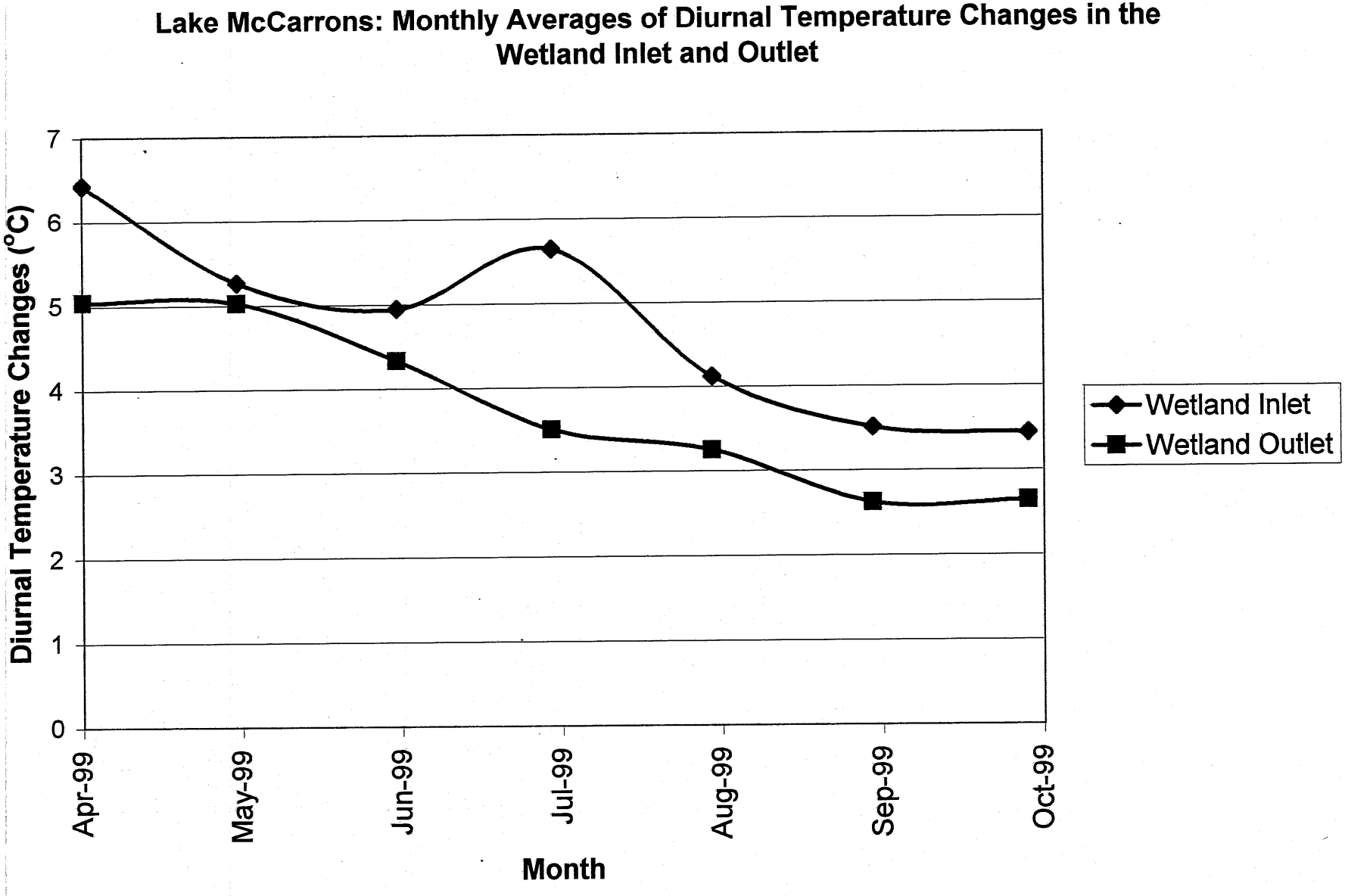

Figure V-8. Monthly average of the diurnal water temperature fluctuation at the inlet and the outlet of the Lake McCarrons wetland.

VI. LAKE TEMPERATURE DYNAMICS

The recorded average daily lake water temperature data for the entire summer period of 1999 are plotted in Figures VI-1 and VI-2. Daily averages were used to give the isotherm patterns in Figures VI-3 and VI-4. It is evident that a temperature stratification is established in the lake before the start of the record, i.e. April 29, and that it continues throughout the summer until the end of the record, i.e. October 18. A surface mixed layer of 2 m or less depth is established by the end of April and lasts until about the end of July, when the surface lake waters begin to cool. The surface mixed layer then deepens to 3 m until the beginning of September. From then on the surface mixed layer deepens rapidly due to surface cooling and the potential for algal blooms diminishes accordingly. The stratification/isotherm patterns shown in Fig. VI-3 are very similar to those observed in many previous years and shown in Appendix A.

The inflow from the wetland enters the lake in the littoral zone, and one may ask whether water temperatures measured in the center of the lake are representative of the littoral waters. To make that comparison, water temperatures were also recorded at a littoral station. The daily littoral water temperatures are shown in Figs. VI-2. The isotherms at the littoral location are plotted in Fig. VI-4. As can be seen, the temperature stratifications (isotherms) are very similar in Figs. VI-3 and VI-4. A minor difference is that surface mixed layer depths are slightly smaller in the littoral waters than in the center of the lake.

The short time scales have been suppressed in Figs. VI-1 to VI-4 by using daily average temperatures. A more dynamic picture is obtained by plotting the 10-min data against time (Fig. VI-5). Temperature variations on the order of 1 to 2°C are apparent in the bandwidth of each trace. Only at the greatest depths (14.6 m and 17 m) are the fluctuations less than 1°C. For most depths these fluctuations can be attributed to internal waves. Near the surface (0.1 m and 1.1 m depths) one can also identify a daily (periodic) heating and cooling pattern. Longer periodicities of several days duration are attributable to mesoscale weather system moving through the area. The data in Fig VI-4 are from the center (deeper part) of the lake. Those in the shallow littoral location (Fig. VI-6) are even more dynamic with daily temperature excursion up to 5°C at times due to the smaller thermal inertia of the shallow water.

The diurnal periodicities are made more clearly visible in Figs. VI-7 and VI-8 where only data for July have been plotted. Diurnal amplitudes are clearly seen only at water depths of 0.1 and 1.1 m in the center of the lake, and at water depths of 0.1, 0.3 and 0.6 m in the shallow littoral waters. Diurnal surface water temperature amplitudes in July are on the order of 2°C with a range from about 1 to 4°C in the center of the lake, and larger in the littoral water.

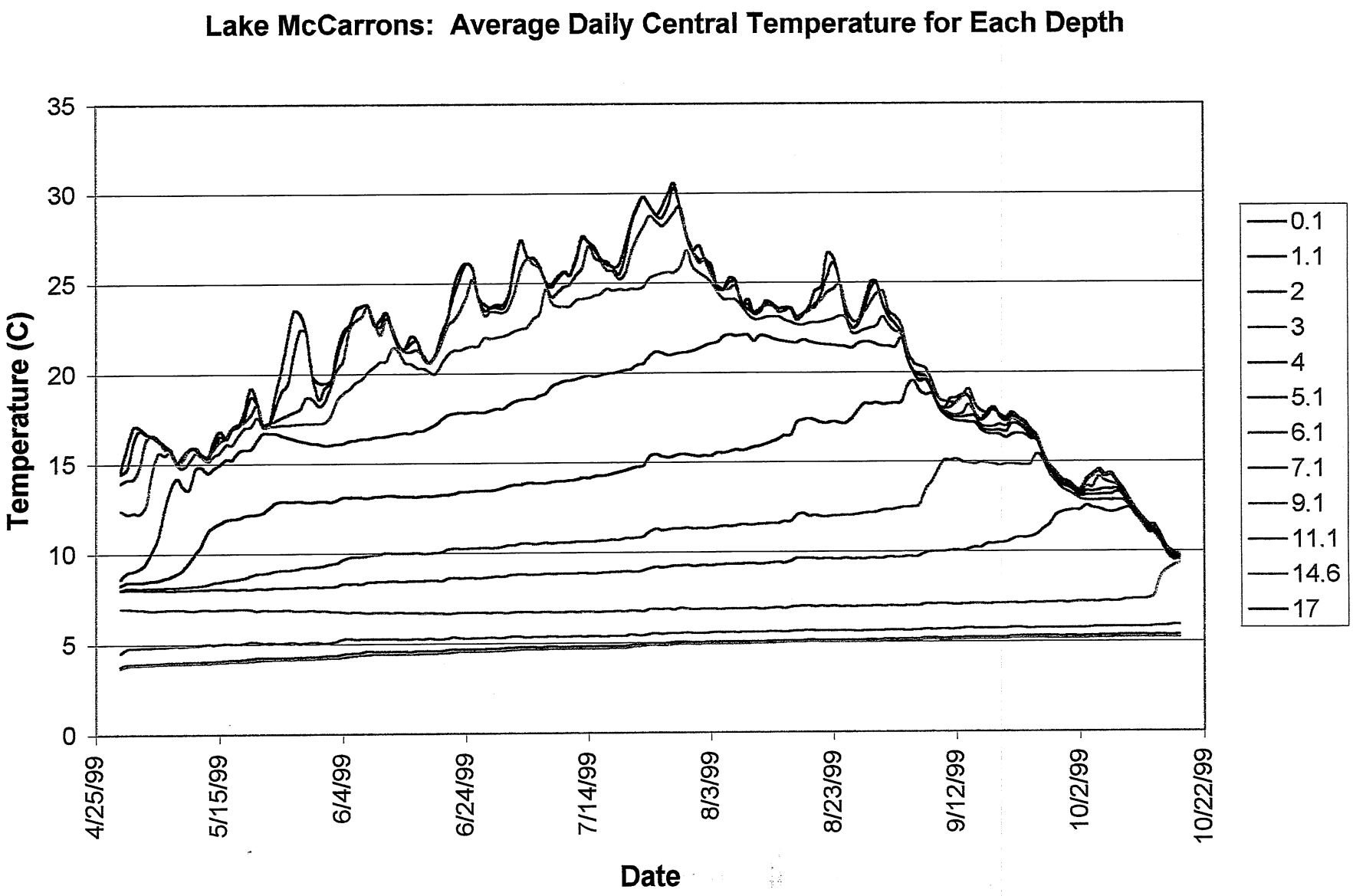

Figure VI-1 Daily average water temperature recorded at the central raft location at depths from 0.1 to 17.0 m.

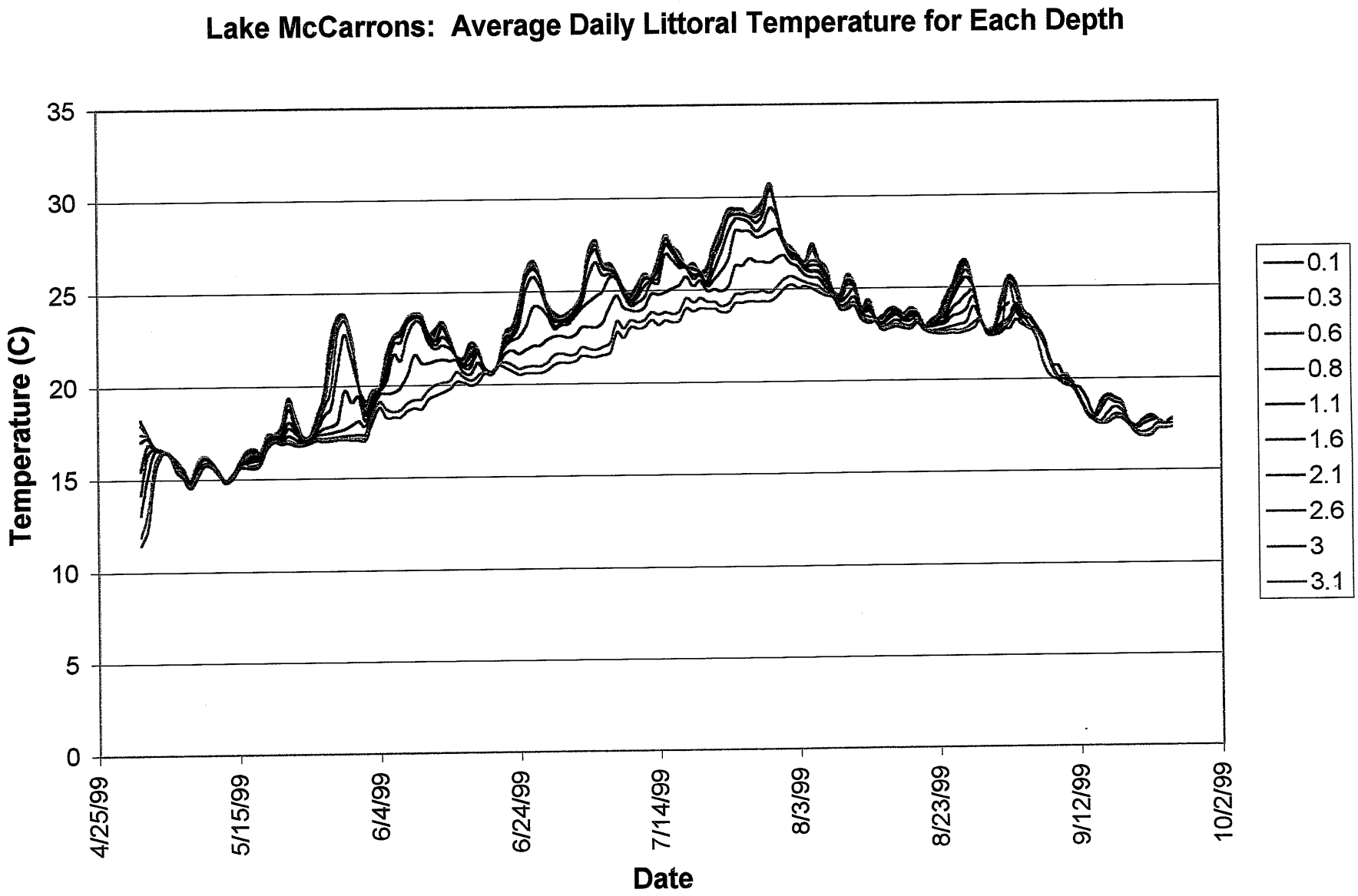

Figure VI-2 Daily average water temperature recorded at the littoral raft location at depths from 0.1 to 3.1 m.

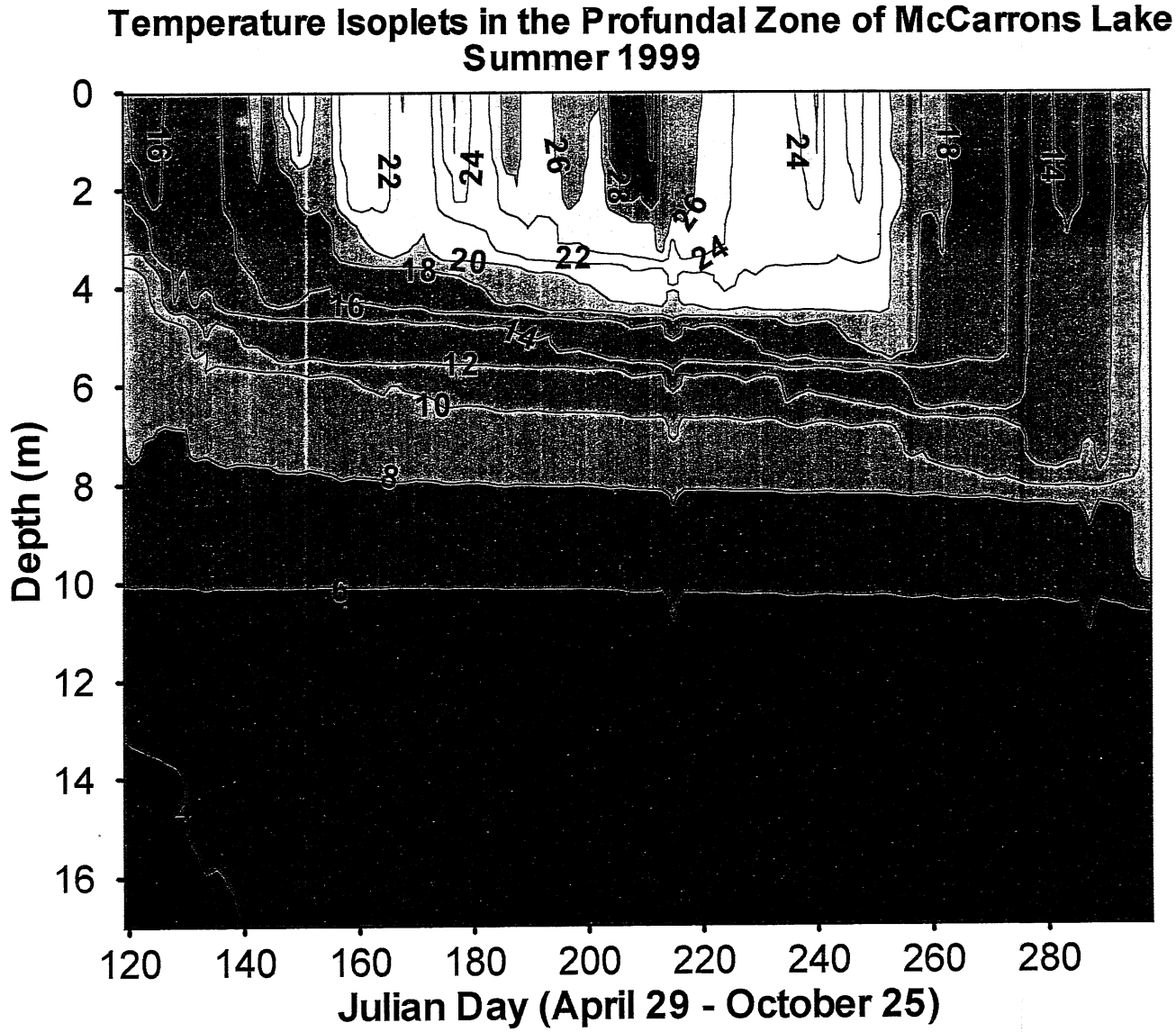

Figure VI-3 Isotherms in Lake McCarrons in 1999 (interpolated from average daily water temperatures). (Temperature in °C)

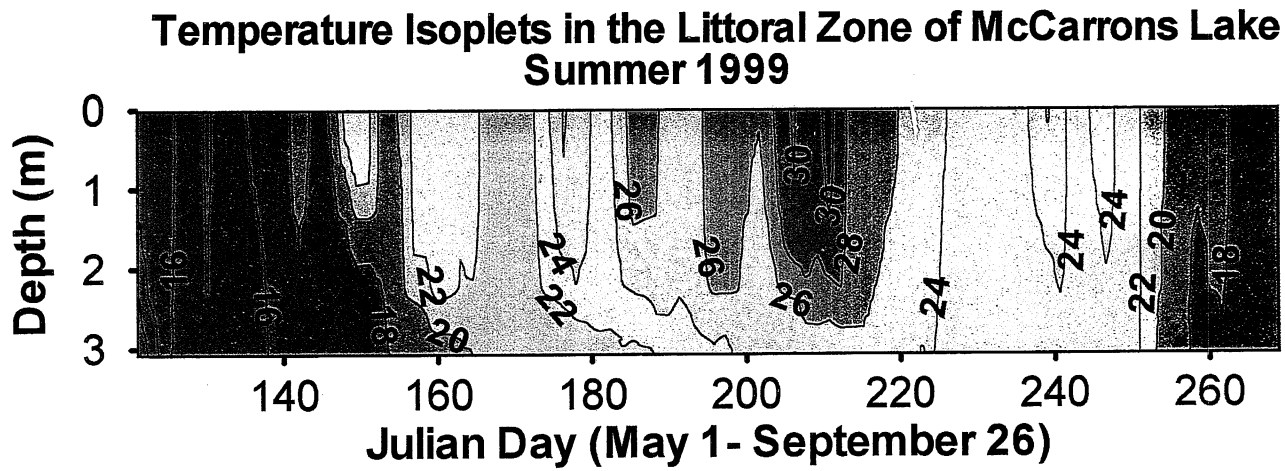

Figure VI-4 Isotherms in the littoral water of Lake McCarrons in 1999 (interpolated from average daily water temperatures). (Temperature in °C)

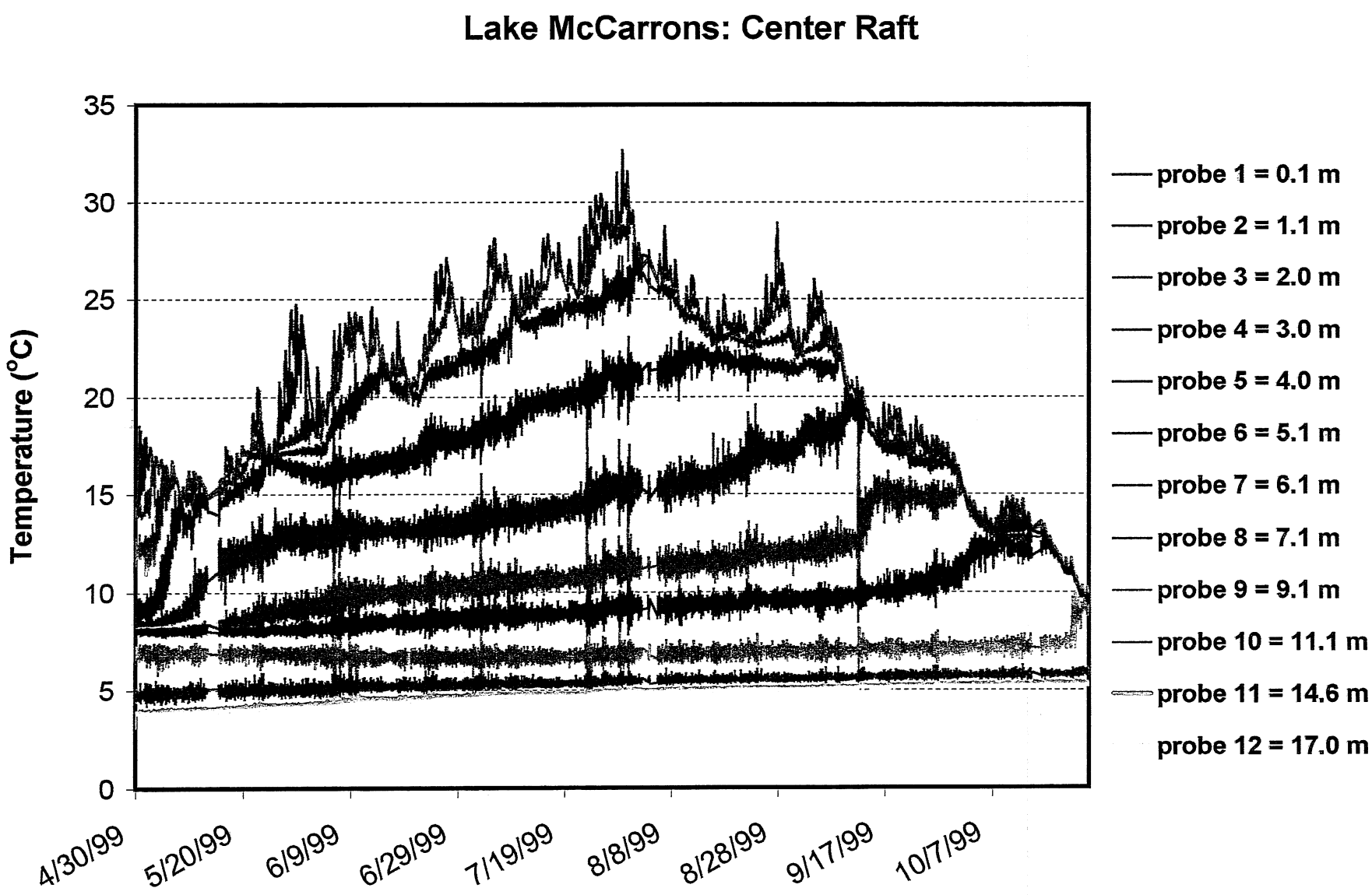

Figure VI-5 Water temperatures (10 minute averages at 12 depths) in Lake McCarrons in 1999.

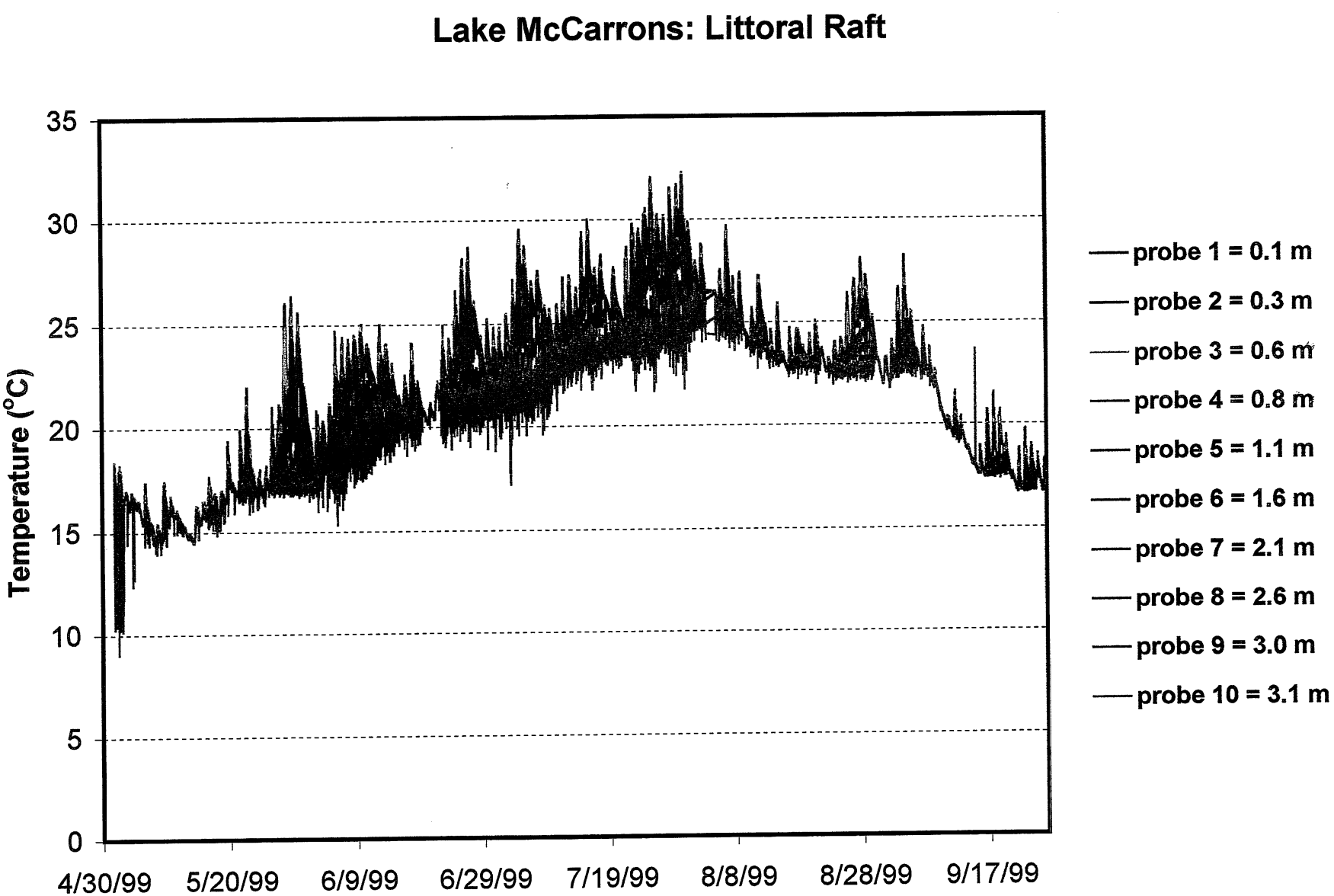

Figure VI-6 Water temperatures (10 minute averages at 10 depths) in the littoral waters of Lake McCarrons in 1999.

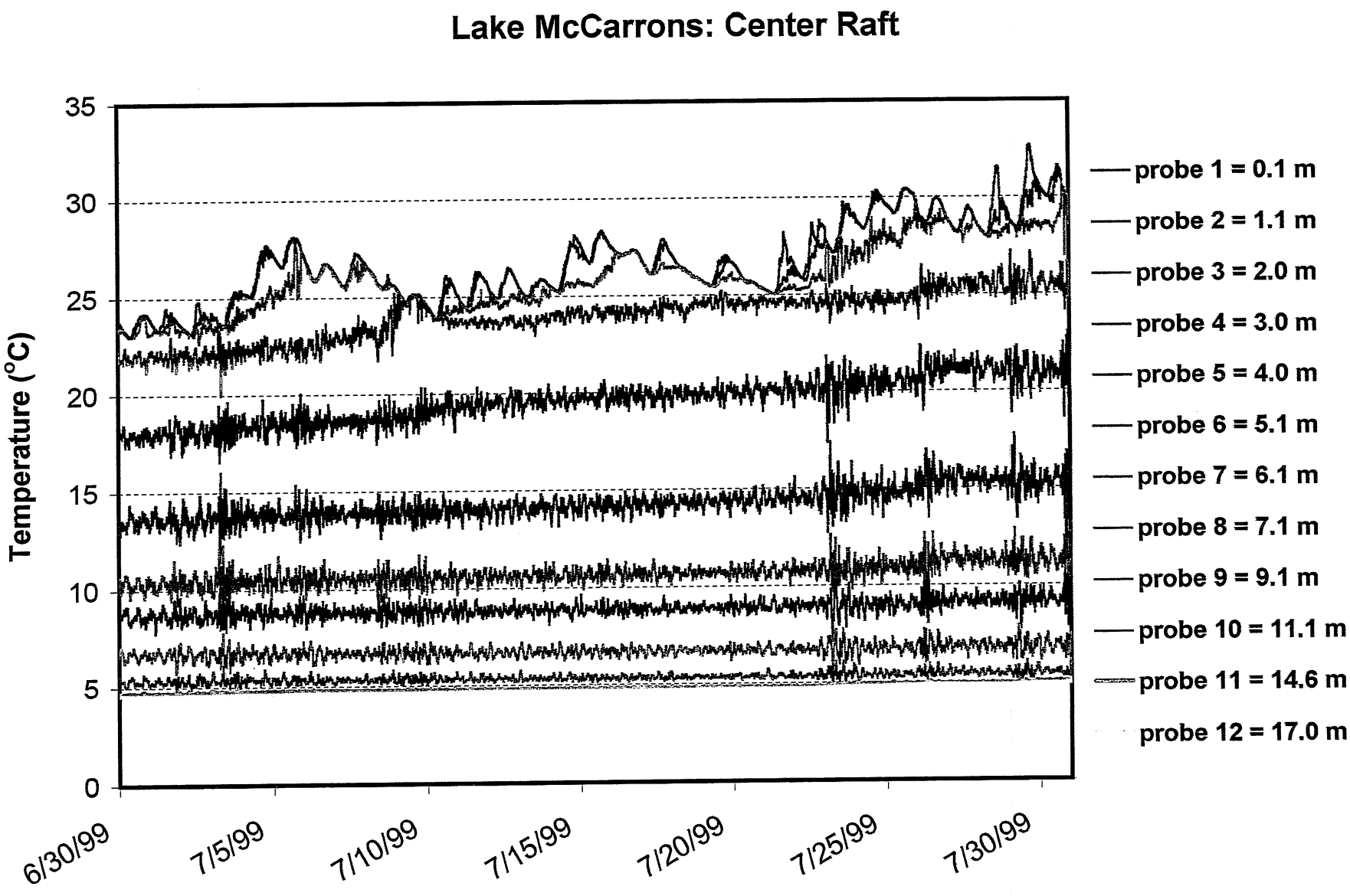

Figure VI-7 Water temperatures (10 minute averages at 12 depths) in Lake McCarrons in July 1999.

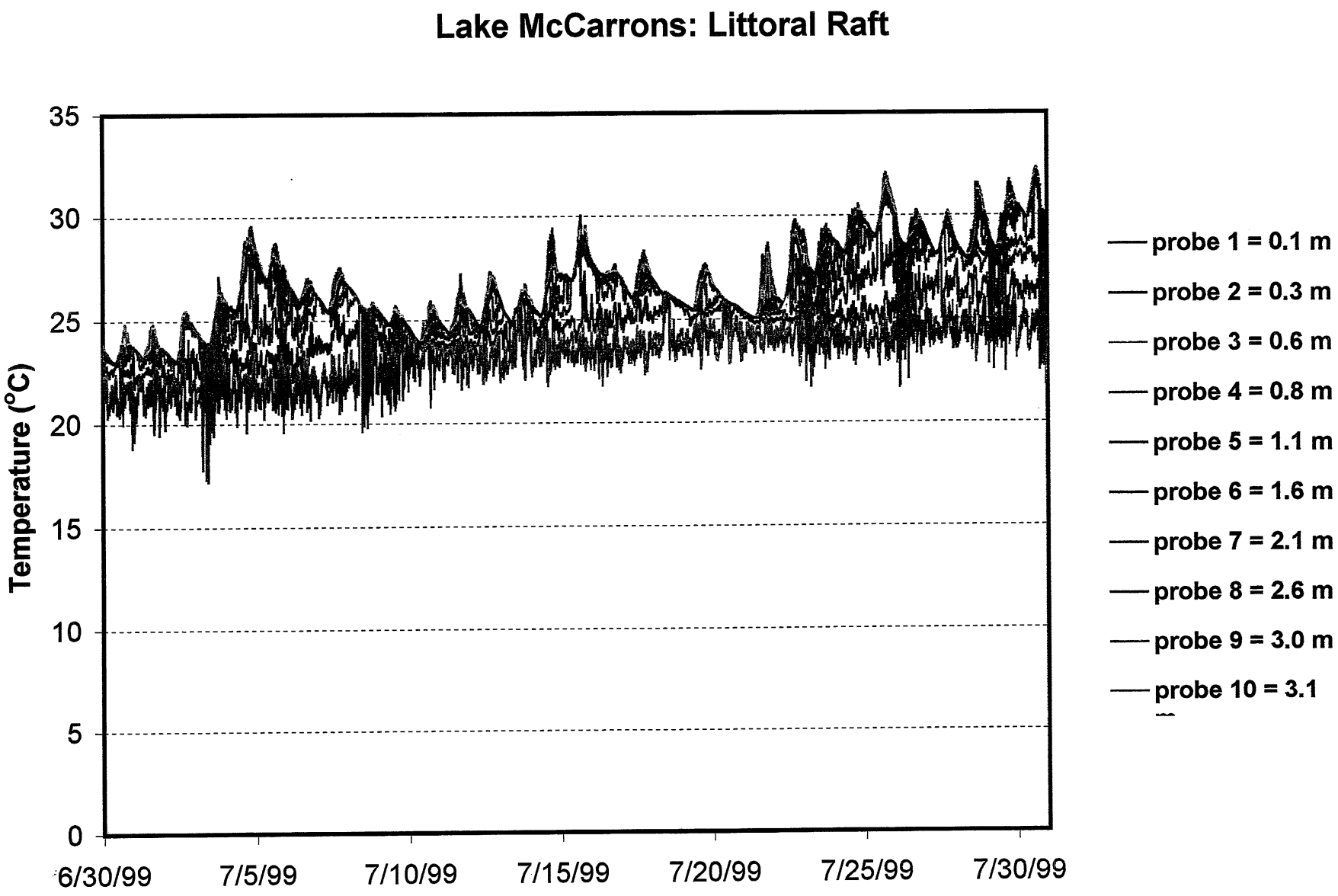

Figure VI-8 Water temperatures (10 minute averages at 10 depths) in the littoral waters of Lake McCarrons in July 1999.

A temporary deepening of the surface mixed layer from 2 m on May 4 to 4 m on May 8 is illustrated in Fig. VI-9. This event was driven by increased windspeeds during that period. Intermittent stratification and destratification of the littoral waters is shown in Fig. VI-10. Periods of stratification of littoral waters in Fig. VI-10 are usually associated with rising air temperatures and heating of the waters by atmospheric heat input; complete mixing of littoral waters in Fig. VI-10 coincides with falling air temperatures and/or higher windspeeds. This linkage is illustrated in Fig. VI-11 where air temperatures have been plotted in addition to water temperature. Windspeeds in m/s recorded on the littoral raft are also shown in Fig. VI-11. The effect of short time-scale dynamics on surface mixed layer dynamics throughout the summer is illustrated by the isotherm plots in Appendix F. Surface mixed layer depths are identified by the downward extent of isothermal warm water below the water surface.

Water temperature variations over a 24-hour period are substantial and found at all depths. To summarize their magnitude at different times of the season, the difference between the recorded daily maximum and minimum water temperatures were calculated and averaged by month. The mean monthly diurnal amplitudes are plotted by depth in Figs. VI-12 and VI-13.

Water temperature variations near the water surface (0 to 1.5 m) are attributable to daytime heating and night-time cooling. From 2 to about 6 m, i.e. in the thermocline, they are attributable to internal waves and intrusions. Below 6 m, i.e. in the hypolimnion, they are due to internal waves. As can be seen in Figure VI-12, diurnal amplitudes vary significantly with season and depth. Amplitudes are strongest on the lake surface and in the thermocline. During the lake warming season (through July) they are about equally strong at the surface and in the thermocline. After lake cooling begins (August), the diurnal water temperature fluctuations in the thermocline are the strongest. In the littoral waters (Fig. VI-13) the seasonal trend is inverse from the deep water (Fig. VI-12) and the amplitudes are larger.

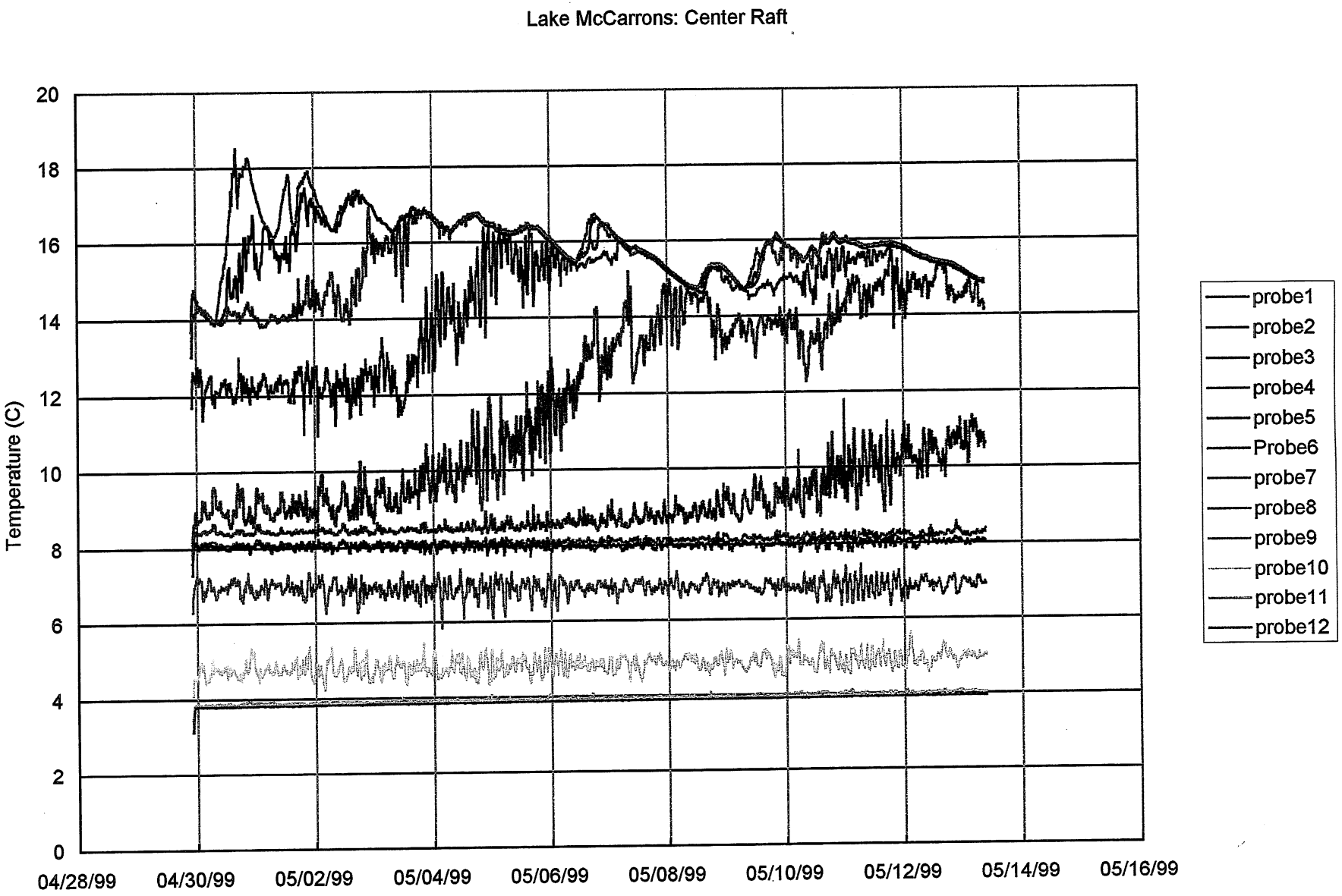

Figure VI-9 Water temperature time series illustrating a deepening of the surface mixed layer in Lake McCarrons April 30 and May 13, 1999.

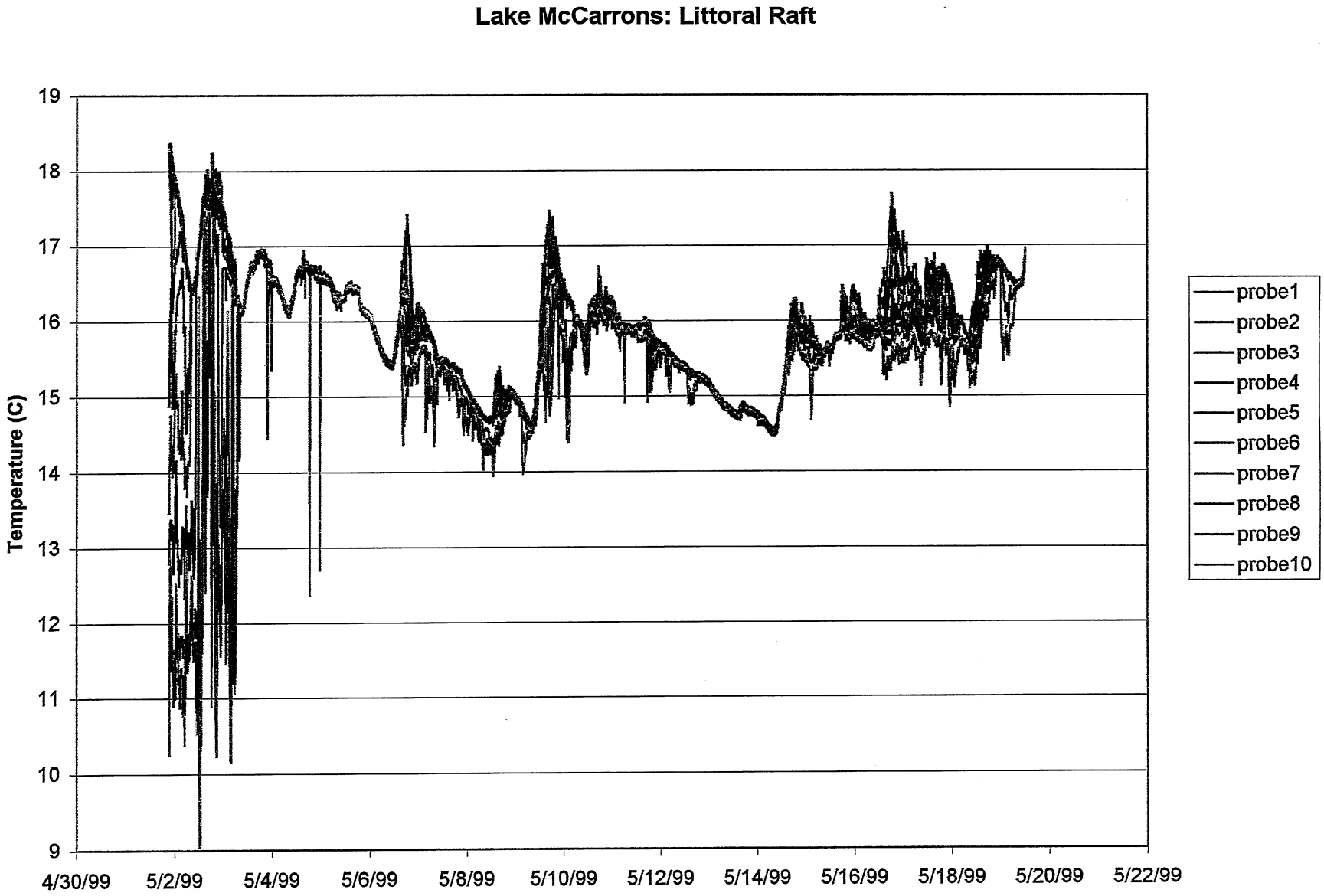

Figure VI-10 Water temperature time series illustrating sequences of stratification and mixing in the littoral waters Of Lake McCarrons in May 1999.

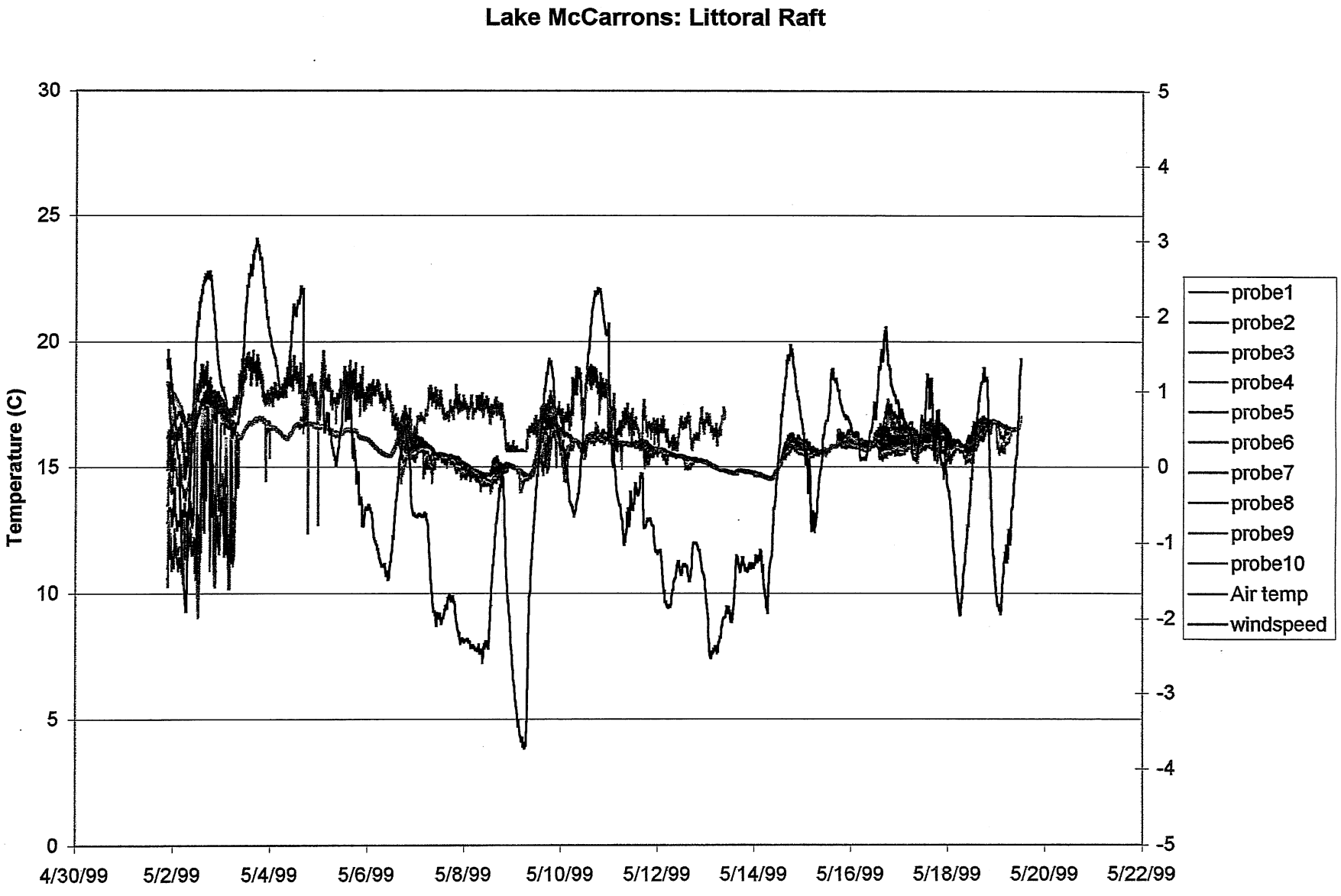

Figure VI-11 Air temperatures and windspeeds (m/s) added to Figure VI-10.

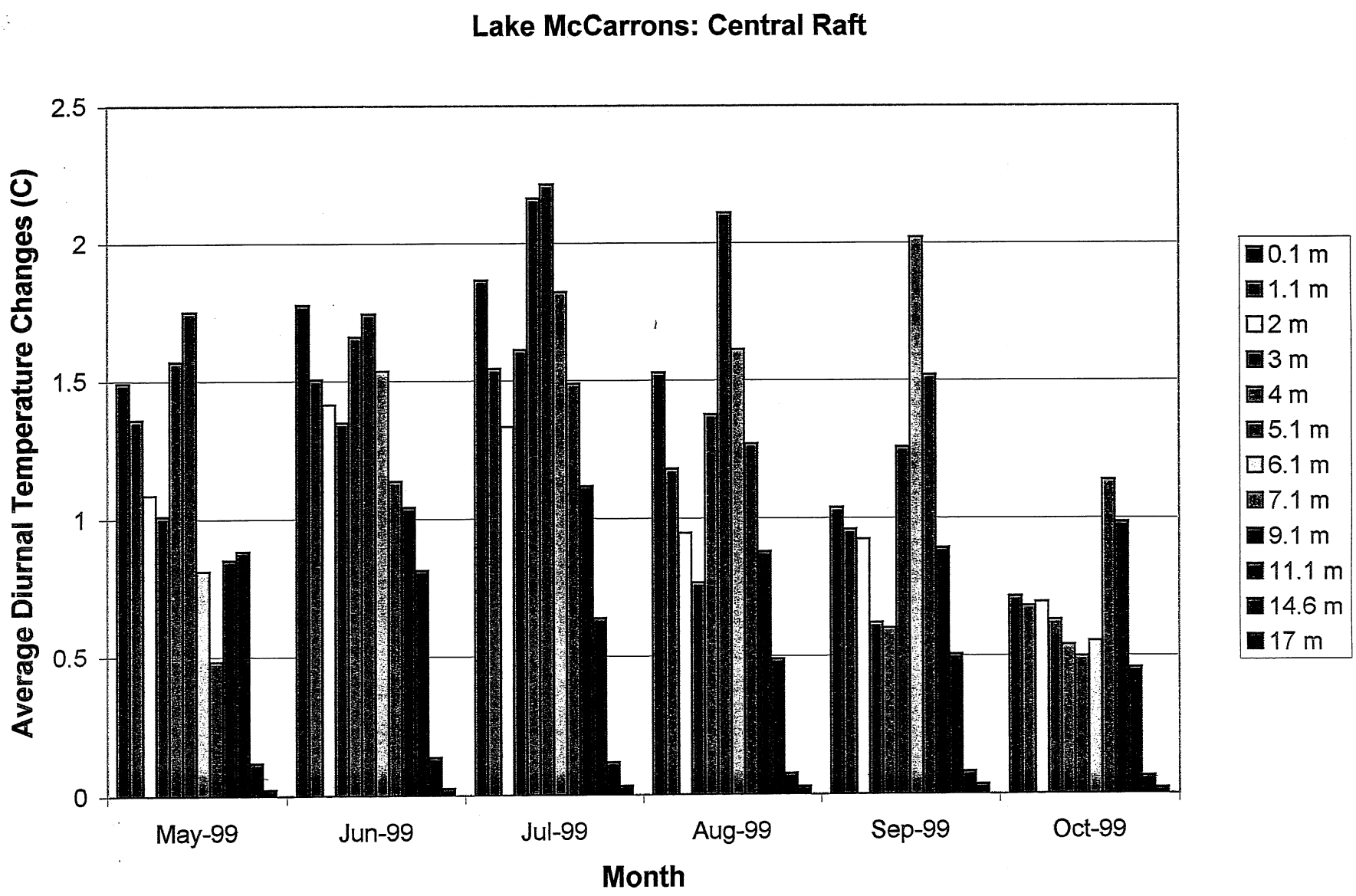

Figure VI-12 Monthly average of the diurnal water temperature change at the central raft location at depths from 0.1 to 17.0 m.

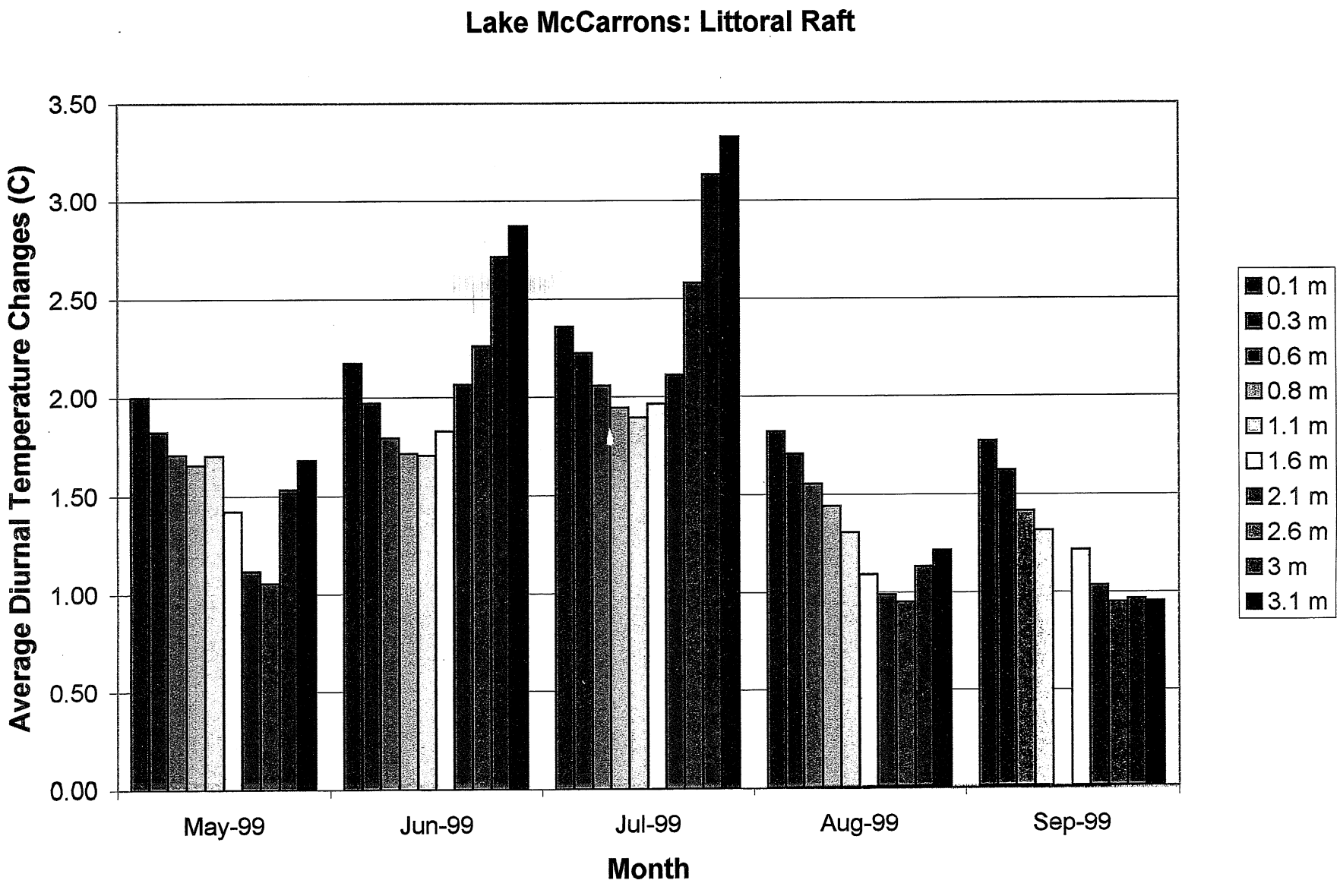

Figure VI-13 Monthly average of the diurnal water temperature change at the littoral raft location at depths from 0.2 to 17.0 m.

VII. SIMULATIONS OF PHYTOPLANKTON GROWTH DYNAMICS

1. Concept

Projecting the direct impact of inflow modification or other management alternatives requires identification and quantification of ecological responses to nutrient loading, light availability, mixing, etc. A numerical simulation model is available for this purpose and will be briefly described.

2. Model Development

MINLAKE98 (Figure VII-1) simulates a lake as a series of stacked layers of varying thickness. The layers include snow, ice, water and sediment. Each of the water layers is considered well mixed. All of the water layers are in contact with the sediment of the lake. Only the surface layer is in contact with the atmosphere during the open water season. A schematic diagram of the water mass balance for the entire lake used in MINLAKE98 is presented in Figure VII-2. A description of subsections of the MINLAKE98 model (West and Stefan, 1999) are reproduced in Appendix E.

3. MINLAKE98 Model Application to Lake McCarrons

3.1. Data base

Lake McCarrons was extensively monitored from 1982 to 1997 (Table VII-1) by the Metropolitan Council. The field data were retrieved from the EPA database STORET.

Inflow rates from the wetland were calculated from rainfall data or from water level measurements at the outflow gage. Inflow temperature and phosophorus concentrations were from records; dissolved oxygen was set to the saturated value, and BOD to 11 mg/L. Suspended and dissolved solids, silica, nitrate + nitrite, and ammonia were set to 0.0 mg/L, as these parameters were not simulated.

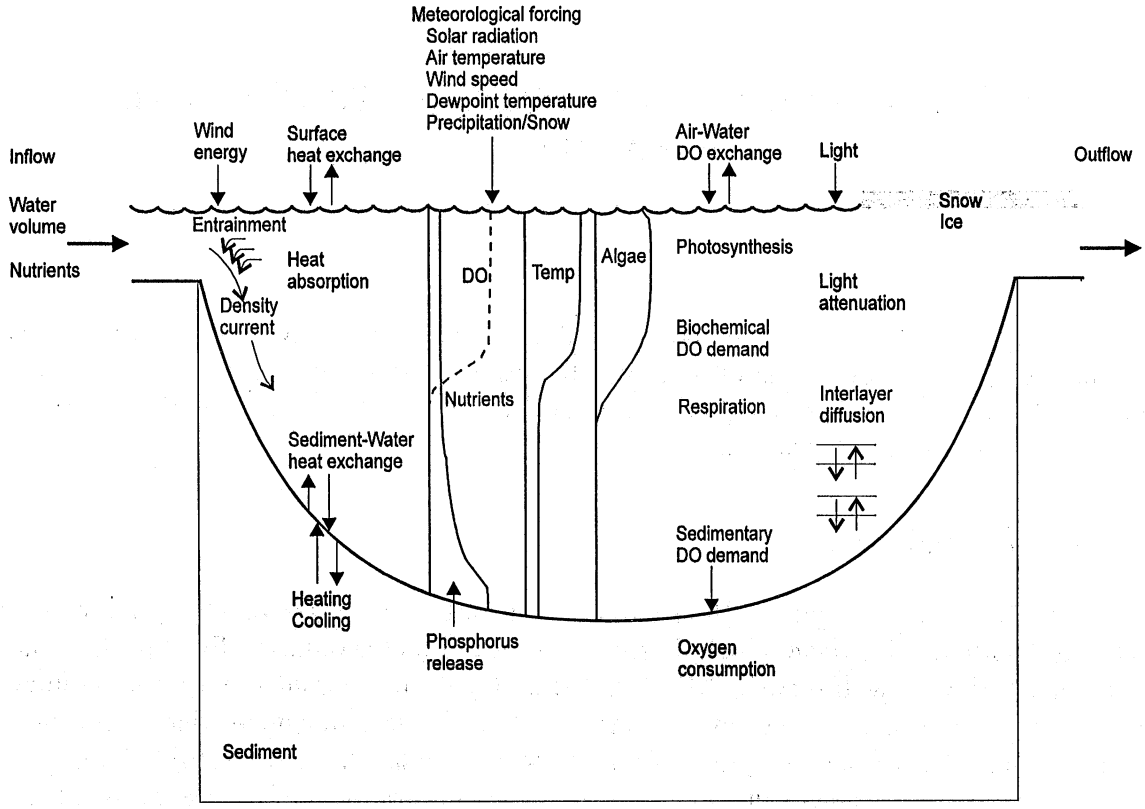

Figure VII-1. Schematic representation of processes in MINLAKE 98.

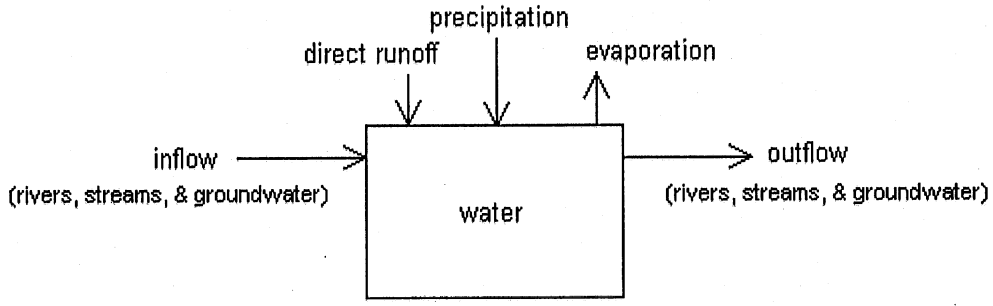

Water Mass Balance

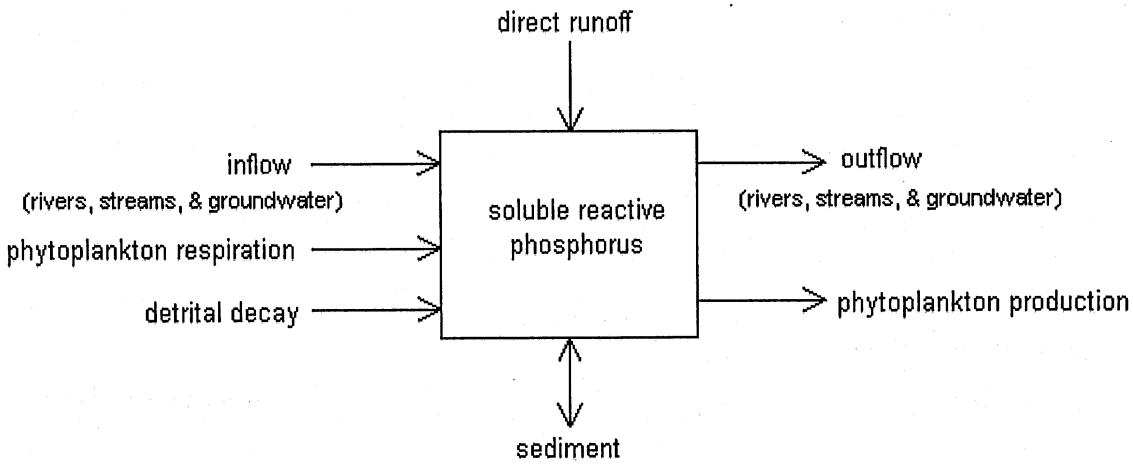

Phosphorus Mass Balance

Figure VI-2. Whole lake mass balance diagrams for MINLAKE98.

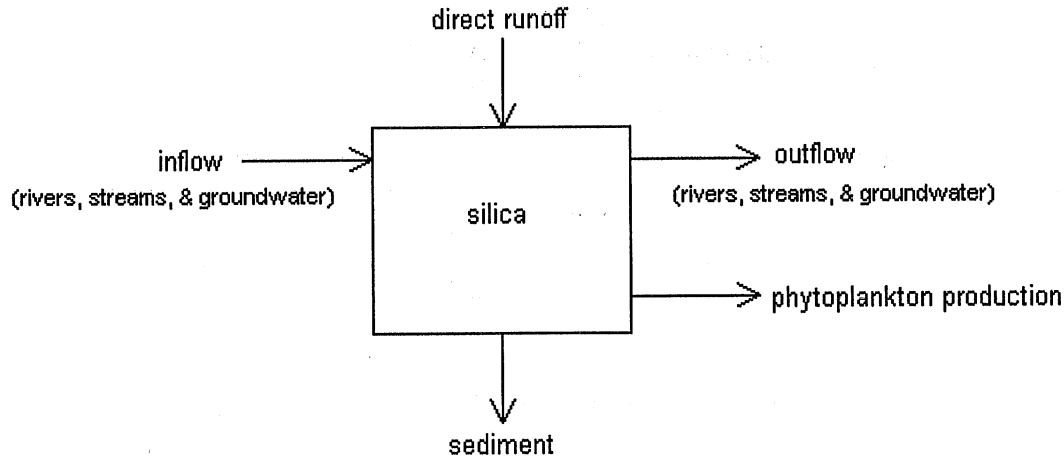

Silica Mass Balance

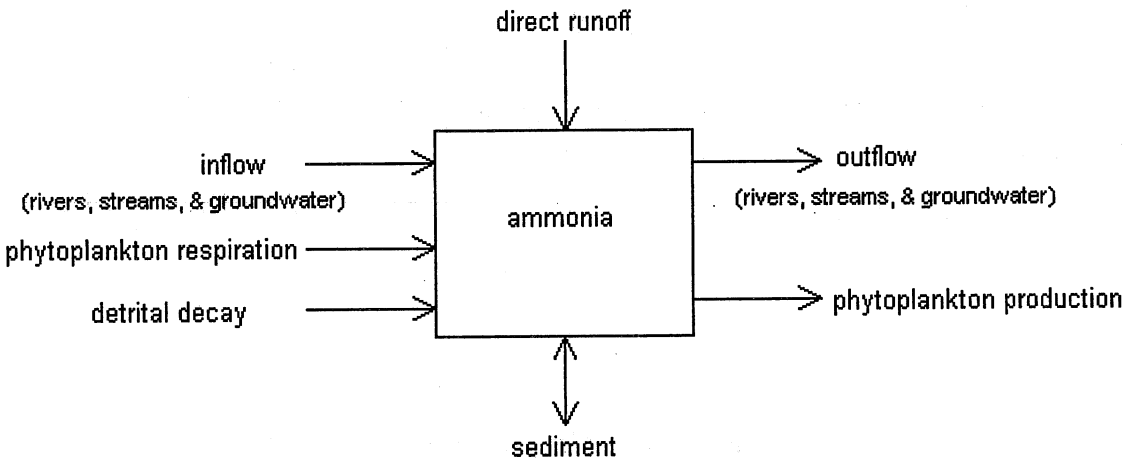

Ammonia Mass Balance

Figure VI-2. (Cont'd) Whole lake mass balance diagrams for MINLAKE98.

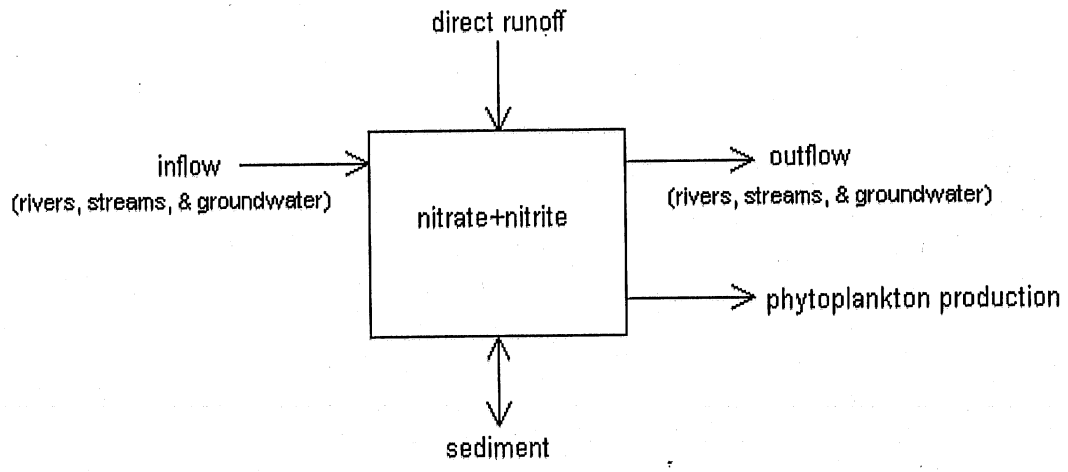

Nitrate+Nitrite Mass Balance

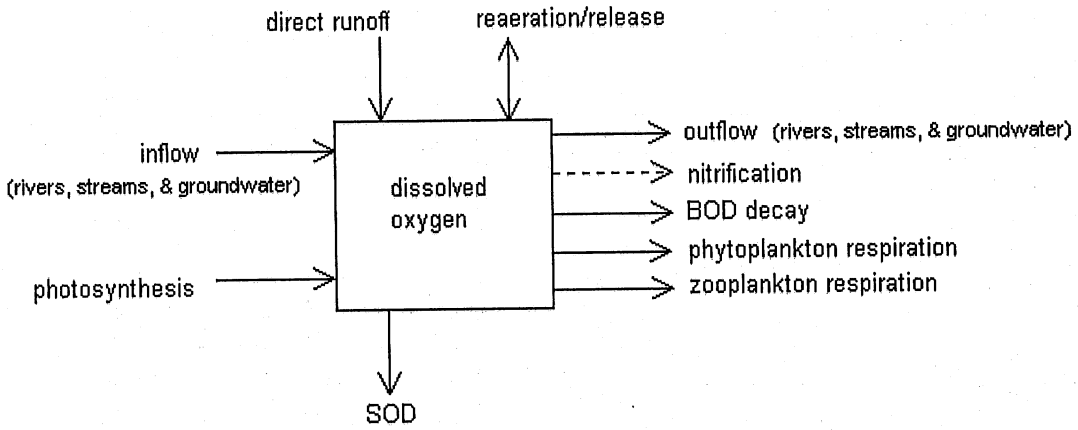

Dissolved Oxygen Mass Balance

Figure VI-2. (Cont'd) Whole lake mass balance diagrams for MINLAKE98.

3.2. N:P Ratio for Lake McCarrons

The nitrogen to phosphorus ratios (N:P) for Lake McCarrons were computed using total nitrogen and total phosphorus. (Concentrations for the bioavailable forms are not available.) The total nitrogen was estimated using the sum of total Kjeldahl nitrogen (which consists primarily of organic nitrogen and ammonia) and nitrate + Nitrite measurements. The average TN:TP ratio for 1993 to 1997 was 29 ± 13 (Table VII-1). In Figure VII-3 the individual TN:TP ratios for 1993 to 1997 and in Figure VII-4, the individual TN:TP ratios for 1984 to 1997 are presented. Ratios of N:P greater than 20 are considered to reflect phosphorus limited systems and ratios of N:P less than 5 are considered to reflect nitrogen limited systems (gray dashed lines in Figures VII-3 and VII-4, Thomann and Mueller, 1987, p. 401). Figure VII-3 shows a general trend of an increasingly phosphorus limited system, i.e. the lowest measured TN:TP ratios increase with time (Table VII-2). Lake McCarrons is currently a phosphorus limited lake.

Table VII-1. Number of Field Measurements in Lake McCarrons.

Year	Number of Dates	Temperature	DO	TP	Chla	Secchi
1984	12	197	197	33	12	11
1985	25	350	360	125	44	21
1986	17	260	260	84	23	17
1987	19	358	358	93	38	19
1988	22	396	296	110	33	22
1989	19	348	260	83	21	19
1990	20	3886	281	87	27	20
1991	16	306	251	80	17	16
1992	7	106	106	34	14	6
1993	21	371	371	83	28	21
1994	20	359	361	77	27	20
1995	24	476	176	100	32	24
1996	23	431	430	92	34	23
1997	9	124	136	39	15	9

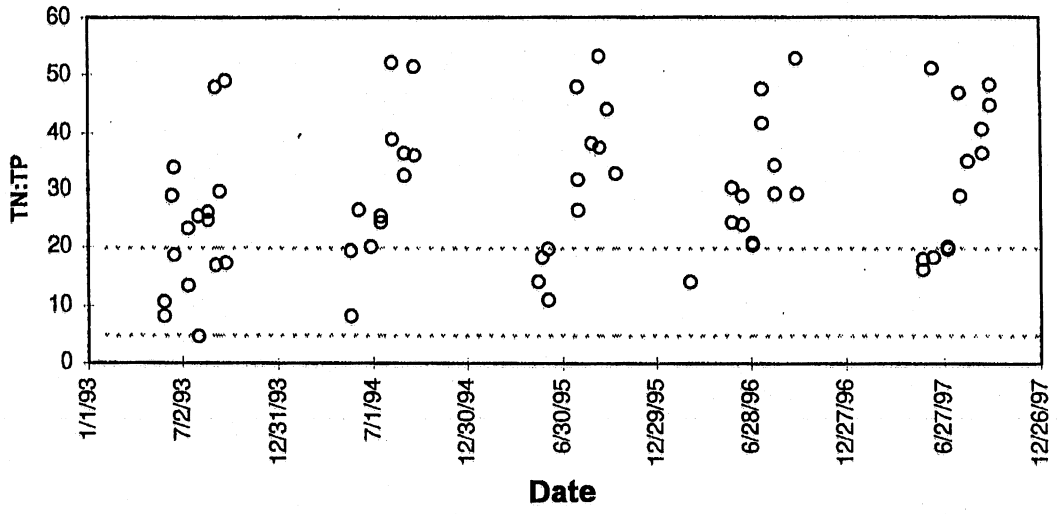

Figure VII-3. Total nitrogen to total phosphorus in Lake McCarrons for 1993 to 1997.

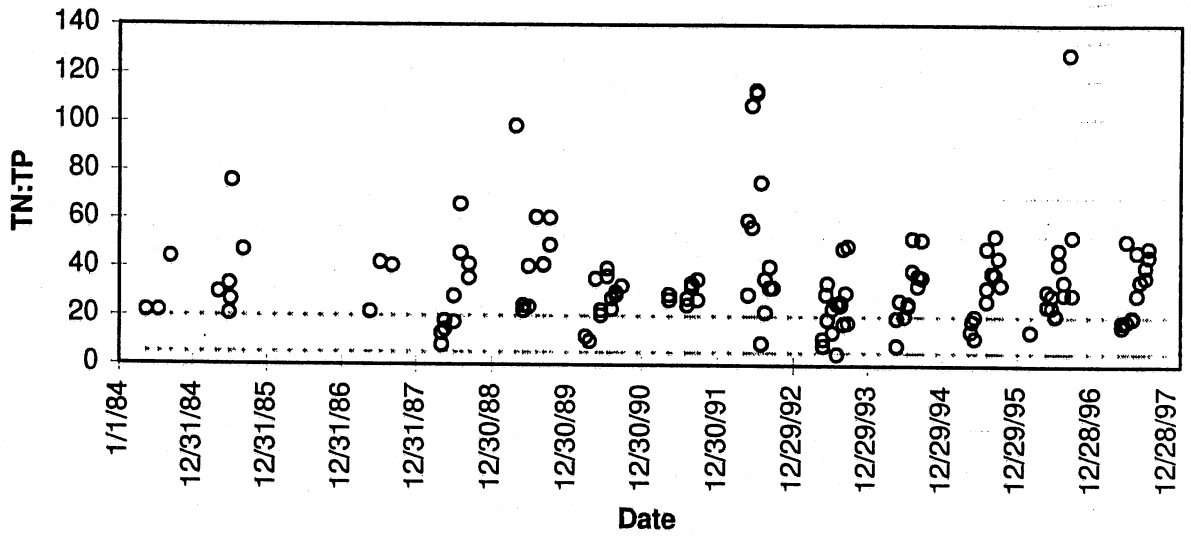

Figure VII-4. Total nitrogen to total phosphorus ratios in Lake McCarrons for 1984 to 1997.

Table VII-2. Total Nitrogen to Total Phosphorus Ratios in Lake McCarrons (1993 to 1997).

Year	Mean ± Standard Dev.	Lowest Value
1993	24 ± 13	4
1994	31 ± 13	8
1995	31 ± 14	11
1996	31 ± 11	14
1997	33 ± 13	16
Mean	29 ± 13	

3.3. Calibration

Simulation of daily water quality profiles was made for the period April 1995 - October 1996. The inflow data were made available by MCES (Oberts and Jensen, personal communication). The model was calibrated using field data. MINLAKE 98 contains some rate coefficients that need to be adjusted to simulate a specific lake. Calibration was based on both statistical and visual comparison with the field data for 1995 and 1996. The simulation results are given in a separate report (West-Mack and Stefan, 2000).

VIII. CONTROL STRATEGIES FOR PRODUCTIVITY

To control primary productivity in Lake McCarrons emphasis has been placed in the past on phosphorus input controls. Another option is to impose a light limitation by artificial deepening of the surface mixed layer.

1. Effect of Mixed Layer Deepening on the Phytoplankton Standing Crop

Increasing the surface mixed layer depth by artificial mixing during the summer stratification period reduces the exposure of algae to light and therefore the standing crop. Oceanographers (Denman et al., 1973) have observed an inverse relationship between phytoplankton concentrations and surface mixed layer depths. Stefan, Skoglund and Megard (1976) and Megard (1978) established a similar relationship for freshwater lakes.

The relationship can be put in the form

$$C_E = \frac{a}{h} - b \qquad \text{(VIII-1)}$$

where C_E = equilibrium concentration of phytoplankton standing crop

h = surface mixed layer depth

a,b = coefficients

$$a = \frac{I_o}{K_\ell k_c}\left(\frac{r_1}{r_2} - 1\right)$$

$$b = \frac{k_w}{k_c}$$

I_o = incident solar irradiance (PAR)

K_ℓ = Michaelis-Menton coefficient for light

k_c = specific radiation attenuation per unit algal concentration

k_w = radiation attenuation coefficient of lake water without algae

r_1 = nutrient and temperature limited growth coefficient

r_2 = loss coefficient for respiration and grazing

To illustrate specifically the influence of mixed layer depths h on standing crops of algae, sample computations are presented in Figure VIII-1 for a eutrophic lake. Results show that only small mixed layer depths support large standing crops of phytoplankton (large C_E values in Figure VIII-1. The second most important parameter is insolation expressed through I_o, and the third is nutrient loading expressed through r_1.

In everyday language this means that sunny and calm weather is required for several days to produce undesired algal blooms. A plot such as presented in Figure VIII-1 can be used to read equilibrium populations for given values of h, I_o, r_1, and r_2. Typically, values of $I_o/K_1[(r_1/r_2) - 1]$ are larger than one. Values above approximately three are typical for algal blooms.

It is therefore possible to control algal growth by artificial deepening of the surface mixed layer. Control of algae growth by artificial mixing has been practiced in South African water supply reservoirs, but has not been applied to natural lakes. Simulations for example in Figure VIII-2 for Lake Calhoun, have shown that artificial deepening of the surface mixed layer is theoretically very effective in controlling phytoplankton growth. Maintaining surface mixed layer depths at 6 m to 8 m depth is sufficient to limit algae growth by self-shading (light limitation). Jet mixing devices to do this are energy efficient and relatively simple, but require some maintenance. Simulations such as shown in Figure VIII-2 can also be made for Lake McCarrons. The amount of energy required for the mixing can be calculated (Gu and Stefan, 1988; Stefan and Gu, 1991, 1992) and is not excessive.

If the phytoplankton concentration in a lake is decreased, its transparency is increased. This inverse relationship is shown for Lake McCarrons in Fig. VIII-3. Higher transparency is usually desired for recreational lake uses. Figure VIII-3a shows the plot of Secchi depths vs. chlorophyll concentrations for Lake McCarrons using field data from 1984 to 1996. Figure VII-3b shows the correlation between Secchi depth and chlorophyll-*a* concentration. The resulting relationship is

$$\log_{10} \text{Secchi depth} = -0.5096 \log_{10} [\text{chl } a] + 0.8825 \qquad \text{(VIII-2)}$$

It is similar to that given by Rast and Lee (1978) for other natural water bodies.

2. Control of Phytoplankton Standing Crop by Phosphorus Management

In the reports by Osgood (1988, 1989) and Oberts and Osgood (1988), one can find a considerable amount of information and discussion of the potential options and effects of phosphorus management on phytoplankton growth in Metropolitan area lakes in general and Lake McCarrons specifically. Here we shall use the lake water quality model MINLAKE98 to explore several options for phosphorus reduction in Lake McCarrons sand their potential effects on phytoplankton standing crops. Strategies that were considered are:

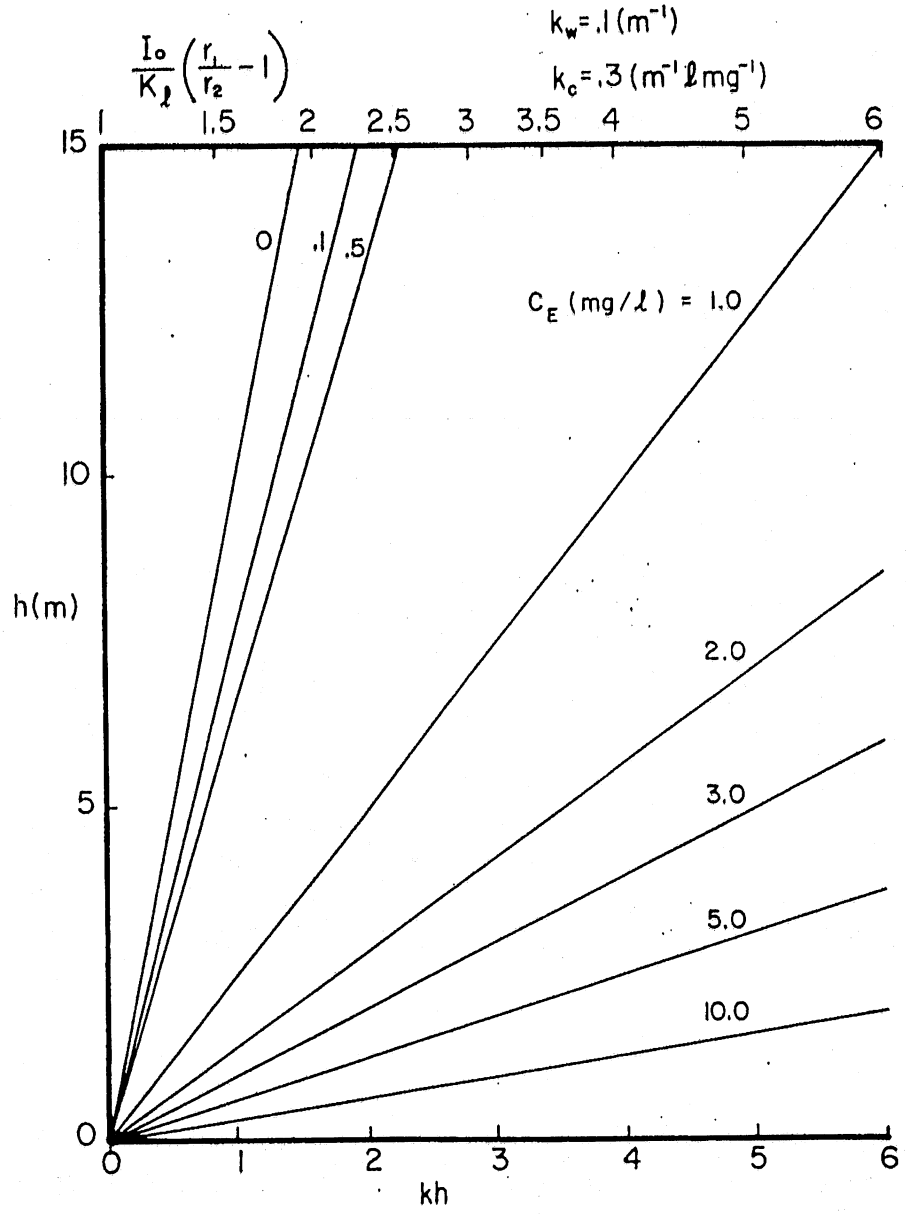

Figure VIII-1 Effect of surface mixed layer depth h and specific net growth coefficient $I_0 / K_\ell[(r_1 / r_2 - 1)]$ on equilibrium photoplankton concentration C_E (Example for k_w=0.1 m^{-1} and k_c=0.3 m^{-1} l mg^{-1}) (after Skoglund et al., 1973).

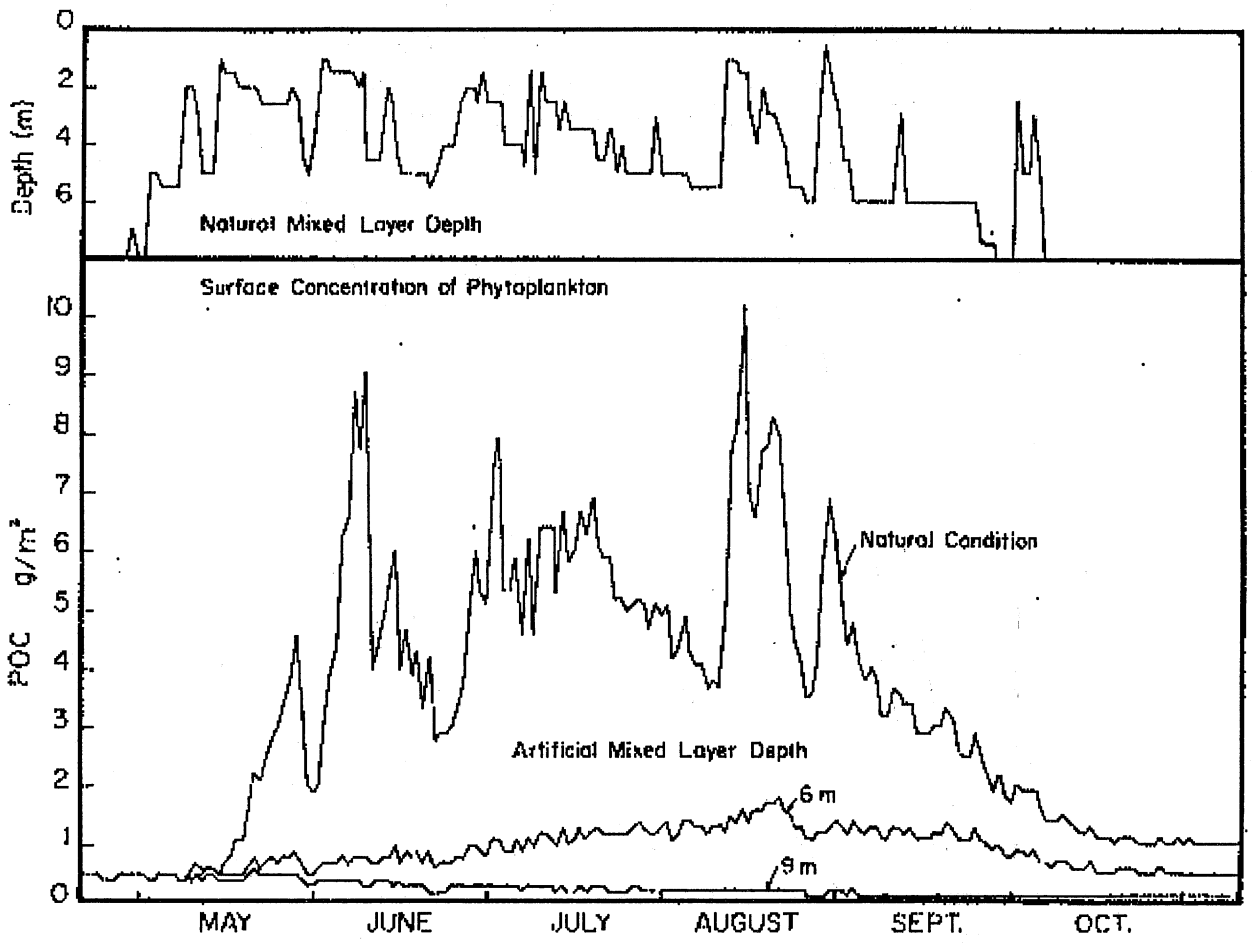

Figure VIII-2 Sample computations showing seasonal variations in surface mixed layer depths and resulting integral phytoplankton concentrations in the surface mixed layer of Lake Calhoun (after Skoglund et al., 1973).

a) Routing of the tributary inflow through the lake by a pipeline.
b) Phosphorus reduction in the inflow during the summer.
c) Sealing of lake sediments to eliminate phosphorus release from the lake sediments in summer.
d) Removal/precipitation of phosphorus from the lake water in spring.

To explore the potential effectiveness of each of the above actions (before implementation), the dynamic lake water quality simulation model, MINLAKE98 was used. The model is driven by hydrologic and weather data. The model simulates lake stratification on a time scale of one day. Simulations progressed from current existing conditions to each management option considered. Actions can be simulated by modifications in the model input or the model coefficients and constraints. Surface mixed layer depth deepening effects on phytoplankton were explored by imposing daily desired depths in the surface mixed layer module.

Simulations were made for the open water period (April to October) using weather conditions recorded in 1995 and 1996. Results are given in a separate report (West-Mack and Stefan, 2000). From the model output statistically significant parameters can be extracted. These are e.g. maximum daily and mean summer chlorophyll concentrations, and minimum, maximum and mean summer Secchi depths. Such parameter values can be used as indicators for the most effective lake management strategies.

The most effective strategies as identified by the water quality simulations can be further explored for technical feasibility. By this we mean a preliminary study of the technical requirements in terms of materials, overall design, energy requirements and operational procedures. These technical design aspects will have to be considered in a future study.

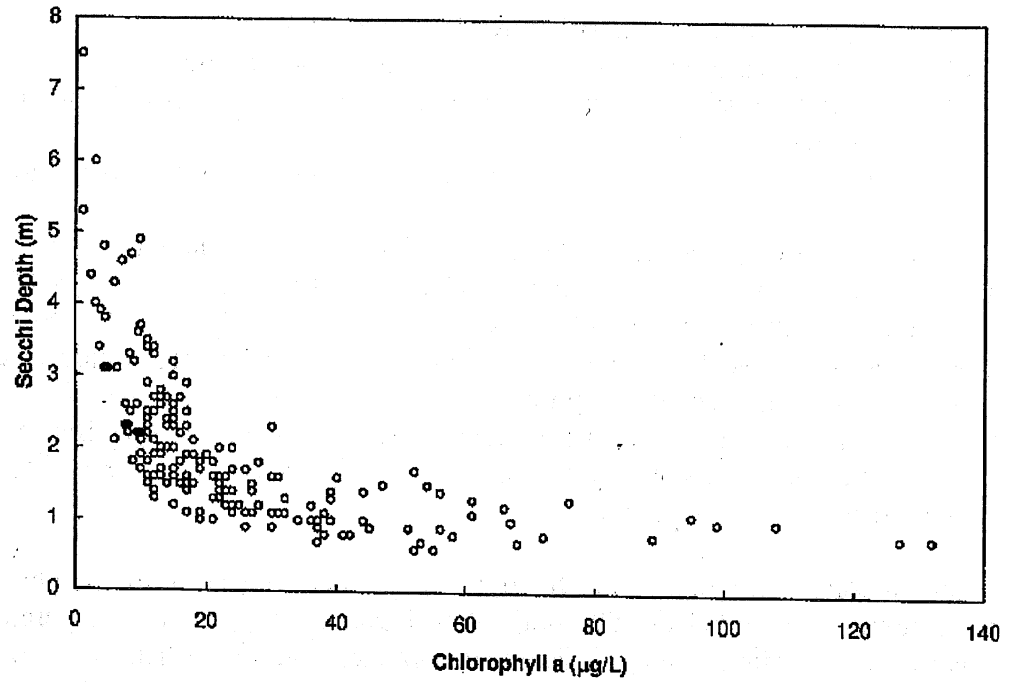

Figure VIII-3a Secchi depth and chlorophyll-a relationship in Lake McCarrons.

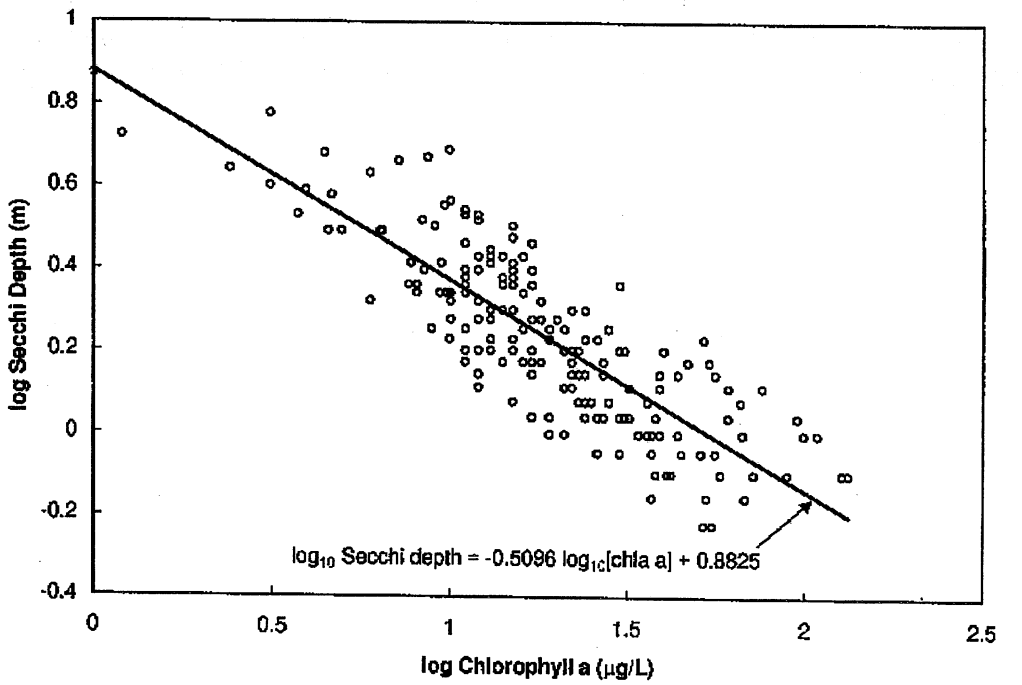

Figure VIII-3b Log-log plot of Secchi depth and chlorophyll-a in Lake McCarrons.

REFERENCES

Andradottir, H. O. and H. M. Nepf. Thermal mediation by littoral wetlands and impact on lake intrusion depths, *Water Resources Research*, Vol. 36, No. 3, 725-736, March 2000.

Denman, K. L. A time-dependent model of the upper ocean, *J. Phys. Oceanography*, 3, 173-184, 1973.

Gu, R. and H. G. Stefan. Mixing of temperature-stratified lakes and reservoirs by jets, *J. Environmental Engineering*, 114(4):898-914, August 1988.

Jensen, K. M.. Trophic State in the Minneapolis Chain of Lakes: Current Conditions and Historical Trends, M.S. Thesis, University of Minnesota, Department of Civil Engineering, October 1998, 1988, 300 pp.

Jirka, G. H. and M. Watanabe. Steady-state estimation of cooling pond performance, *J. Hydraulic Division*, ASCE, 106(H6):1116-1123, 1980.

MCES. Lake McCarrons Wetland Treatment System - Phase III Study Report, Metropolitan Council Environmental Services, St. Paul, MN, September 1997, 250 pp.

Oberts, G. L. and R. A. Osgood. Lake McCarrons Wetland Treatment system: Final Report on the Function of the Wetland Treatment System and the Impact on Lake McCarrons, Publication No. 590-88-095, Metropolitan Council of the Twin Cities Area, St. Paul, MN, October 1988, 220 pp.

Osgood, R. A. The Limnology, Ecology and Management of Twin Cities Metropolitan Area Lakes, Publication No. 590-88-123, Metropolitan Council of the Twin Cities Area, St. Paul, MN, December 1988, 117 pp.

Osgood R. A. An Evaluation of the Effects of Watershed Treatment systems on the Summertime Phosphorus Concentration in Metropolitan Area Lakes, Publication No. 590-89-062b, Metropolitan Council, St. Paul, MN, June 1989, 80 pp.

Rast, W. and G. F. Lee. Summary Analysis of the North American (US Portion) OECD Eutrophication Project: Nutrient Loading-Lake Response Relationship and Trophic State Inices, USEPA, Corvallis Environmental Research Laboratory, Corvallis, OR, 454 pp. EPA-600/3-78-008 (as given by Thomann and Mueller, 1987, p. 414.), 1978.

Stefan, H. G. and R. Gu. Conceptual design procedure for hydraulic destratification systems in small ponds, lakes or reservoirs for water quality improvements, *Water Resources Bulletin,* AWRA, 27(6), 1991.

Stefan, H., T. Skoglund and R. O. Megard. Wind control of algae growth in eutrophic lakes, *J. Environmental Engineering Division*, ASCE, 102(EE6):1201-1213, December 1976.

West, D. E. and H. G. Stefan. Simulation of Lake Water Quality using a One-dimensional Model with Watershed Input: Model Description and Application to Lake Riley and Lake Elmo, *Project Report No. 430*, St. Anthony Falls Laboratory, University of Minnesota, Minneapolis, MN, December 1998, 104 pp.

West-Mack, D.E. and H. G. Stefan. Simulation of Water Quality and Primary Productivity Control Strategies for Lake McCarrons, Project Report No. 426, St. Anthony Falls Laboratory, University of Minnesota, Minneapolis, MN, July 2000, 43 pp.

APPENDIX A. HISTORICAL LAKE MCCARRONS SUMMER TEMPERATURE STRATIFICATION (1984 TO 1997)

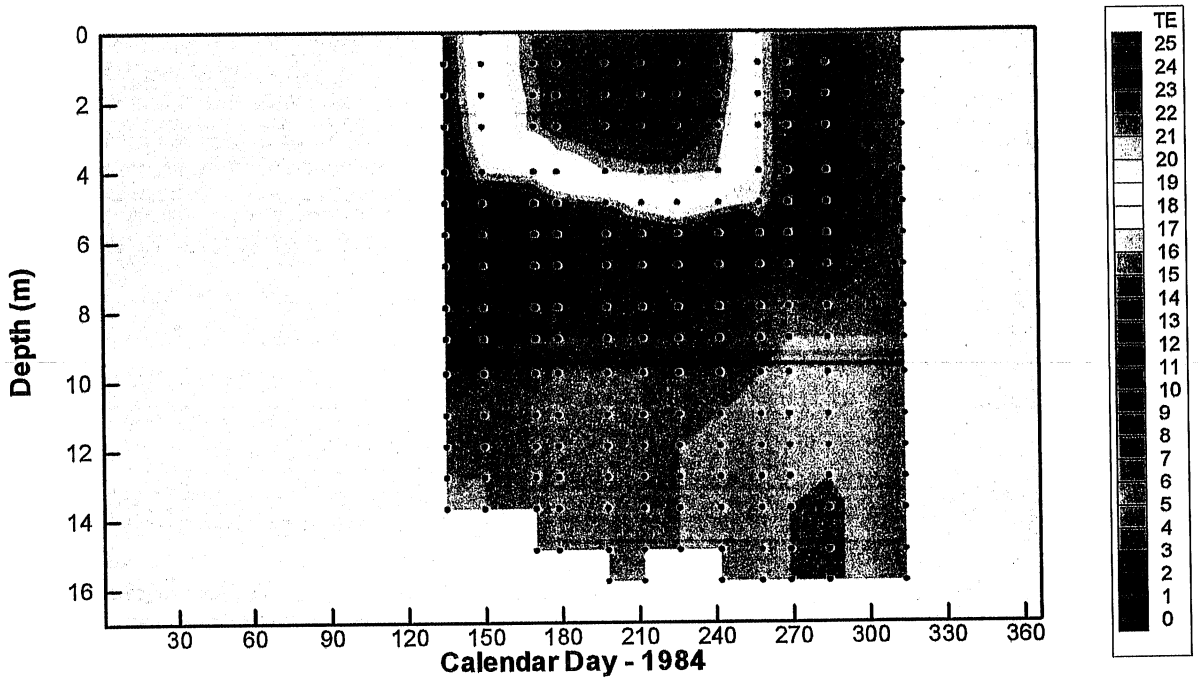
Depth (m)
0
2
4
6
8
10
12
14
16
30
60
90
120
150
180
210
240
270
300
330
360
Calendar Day - 1984
TE
25
24
23
22
21
20
19
18
17
16
15
14
13
12
11
10
9
8
7
6
5
4
3
2
1
0

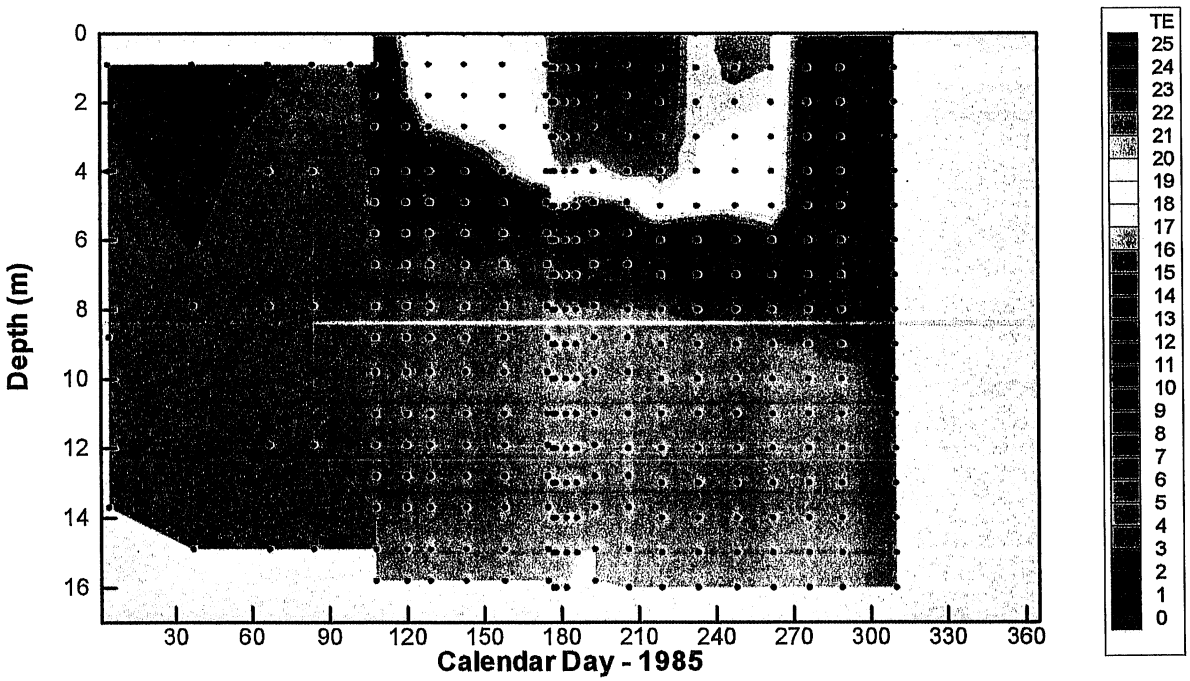
Depth (m)
0
2
4
6
8
10
12
14
16
30
60
90
120
150
180
210
240
270
300
330
360
Calendar Day - 1985
TE
25
24
23
22
21
20
19
18
17
16
15
14
13
12
11
10
9
8
7
6
5
4
3
2
1
0

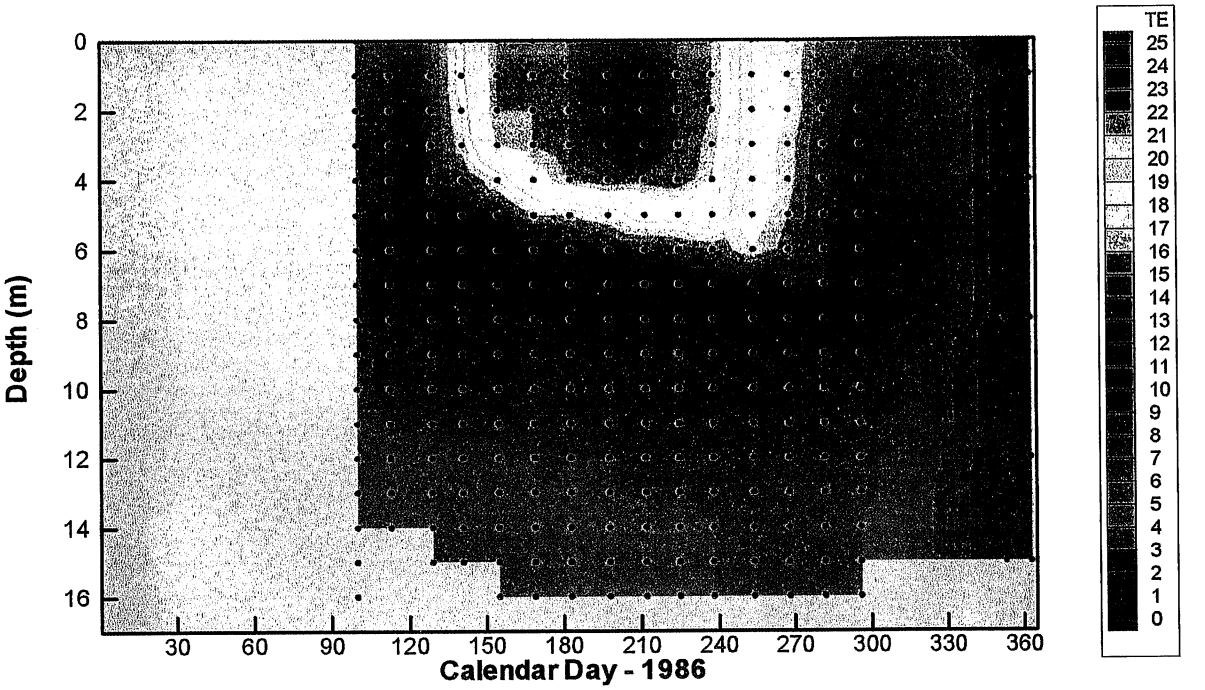
Depth (m)
0
2
4
6
8
10
12
14
16
30
60
90
120
150
180
210
240
270
300
330
360
Calendar Day - 1986
TE
25
24
23
22
21
20
19
18
17
16
15
14
13
12
11
10
9
8
7
6
5
4
3
2
1
0

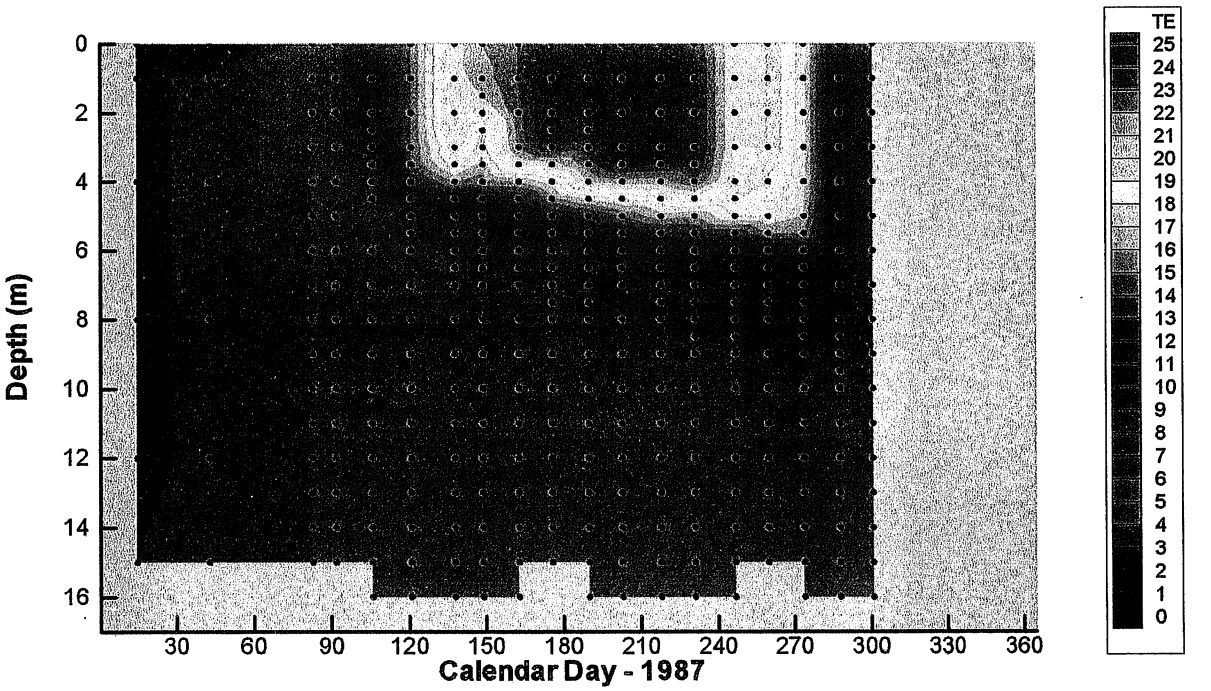
Depth (m)
0
2
4
6
8
10
12
14
16
30
60
90
120
150
180
210
240
270
300
330
360
Calendar Day - 1987
TE
25
24
23
22
21
20
19
18
17
16
15
14
13
12
11
10
9
8
7
6
5
4
3
2
1
0

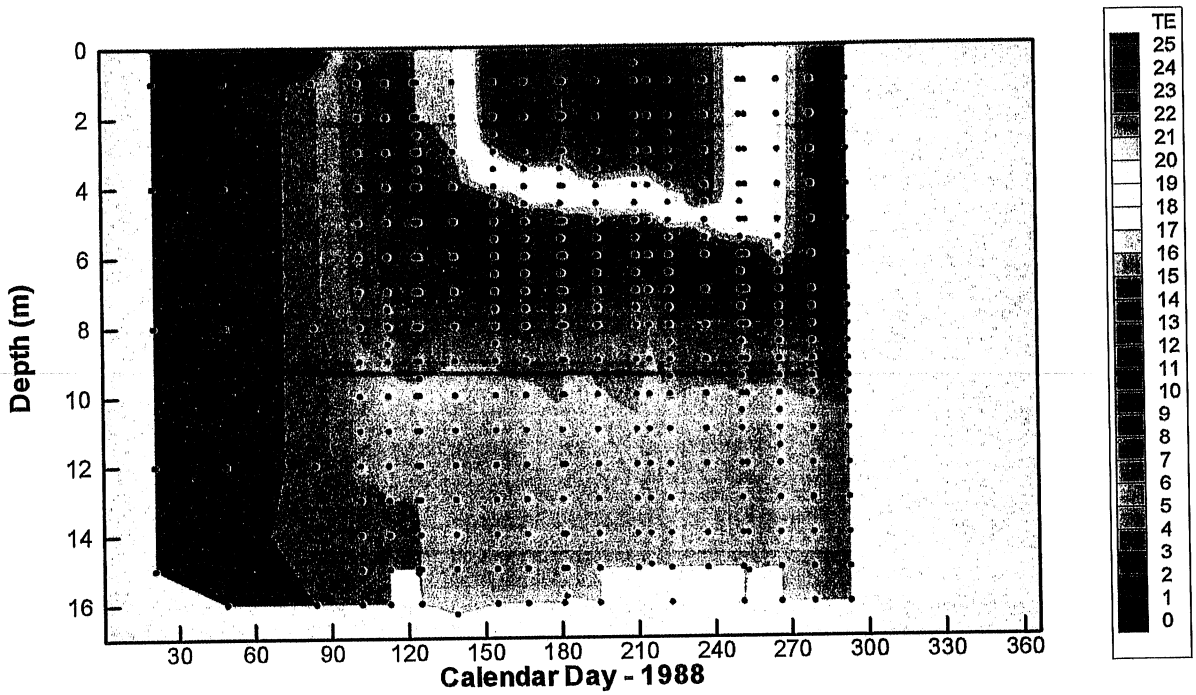
Depth (m)
0
2
4
6
8
10
12
14
16
30
60
90
120
150
180
210
240
270
300
330
360
Calendar Day - 1988
TE
25
24
23
22
21
20
19
18
17
16
15
14
13
12
11
10
9
8
7
6
5
4
3
2
1
0

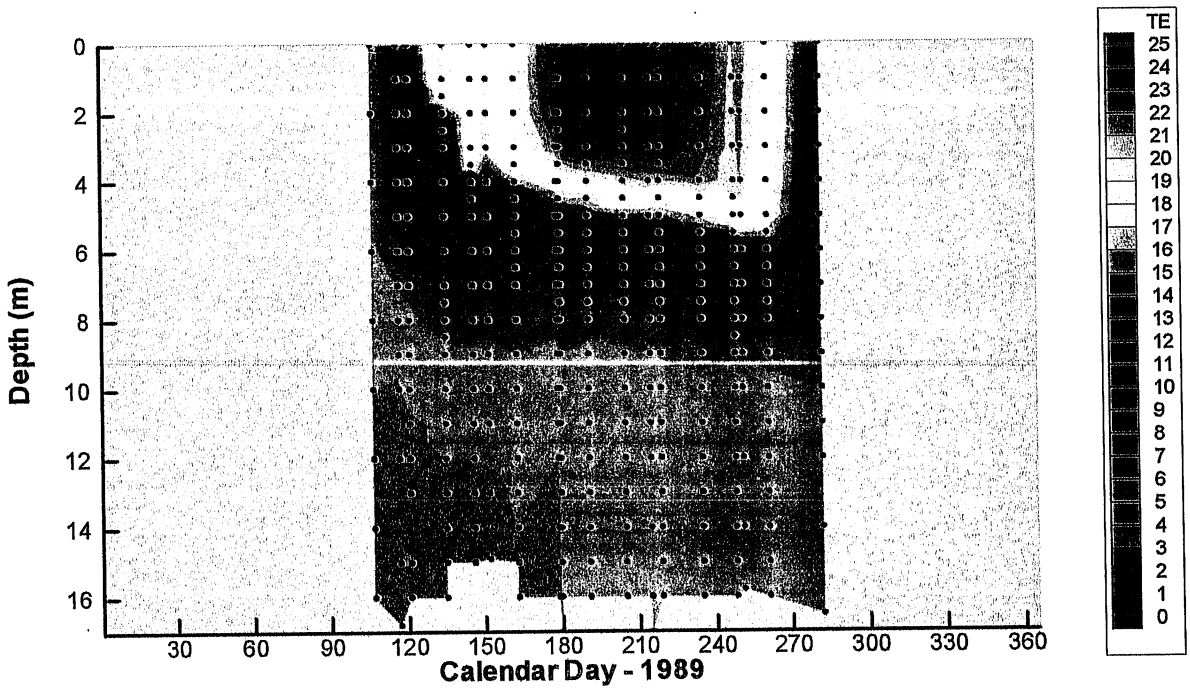
Depth (m)
0
2
4
6
8
10
12
14
16
30
60
90
120
150
180
210
240
270
300
330
360
Calendar Day - 1989
TE
25
24
23
22
21
20
19
18
17
16
15
14
13
12
11
10
9
8
7
6
5
4
3
2
1
0

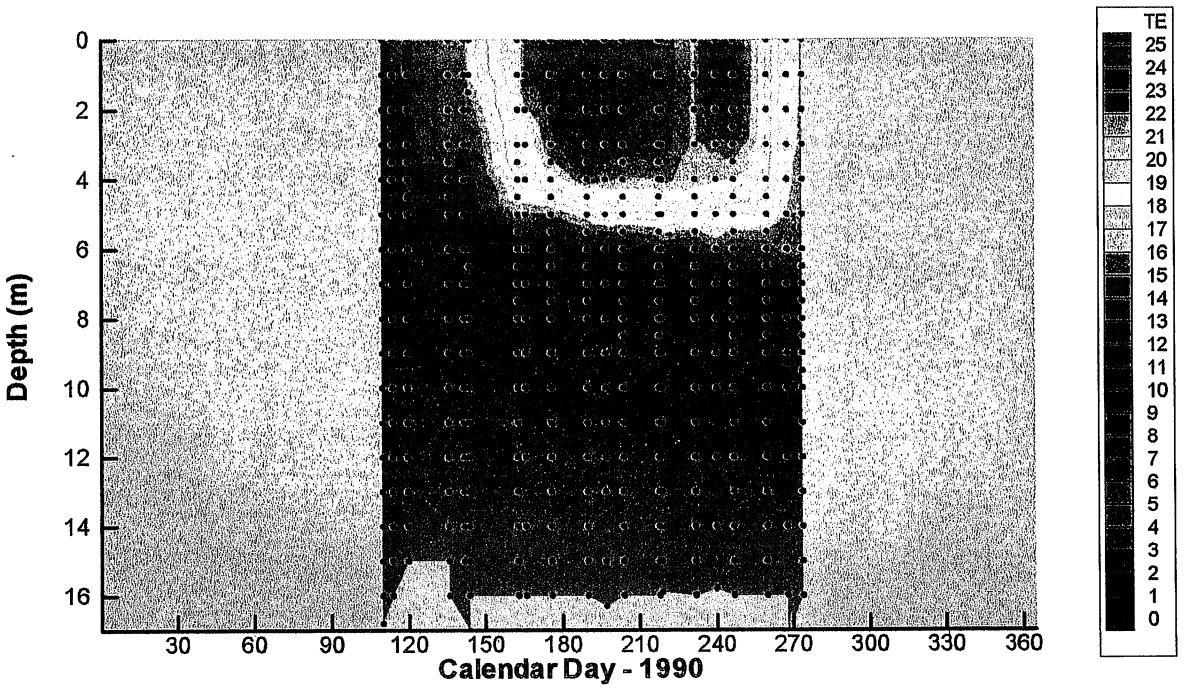
Depth (m)
0
2
4
6
8
10
12
14
16
30
60
90
120
150
180
210
240
270
300
330
360
Calendar Day - 1990
TE
25
24
23
22
21
20
19
18
17
16
15
14
13
12
11
10
9
8
7
6
5
4
3
2
1
0

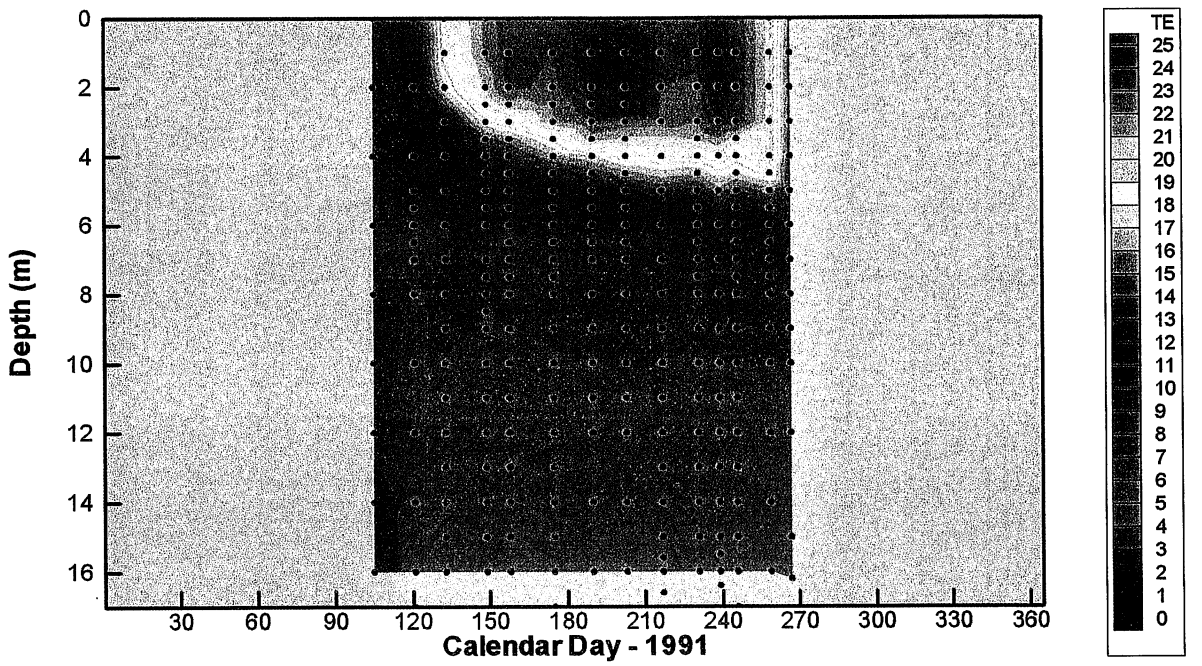
Depth (m)
0
2
4
6
8
10
12
14
16
30
60
90
120
150
180
210
240
270
300
330
360
Calendar Day - 1991
TE
25
24
23
22
21
20
19
18
17
16
15
14
13
12
11
10
9
8
7
6
5
4
3
2
1
0

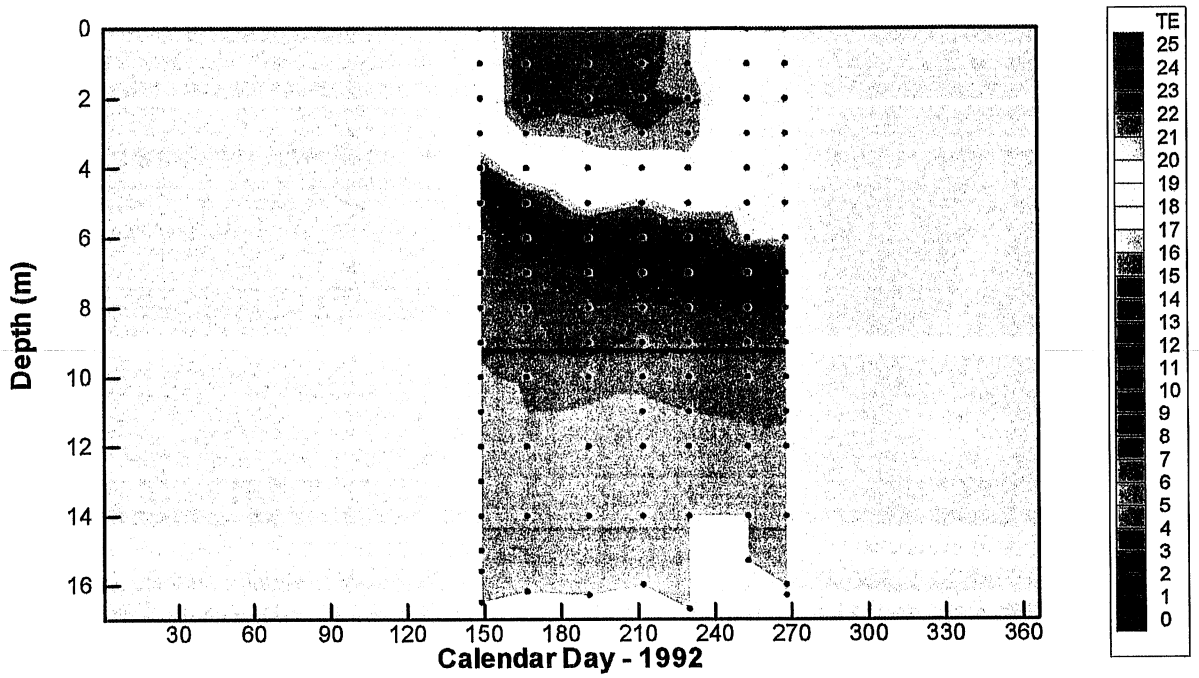
Depth (m)
0
2
4
6
8
10
12
14
16
30
60
90
120
150
180
210
240
270
300
330
360
Calendar Day - 1992
TE
25
24
23
22
21
20
19
18
17
16
15
14
13
12
11
10
9
8
7
6
5
4
3
2
1
0

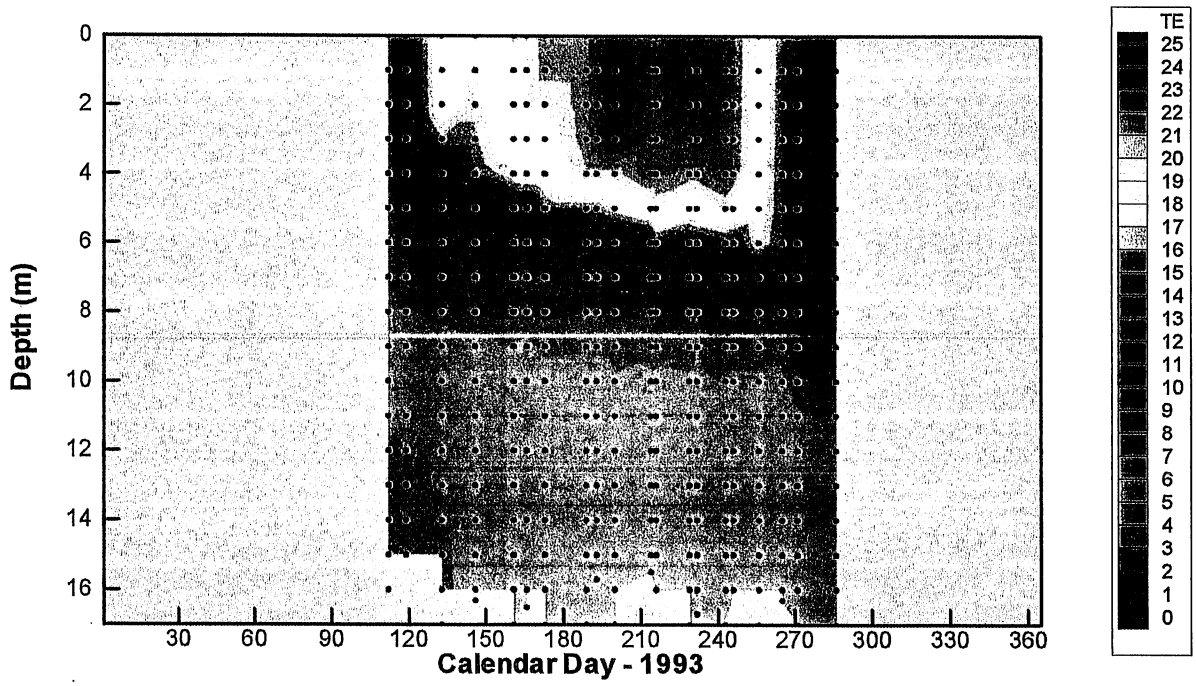
Depth (m)
0
2
4
6
8
10
12
14
16
30
60
90
120
150
180
210
240
270
300
330
360
Calendar Day - 1993
TE
25
24
23
22
21
20
19
18
17
16
15
14
13
12
11
10
9
8
7
6
5
4
3
2
1
0

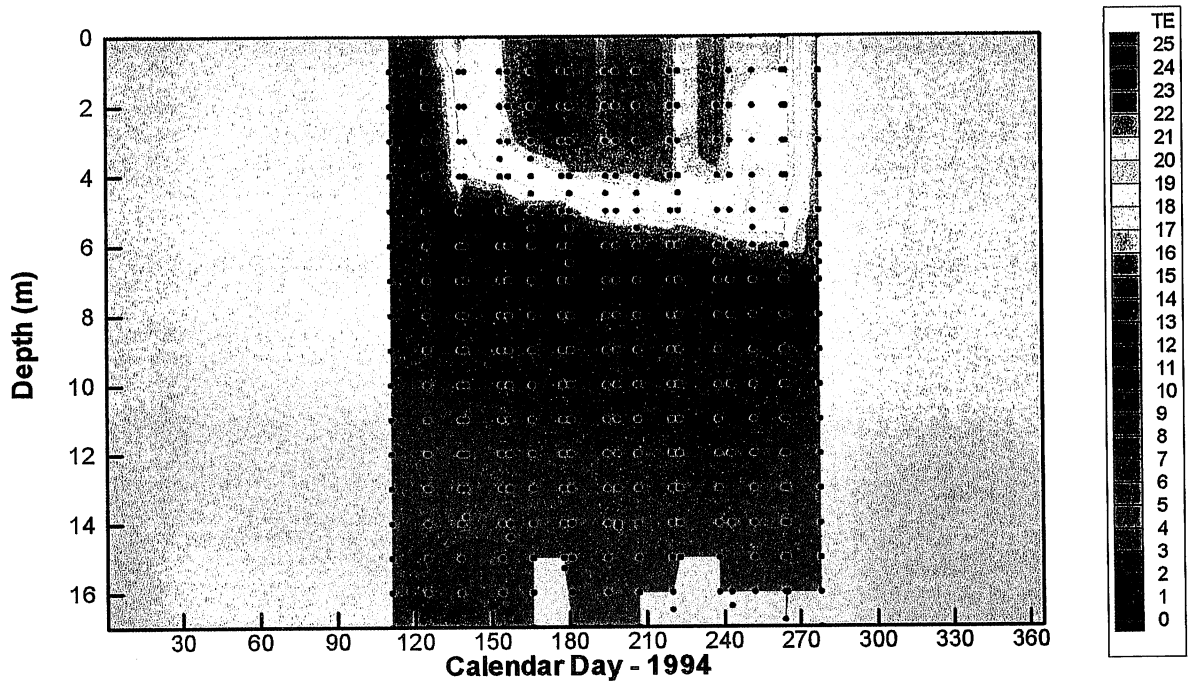
Depth (m)
0
2
4
6
8
10
12
14
16
30
60
90
120
150
180
210
240
270
300
330
360
Calendar Day - 1994
TE
25
24
23
22
21
20
19
18
17
16
15
14
13
12
11
10
9
8
7
6
5
4
3
2
1
0

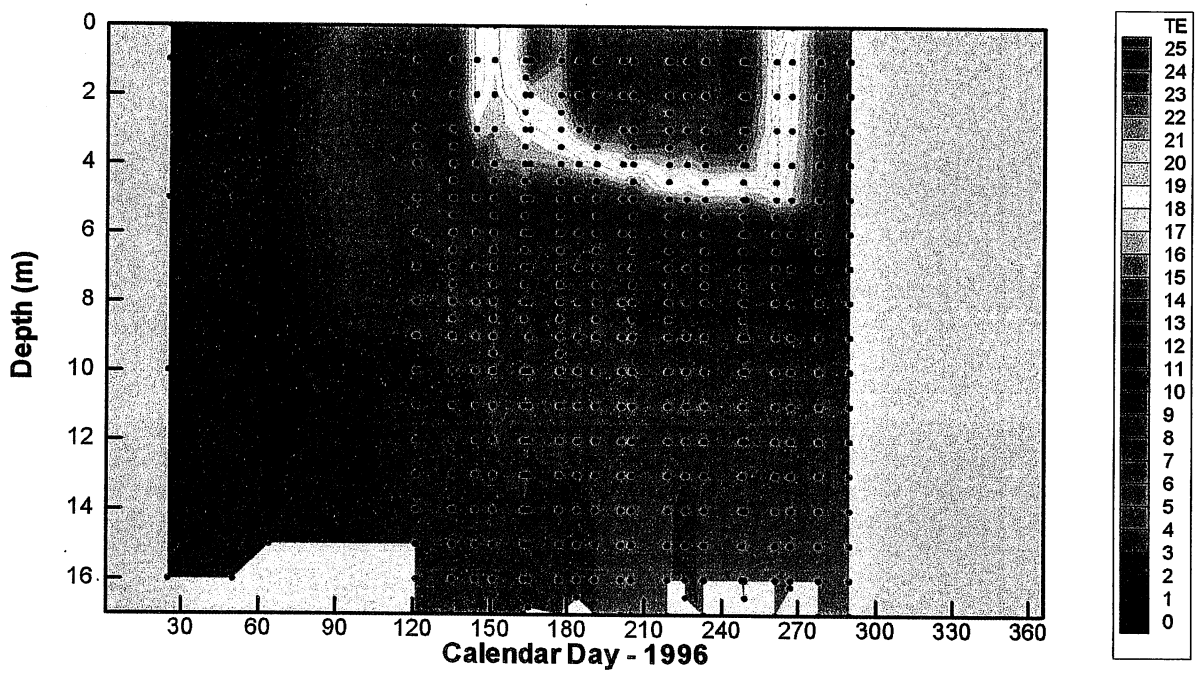
Depth (m)
0
2
4
6
8
10
12
14
16
30
60
90
120
150
180
210
240
270
300
330
360
Calendar Day - 1996
TE
25
24
23
22
21
20
19
18
17
16
15
14
13
12
11
10
9
8
7
6
5
4
3
2
1
0

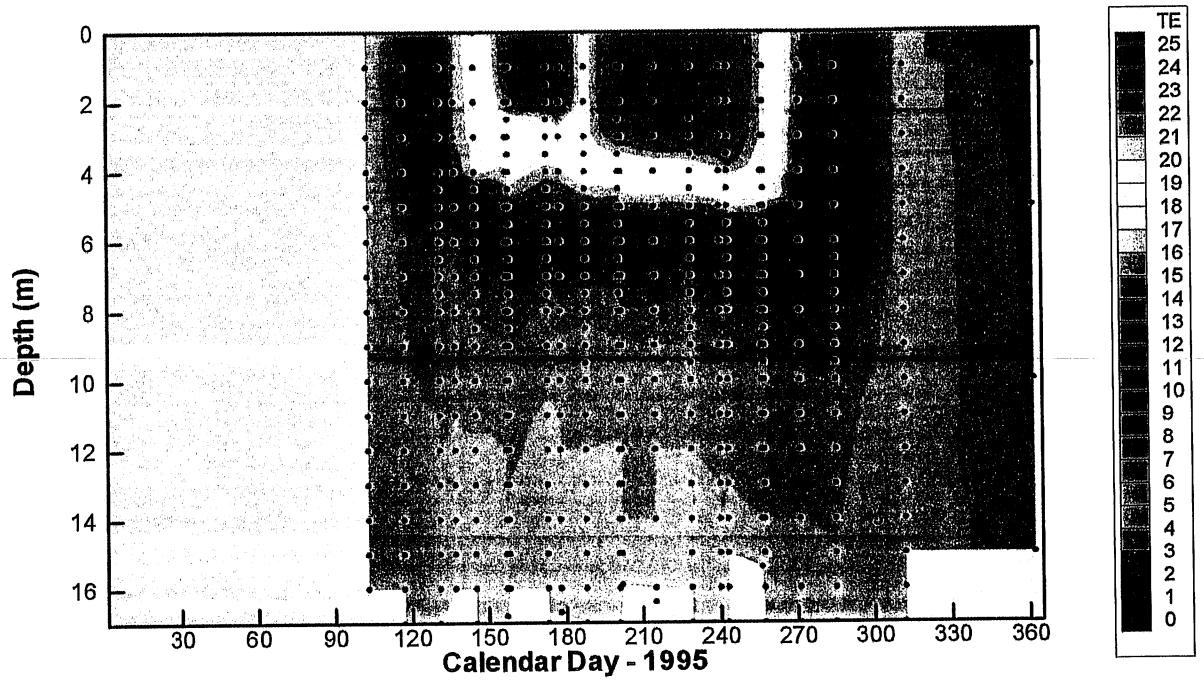
Depth (m)
0
2
4
6
8
10
12
14
16
30
60
90
120
150
180
210
240
270
300
330
360
Calendar Day - 1995
TE
25
24
23
22
21
20
19
18
17
16
15
14
13
12
11
10
9
8
7
6
5
4
3
2
1
0

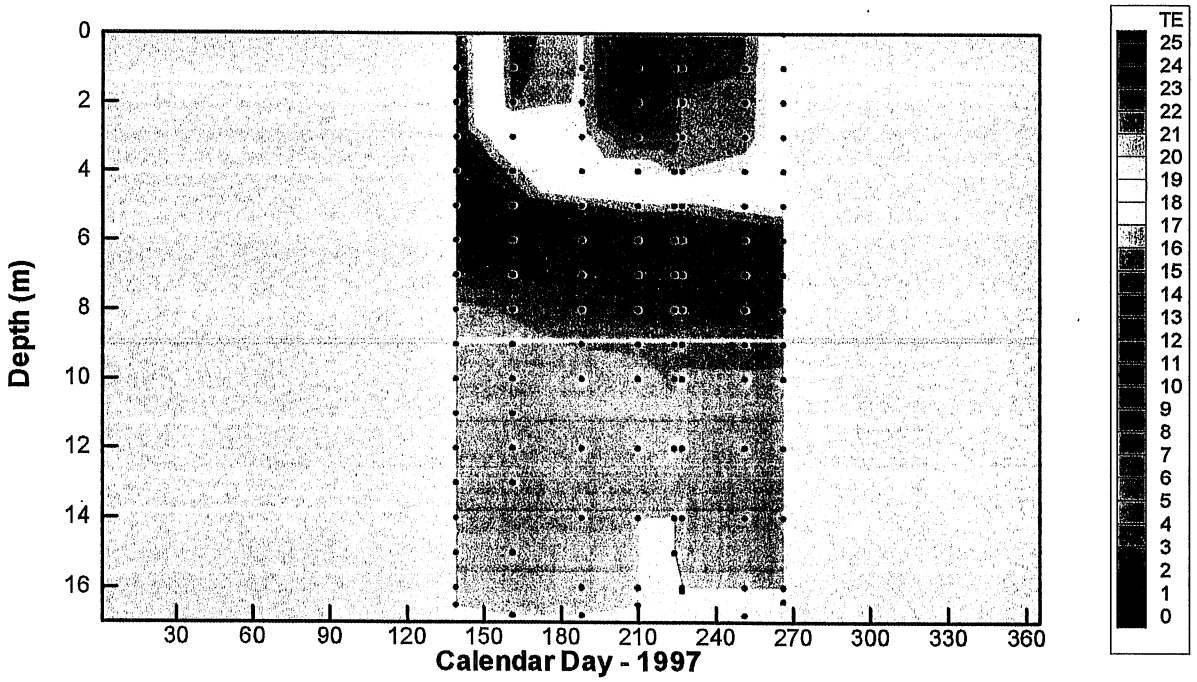
Depth (m)
0
2
4
6
8
10
12
14
16
30
60
90
120
150
180
210
240
270
300
330
360
Calendar Day - 1997
TE
25
24
23
22
21
20
19
18
17
16
15
14
13
12
11
10
9
8
7
6
5
4
3
2
1
0

APPENDIX B. LAKE MCCARRONS WATER TEMPERATURE IN 1999.

(Measurements are 10-minute averages)

Lake McCarrons: Center Raft

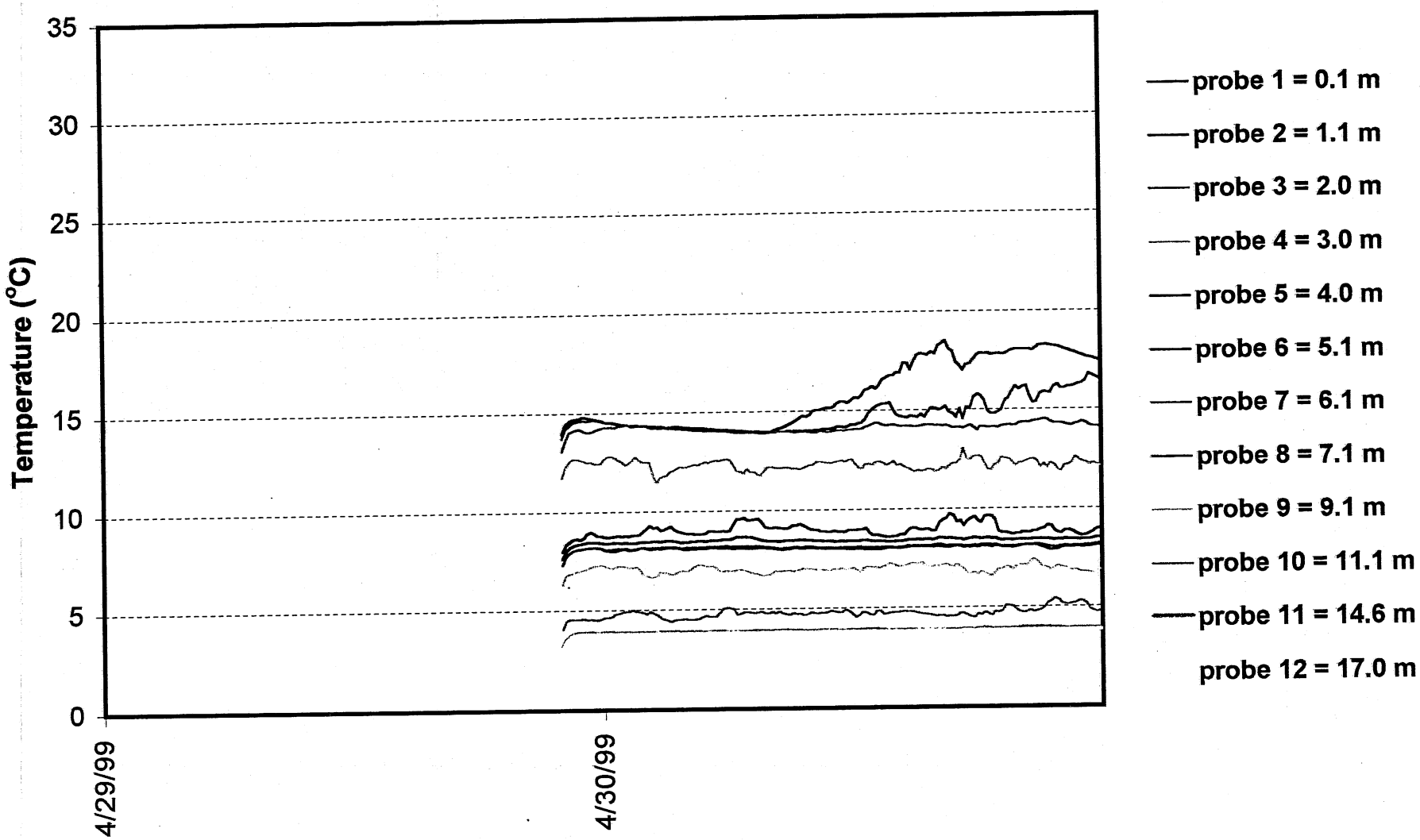

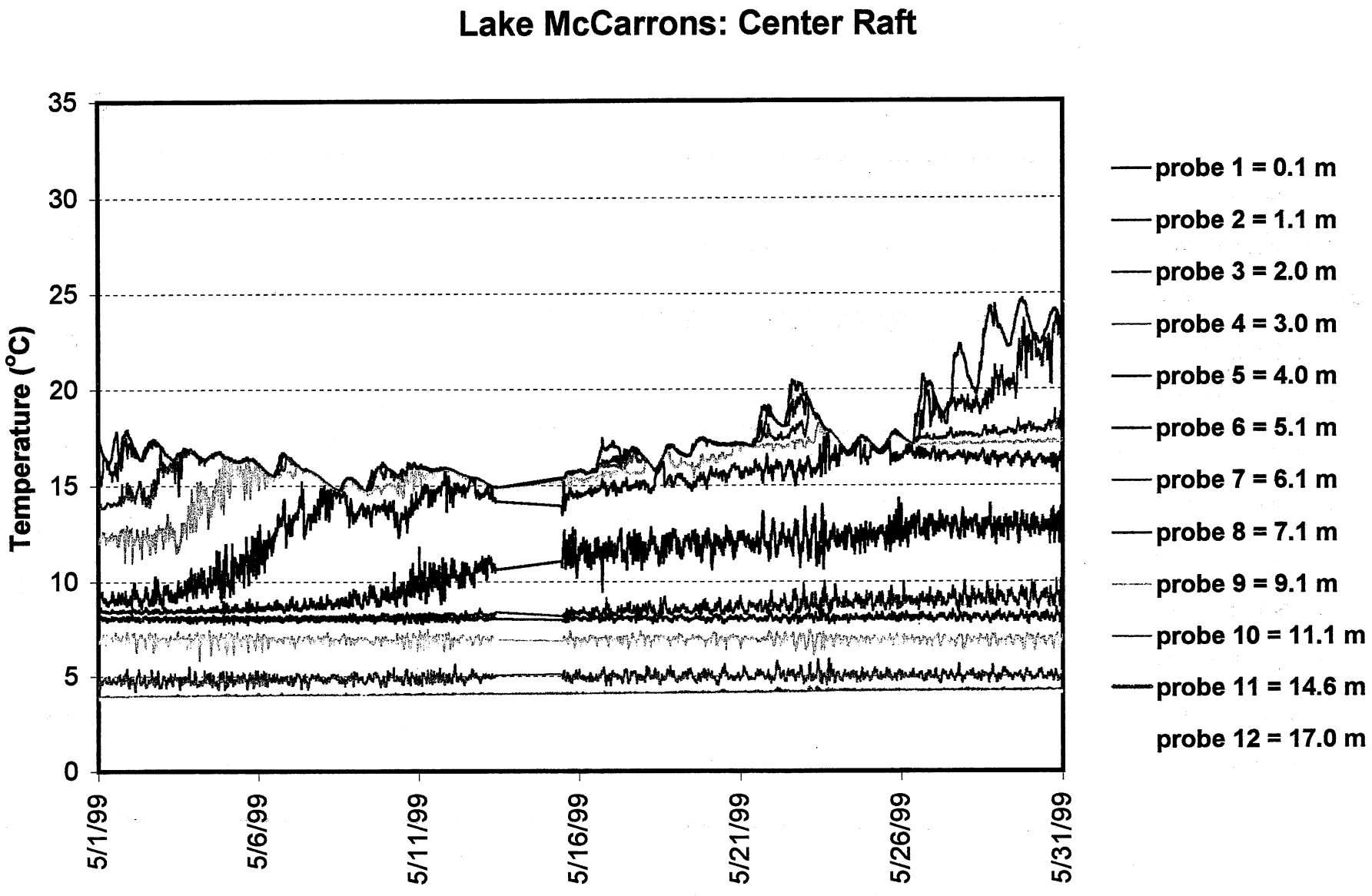
Lake McCarrons: Center Raft
Temperature (°C)
35
30
25
20
15
10
5
0
5/1/99
5/6/99
5/11/99
5/16/99
5/21/99
5/26/99
5/31/99
probe 1 = 0.1 m
probe 2 = 1.1 m
probe 3 = 2.0 m
probe 4 = 3.0 m
probe 5 = 4.0 m
probe 6 = 5.1 m
probe 7 = 6.1 m
probe 8 = 7.1 m
probe 9 = 9.1 m
probe 10 = 11.1 m
probe 11 = 14.6 m
probe 12 = 17.0 m

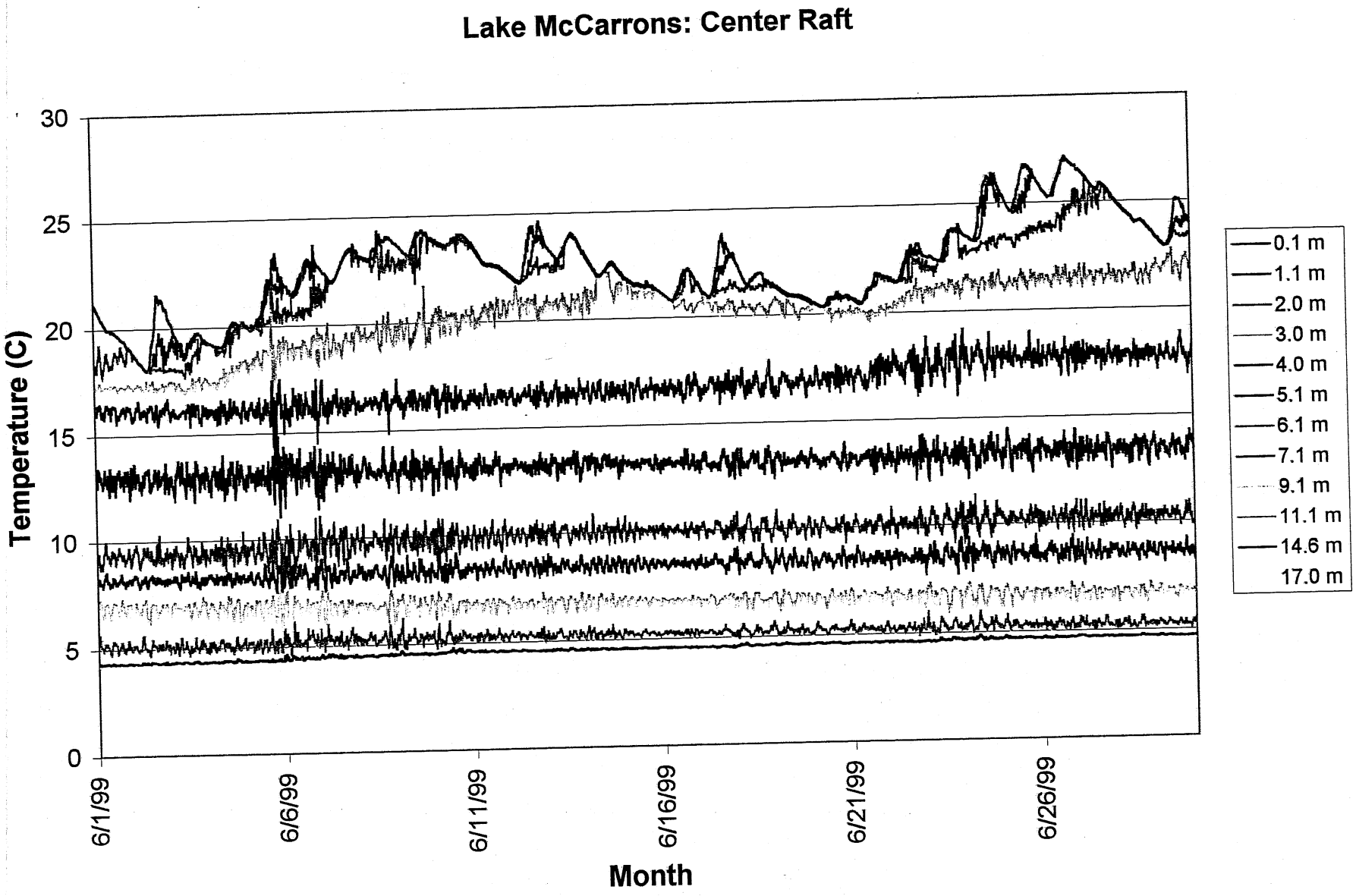
Lake McCarrons: Center Raft
Temperature (C)
30
25
20
15
10
5
0
6/1/99
6/6/99
6/11/99
6/16/99
6/21/99
6/26/99
Month
0.1 m
1.1 m
2.0 m
3.0 m
4.0 m
5.1 m
6.1 m
7.1 m
9.1 m
11.1 m
14.6 m
17.0 m

Lake McCarrons: Center Raft

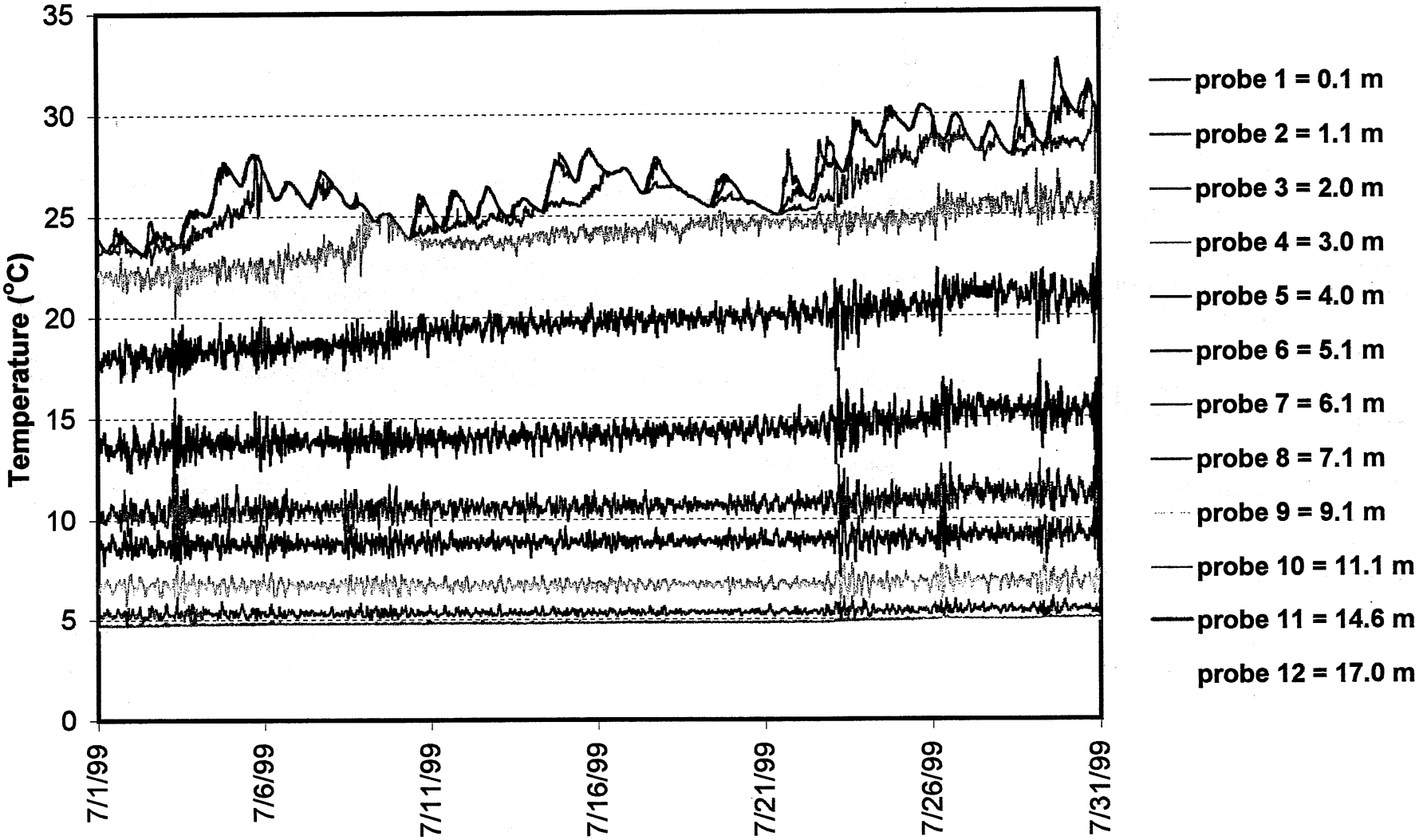

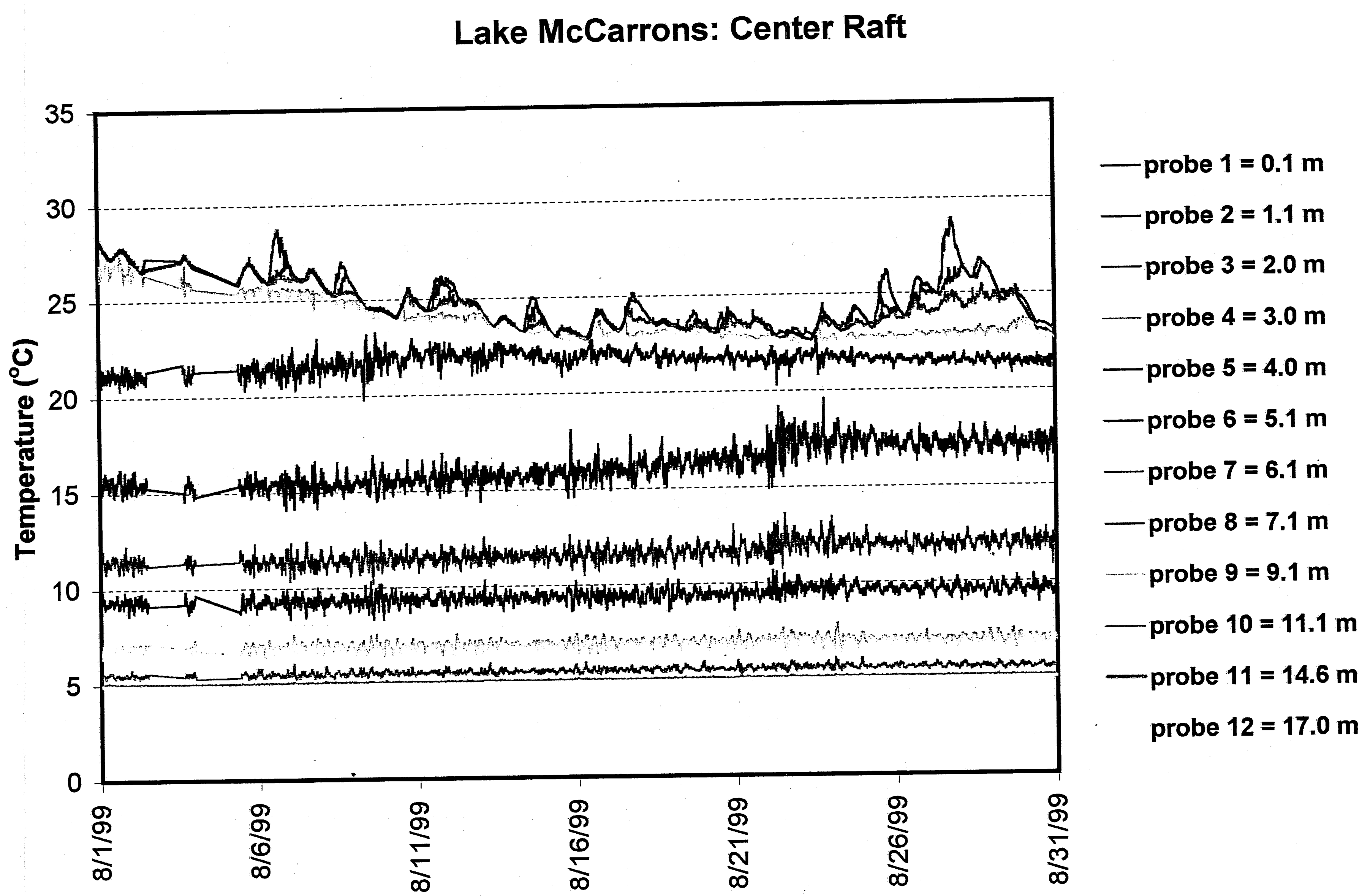
Lake McCarrons: Center Raft
Temperature (°C)
35
30
25
20
15
10
5
0
8/1/99
8/6/99
8/11/99
8/16/99
8/21/99
8/26/99
8/31/99
probe 1 = 0.1 m
probe 2 = 1.1 m
probe 3 = 2.0 m
probe 4 = 3.0 m
probe 5 = 4.0 m
probe 6 = 5.1 m
probe 7 = 6.1 m
probe 8 = 7.1 m
probe 9 = 9.1 m
probe 10 = 11.1 m
probe 11 = 14.6 m
probe 12 = 17.0 m

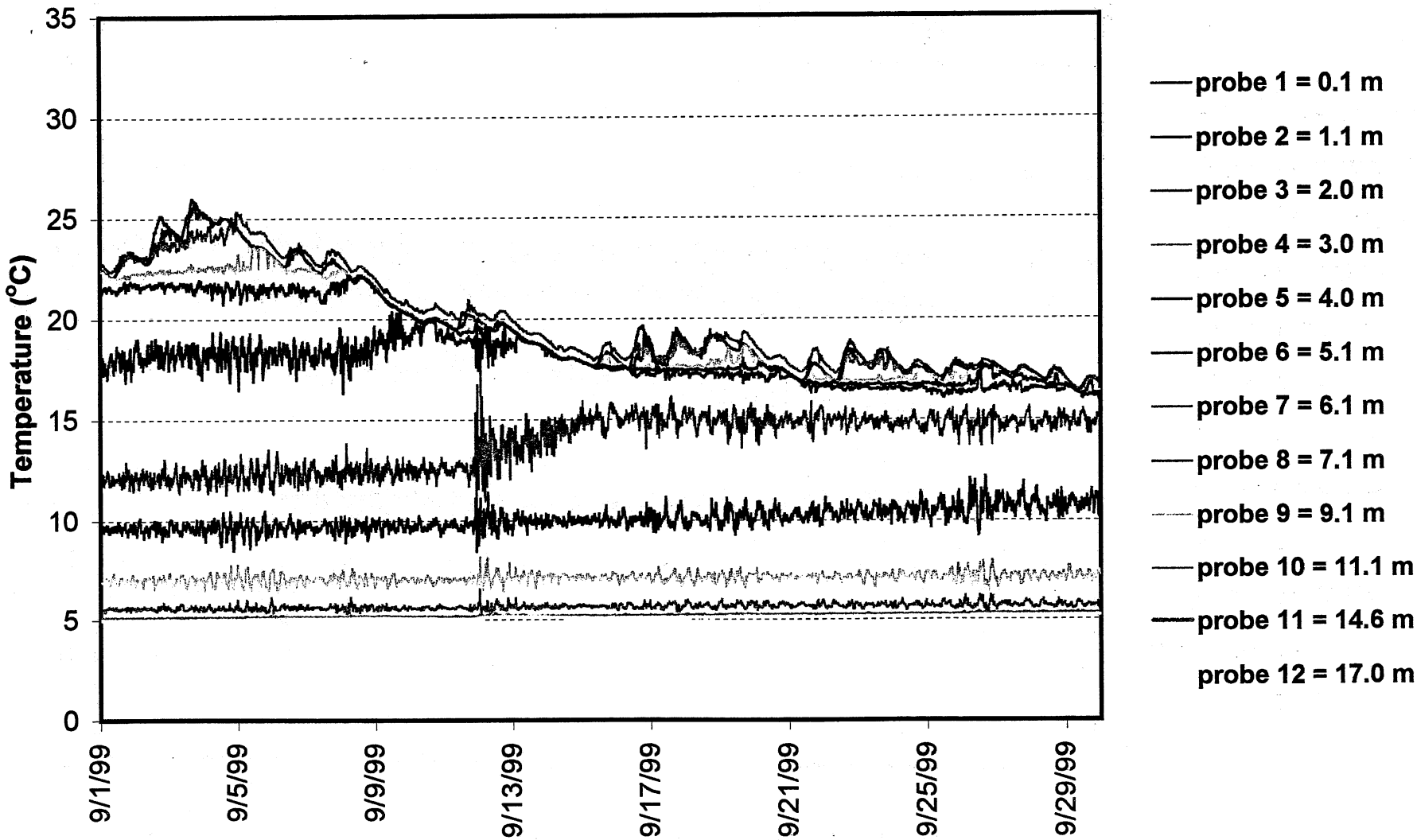
Lake McCarrons: Center Raft
Temperature (°C)
35
30
25
20
15
10
5
0
9/1/99
9/5/99
9/9/99
9/13/99
9/17/99
9/21/99
9/25/99
9/29/99
probe 1 = 0.1 m
probe 2 = 1.1 m
probe 3 = 2.0 m
probe 4 = 3.0 m
probe 5 = 4.0 m
probe 6 = 5.1 m
probe 7 = 6.1 m
probe 8 = 7.1 m
probe 9 = 9.1 m
probe 10 = 11.1 m
probe 11 = 14.6 m
probe 12 = 17.0 m

Lake McCarrons: Center Raft

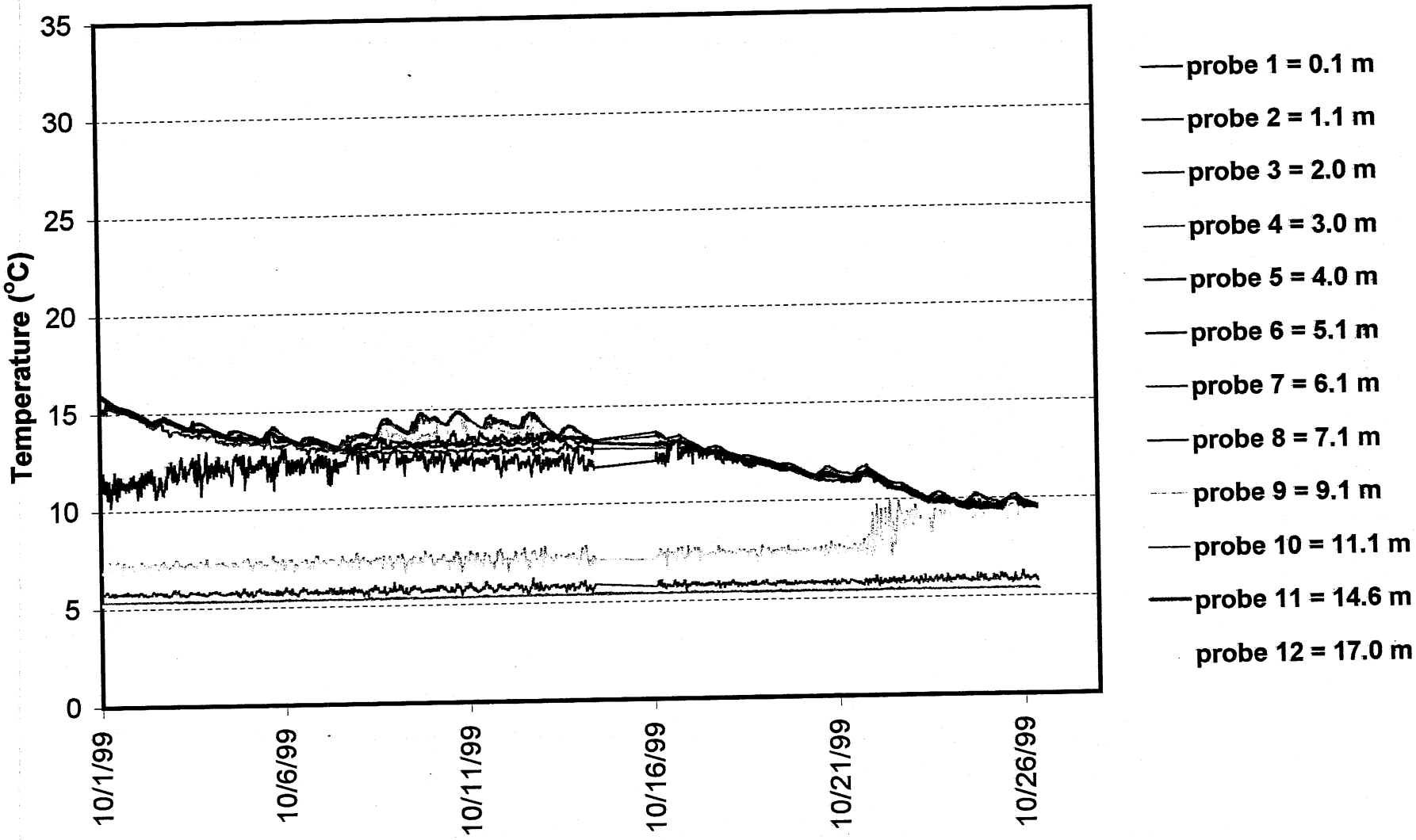

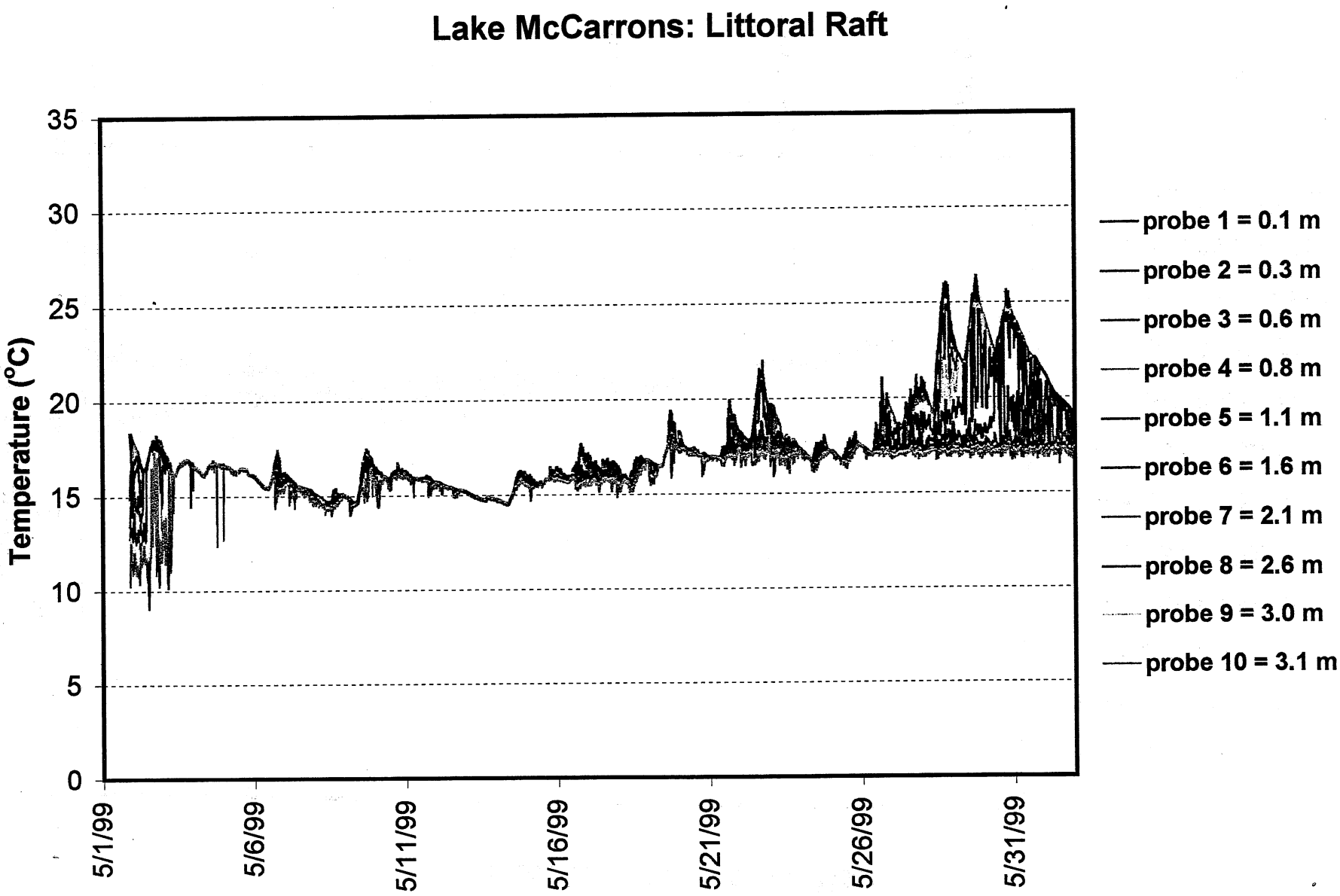
Lake McCarrons: Littoral Raft
Temperature (°C)
35
30
25
20
15
10
5
0
5/1/99
5/6/99
5/11/99
5/16/99
5/21/99
5/26/99
5/31/99
probe 1 = 0.1 m
probe 2 = 0.3 m
probe 3 = 0.6 m
probe 4 = 0.8 m
probe 5 = 1.1 m
probe 6 = 1.6 m
probe 7 = 2.1 m
probe 8 = 2.6 m
probe 9 = 3.0 m
probe 10 = 3.1 m

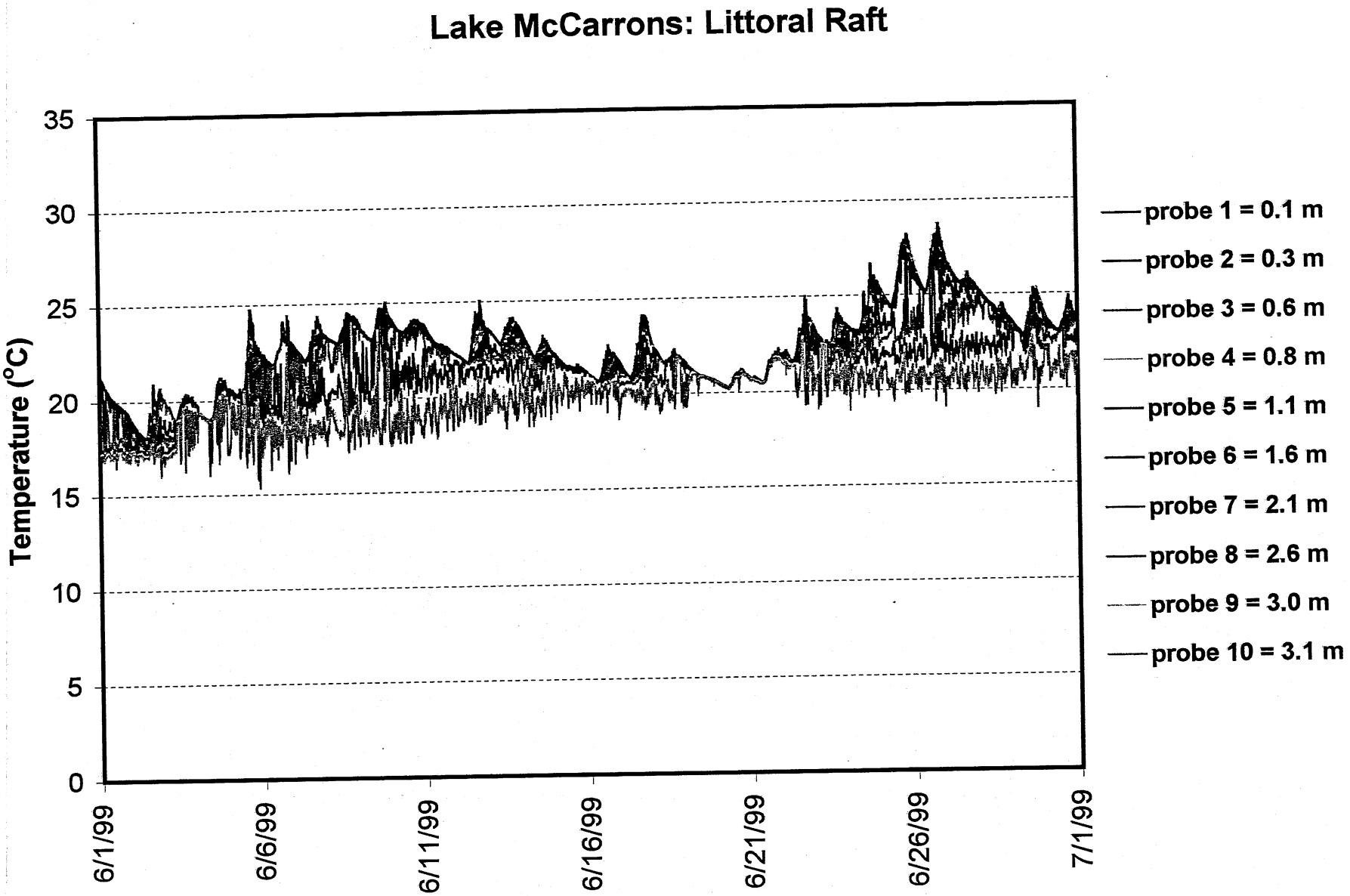
Lake McCarrons: Littoral Raft
Temperature (°C)
35
30
25
20
15
10
5
0
6/1/99
6/6/99
6/11/99
6/16/99
6/21/99
6/26/99
7/1/99
probe 1 = 0.1 m
probe 2 = 0.3 m
probe 3 = 0.6 m
probe 4 = 0.8 m
probe 5 = 1.1 m
probe 6 = 1.6 m
probe 7 = 2.1 m
probe 8 = 2.6 m
probe 9 = 3.0 m
probe 10 = 3.1 m

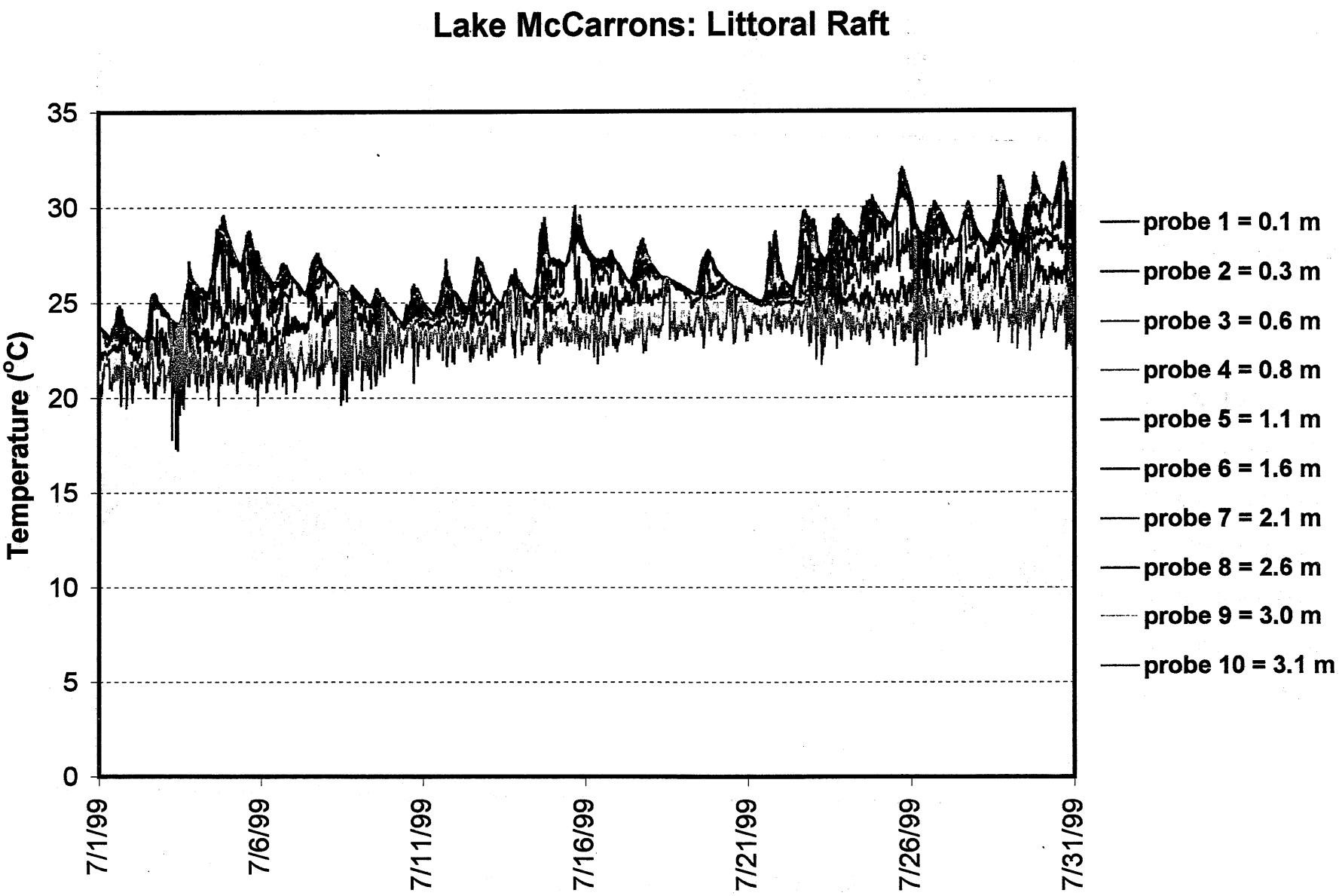
Lake McCarrons: Littoral Raft
Temperature (°C)
35
30
25
20
15
10
5
0
7/1/99
7/6/99
7/11/99
7/16/99
7/21/99
7/26/99
7/31/99
probe 1 = 0.1 m
probe 2 = 0.3 m
probe 3 = 0.6 m
probe 4 = 0.8 m
probe 5 = 1.1 m
probe 6 = 1.6 m
probe 7 = 2.1 m
probe 8 = 2.6 m
probe 9 = 3.0 m
probe 10 = 3.1 m

Lake McCarrons: Littoral Raft

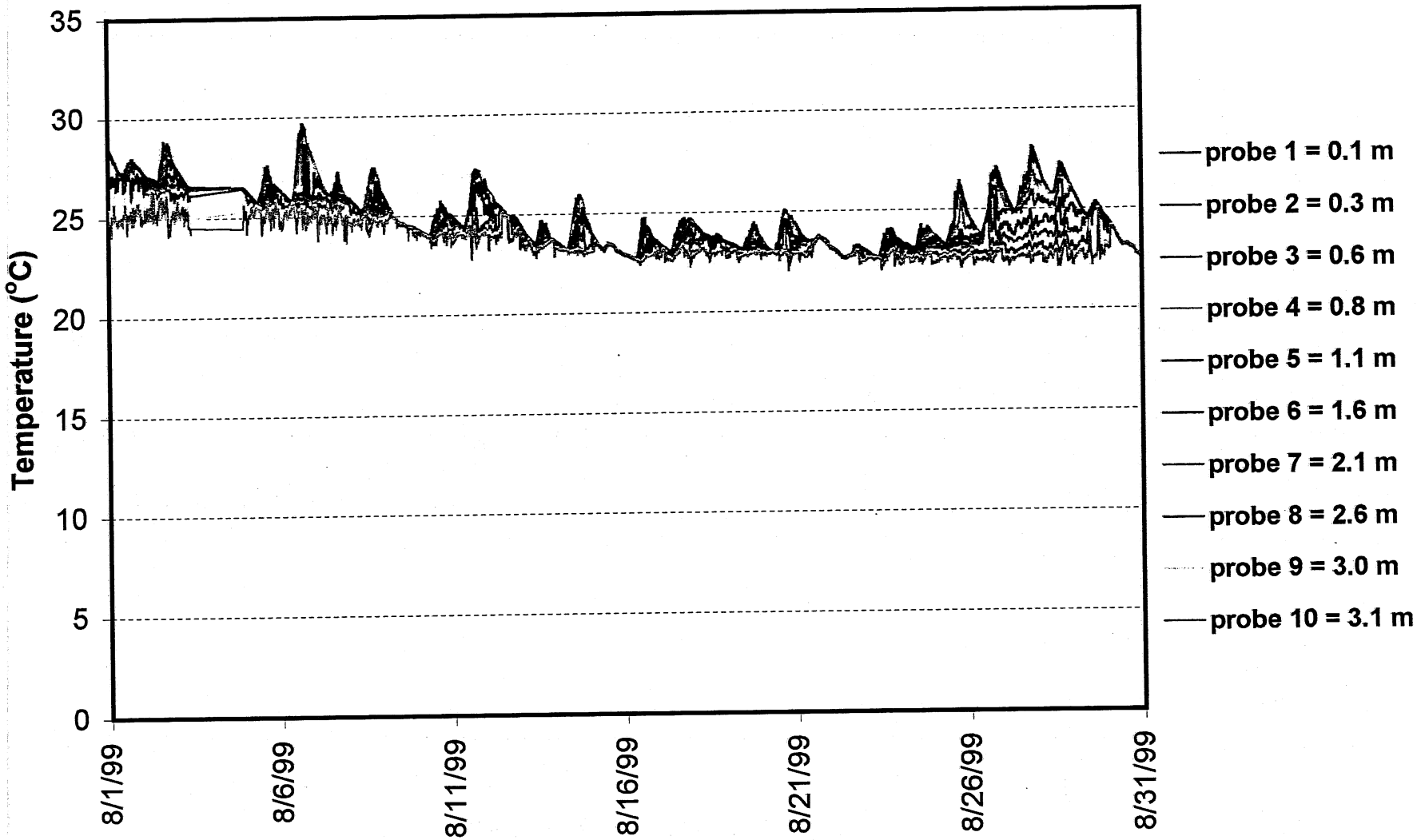

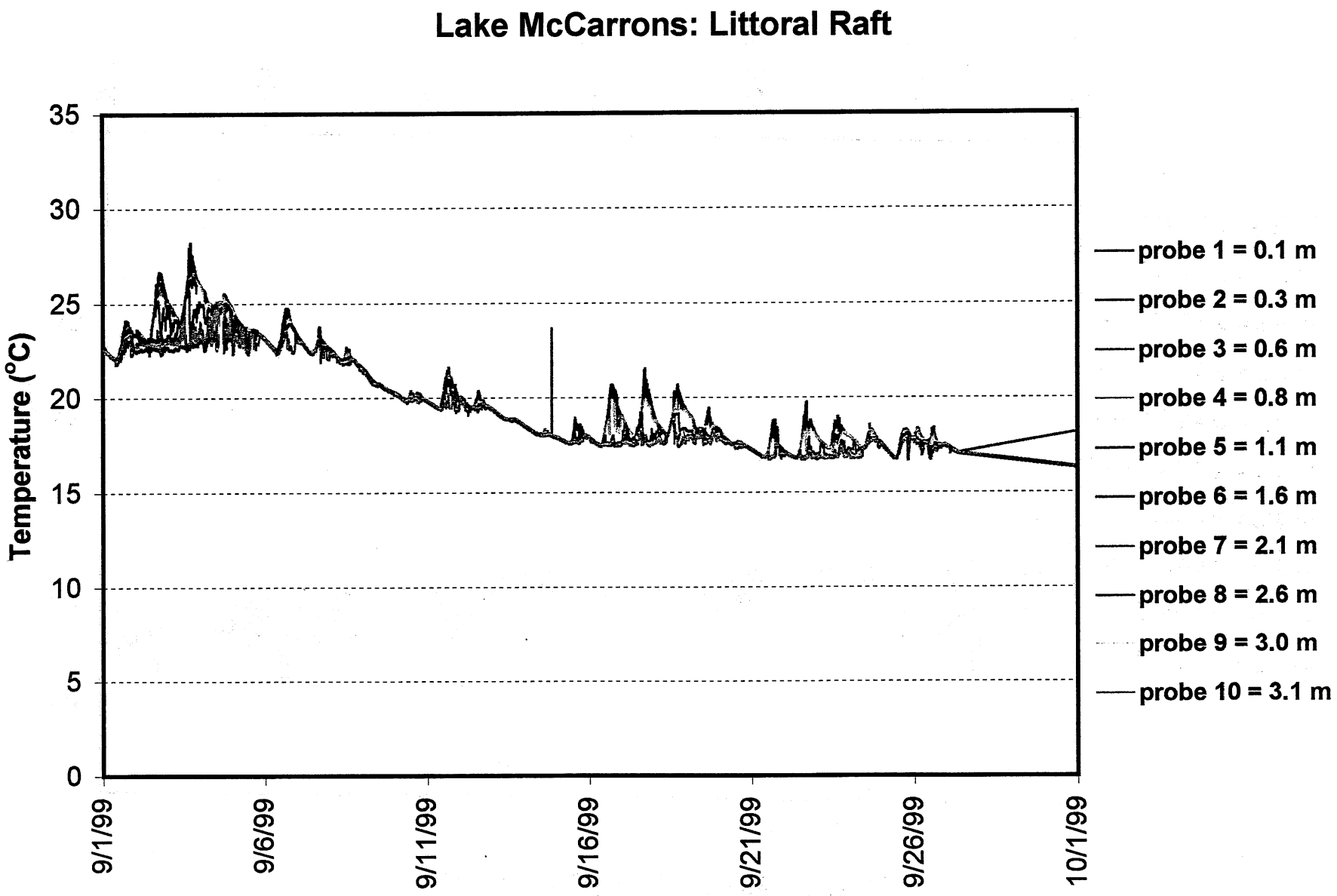
Lake McCarrons: Littoral Raft
Temperature (°C)
35
30
25
20
15
10
5
0
9/1/99
9/6/99
9/11/99
9/16/99
9/21/99
9/26/99
10/1/99
probe 1 = 0.1 m
probe 2 = 0.3 m
probe 3 = 0.6 m
probe 4 = 0.8 m
probe 5 = 1.1 m
probe 6 = 1.6 m
probe 7 = 2.1 m
probe 8 = 2.6 m
probe 9 = 3.0 m
probe 10 = 3.1 m

APPENDIX C. DYE STUDY OF MWTS OUTFLOW INTO LAKE MCCARRONS

On Tuesday, June 19, 1999, from approximately 9:30 am to 12:30 pm a dye study on the wetland outflow into Lake McCarrons in Roseville, MN, was performed by the University of Minnesota, St. Anthony Falls Laboratory and the Twin Cities Metropolitan Council--Environmental Services. The dye study was performed to verify the vertical deposition of the inflow water into Lake McCarrons predicted by the temperature differences of the inflow and the lake water. Inflow water which has a lower density than the surface water of the lake will float to the top of the lake (overflow); inflow water which has a higher density than the lake water will plunge to the bvottom of the lake (underflow); and inflow water which has a density between the low density surface water and higher density bottom water will flow to an intermediate depth (interflow). The density differences of the water are controlled by water temperature and can be estimated using water temperature except when there are large amount of dissolved solids in the water.

Rhodamine WT, a fluorescent tracer approved by the Environmental Protection Agency (EPA), was used for this study. Rhodamine WT is a highly fluorescent material with the unique ability to absorb green light and emit red light. Approximately 290 mL of 2% Rhodamine was added by trickling into the wetland outflow at the weir during a 10-minutes period (Figure C-1). The flow rate out of the wetland during the study was estimated at 0.15 cfs. The turbulence created by the flow over the weir sufficiently mixed the dye into the entire water outflow volume. The water flowing out of the culvert from under the road into the short stream was visibly pink. The stream is approximately 8-10 ft wide, 0.5 ft deep, and runs from the culvert into the lake.

The Rhodamine dyed inflow was visible coming into the lake. The concentration of Rhodamine in the lake near the inflow was measured using a Turner Fluorometer set up for continuous flow measurements. Water was pumped from a specified depth through tubing using a centrifugal pump through the fluorometer and returned to the same depth in the water column. A shallow flat-bottomed boat was used for a sampling platform. The boat was moved between sampling locations by polling to minimize disturbing the natural diffusion.

Vertical profiles of dye concentrations were collected at 15 sites. The location of the study are within Lake McCarrons is presented in Figure C-2. The location of the sampling sites within the study area are presented in Figure C-3. Data were collected starting around 10:35, approximately one hour after dye was added to the inflow. The

complete profile readings for the 15 stations are presented in Table C-1. A depth contour plot of the study is presented in Figure C-3.

At the time of the experiment the inflow temperature ranged from 15.9°C to 16.9°C, the surface water in the center of the lake ranged from 22.9°C to 23.7°C, and the surface water in the littoral region of the lake ranged from 23.0°C to 23.1°C. The water temperature at 1m below the surface in the center of the lake ranged from 22.9°C to 23.4°C and the water temperature at 1m below the surface in the littoral region ranged from 22.8°C to 22.9°C. For the study area with water depth ranging from 0.5 ft to 3.5 ft the inflow water was therefore expected to be plunging.

Contour plots of measured dye concentrations in the surface water and in the bottom water are presented in Figures C-4 and C-5, respectively. Comparison of the two figures shows that the inflow plunged to the bottom as expected. Individual fluorometry readings confirm the existence of a plunging (sinking) flow by the higher dye concentrations in the bottom water (Table C-1). Figure C-5 also shows that the water from the inflow tends towards the east-southeast before dispersing in the deeper parts of the lake. While sampling, it was noted that the area to the northeast of the inflow was shallower than the rest of the area (Figure C-3). It is speculated that this may be due to sediment deposition entering the lake before the wetland outflow was modified. The shallow area to the north may be forcing the water flow to the southeast. The inflow appears to be following the path of the deepest water (Figures C-3 and C-5).

Log contour plots of equal dye concentrations in the surface water and in the bottom water are presented in Figures C-6 and C-7, respectively. The log contour plots emphasize the lower concentration differences, especially in the range between 1 and 10. The log contour plot of the dye in the surface water indicates that most locations have low levels of dye. This is not unexpected, as the water depth is shallow (less than 1.5 ft) in most of the study area. The log contour plot of the bottom water like the cartesian plot shows that the highest concentrations are near the bottom and flow into the lake in a south-easterly direction.

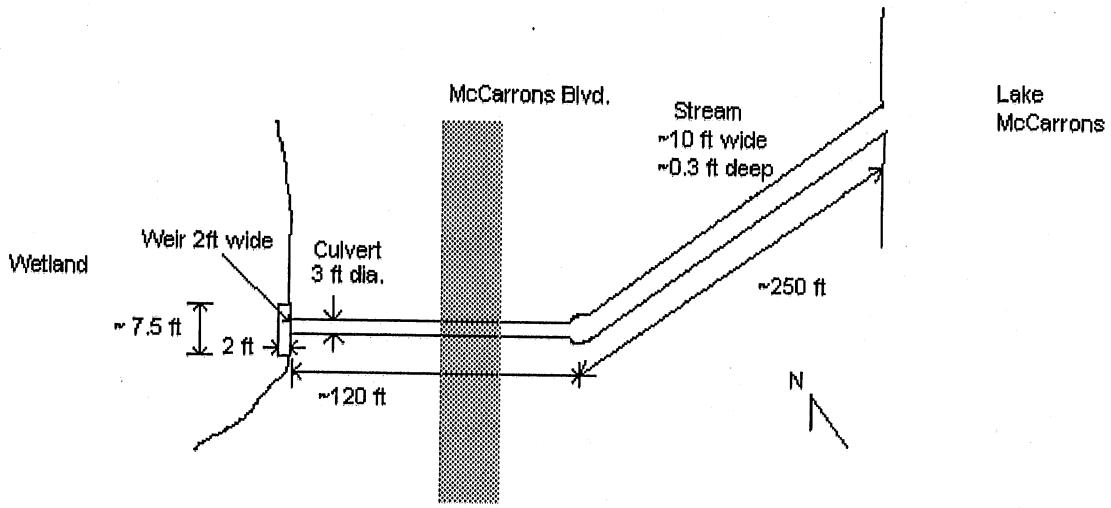

Figure C-1. Connection between Lake McCarrons wetland and Lake (schematic).

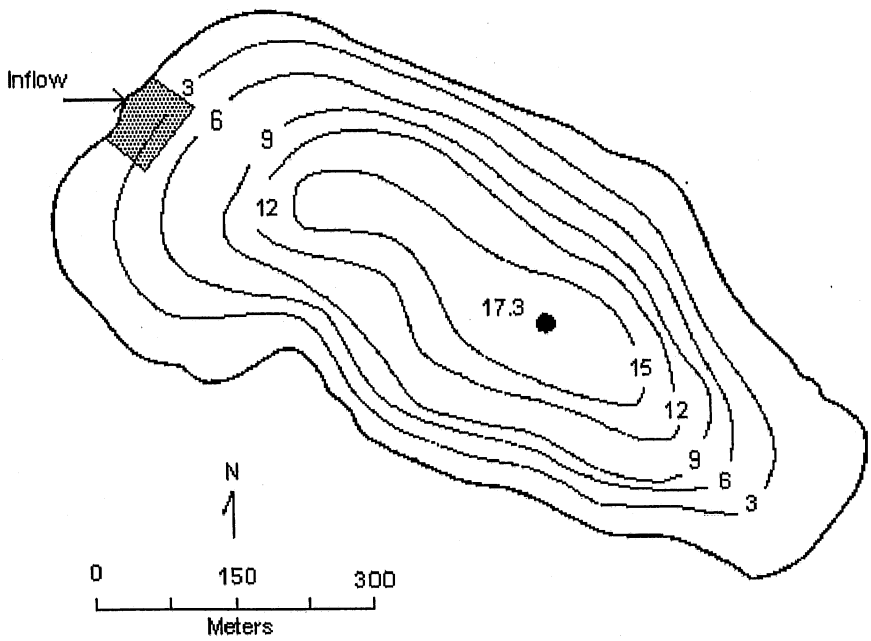

Figure C-2. Location of the study area in Lake McCarrons. Study area is shaded.

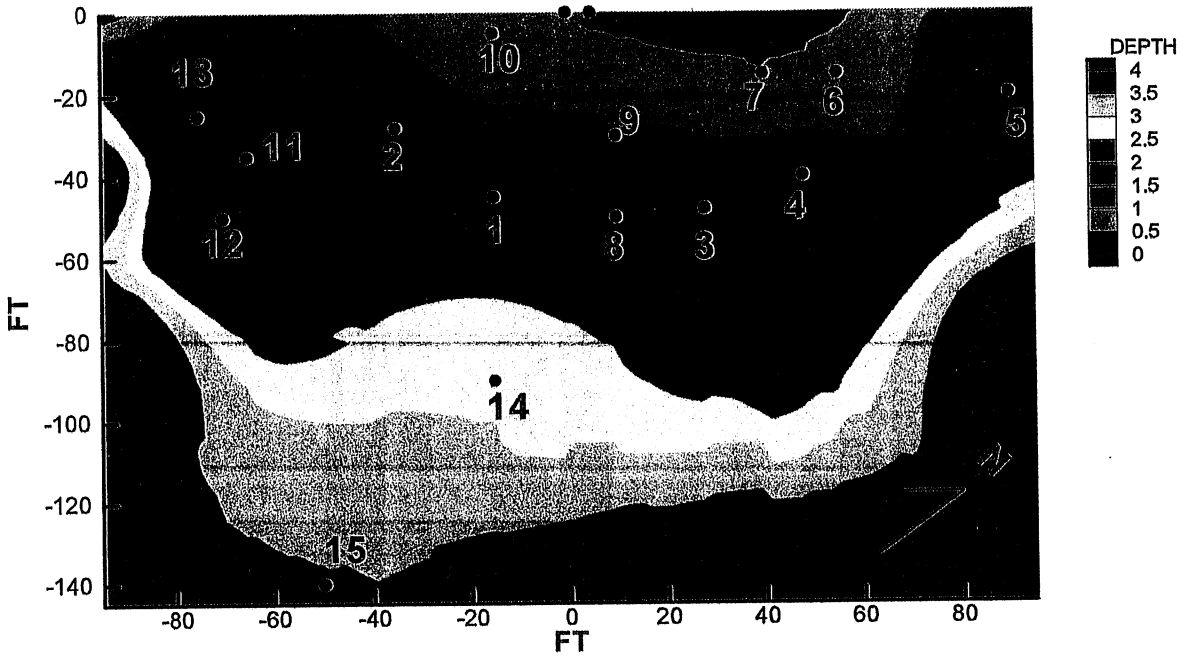

Figure C-3. Site locations in study area and contour plot of the water depth (ft).

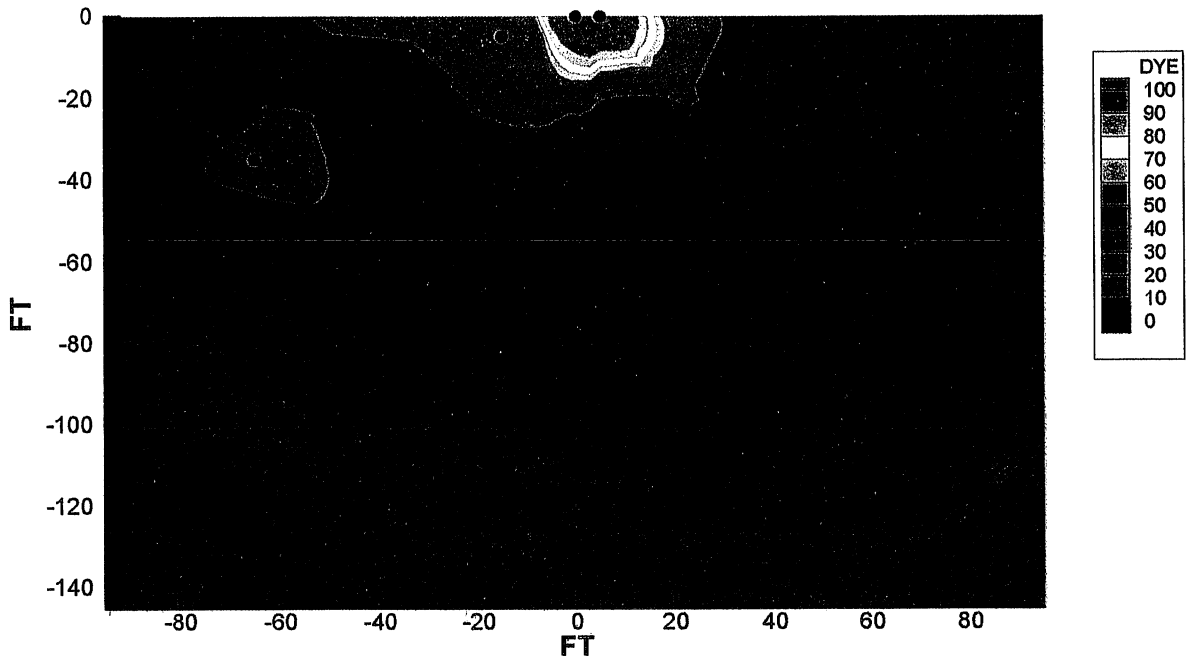

Figure C-4. Contour plot of the Rhodamine concentrations (%) in the surface water of Lake McCarrons.

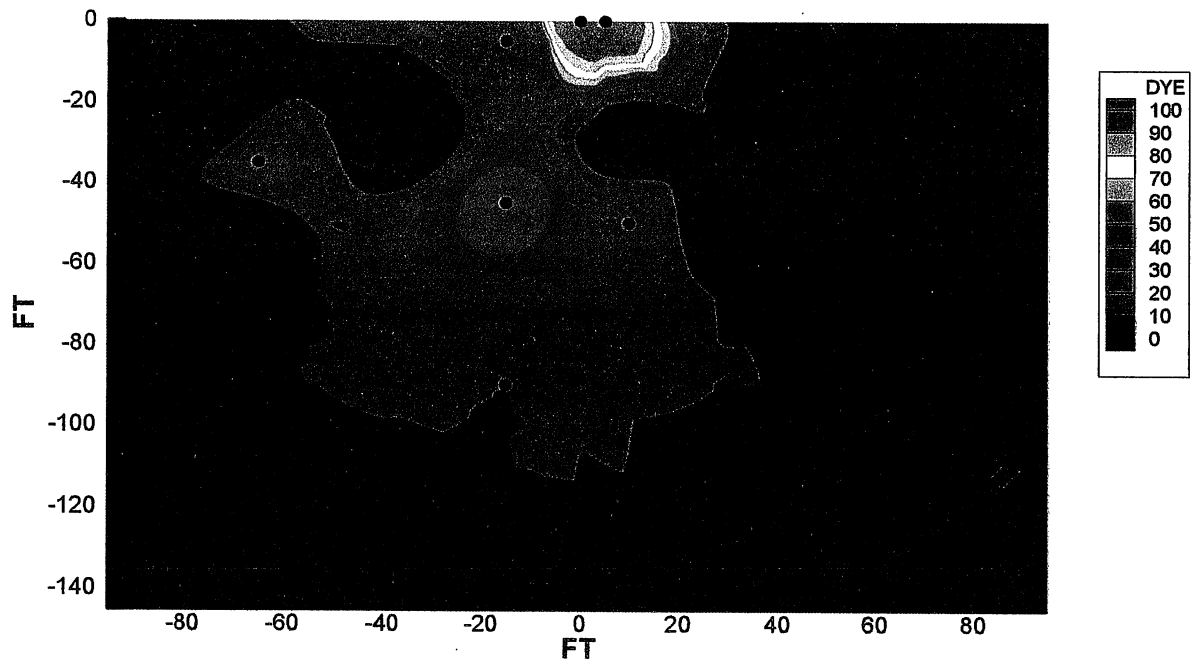

Figure C-5. Contour plot of the Rhodamine concentrations (%) in the bottom water of Lake McCarrons.

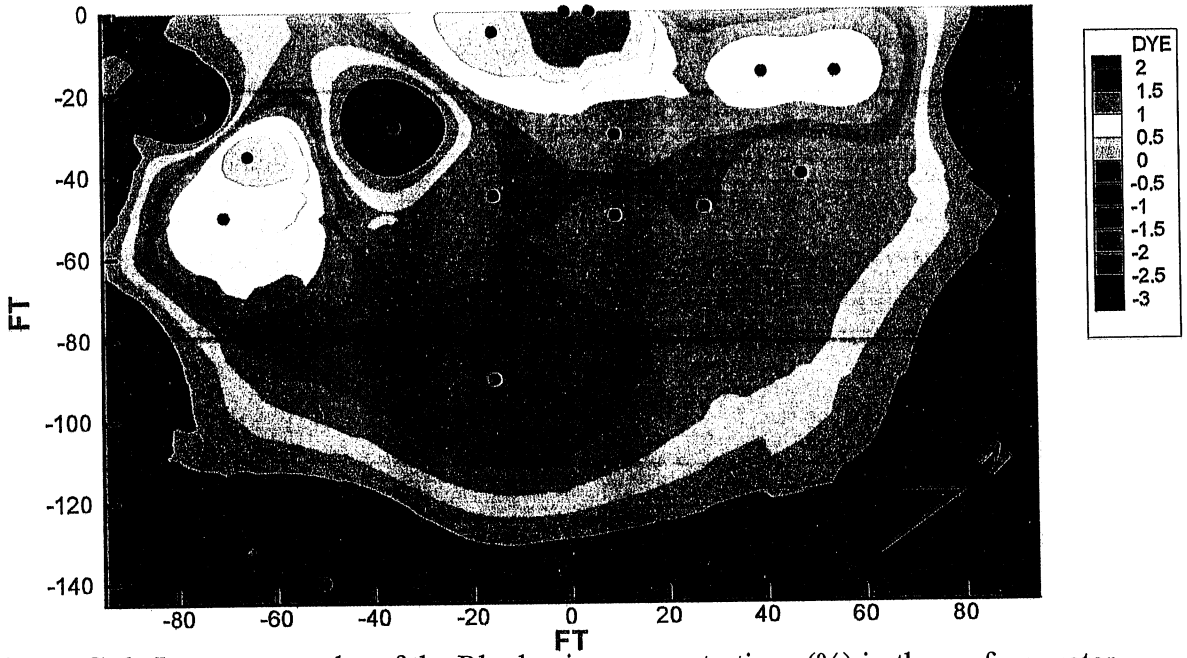

Figure C-6. Log contour plot of the Rhodamine concentrations (%) in the surface water of Lake McCarrons.

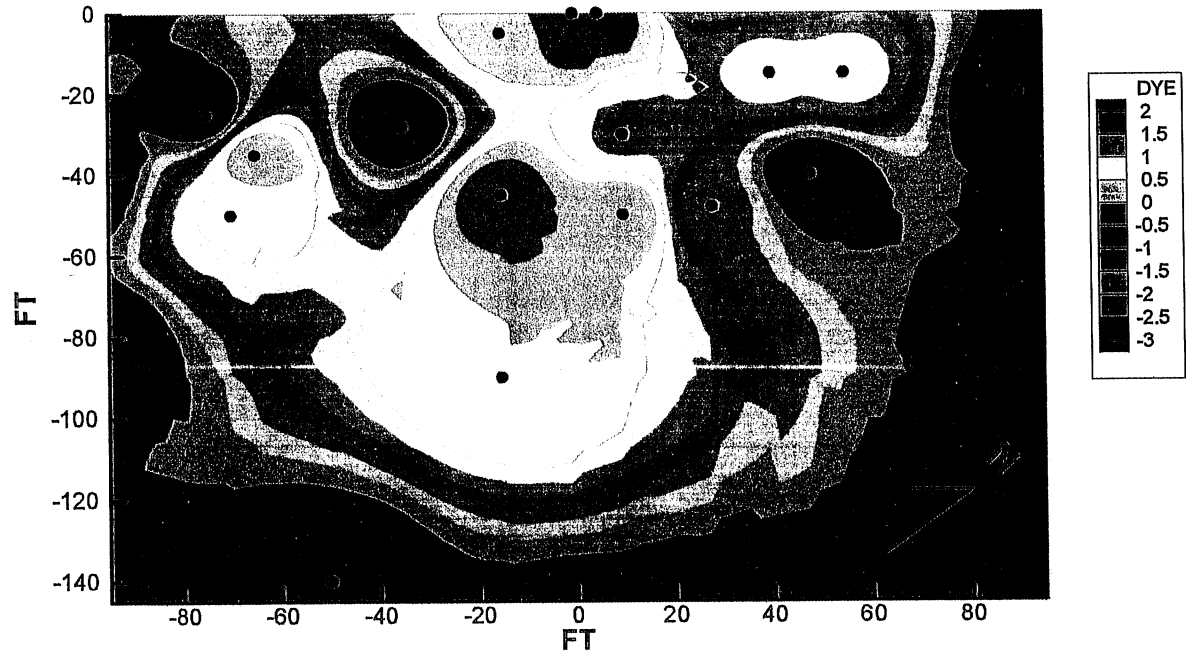

Figure C-7. Log contour lot of the Rhodamine concentrations (%) in the bottom water of Lake McCarrons.

TABLE C-1

Station 1	~10:35
Depth (ft)	Reading
0.5	<0.1
1	0.0 - 0.3
1.5	0.1 - 1.0
1.75	30 - 80

Station depth: 2 ft

Station 2	~10:45
Depth (ft)	Reading
0.5	0
1.25	0

Station depth: 1.5 ft

Station 3	~10:55
Depth (ft)	Reading
0.5	0.1
1	0.05

Station depth: 1.25 ft

Station 4	~11:05
Depth (ft)	Reading
0.5	0.04
1	0
1.25	0

Station depth: 1.3 ft

Station 5	~11:15
Depth (ft)	Reading
0.5	0
1	0
1.5	0
2	0

Station depth: 2.5 ft

Station 6	~11:25
Depth (ft)	Reading
0.25	1.5

Station depth: 0.5 ft

Station 7	~11:35
Depth (ft)	Reading
0.25	1.4

Station depth: 0.5 ft

Station 8	~11:45
Depth (ft)	Reading
0.5	0.08
1	28

Station depth: 1.5 ft

Station 9	~11:55
Depth (ft)	Reading
0.5	0.9

Station depth: 1 ft

Station 10	~12:05
Depth (ft)	Reading
0.25	16

Station depth: 0.5 ft

Station 11	~12:15
Depth (ft)	Reading
0.5	18
1	3-9
1.25	22

Station depth: 1.5 ft

Station 12	~12:25
Depth (ft)	Reading
1	3
1.5	3.6

Station depth: 1.5 ft

Station 13	~12:35
Depth (ft)	Reading
1	0

Station depth: 1.5 ft

Station 14	~12:45
Depth (ft)	Reading
0.5	0.2
1	1.2
1.5	0.6
2	0.7-4
2.5	7.5-10
2.75	10

Station depth: 3.0 ft

Station 15	~12:55
Depth (ft)	Reading
3.5	0

Station depth: 3.5 ft

Table C-1

APPENDIX D: SUPPORTING DATA FOR WETLAND TEMPERATURE MEDIATION STUDY

Table D-1. Approximate Wetland Geometry.

	H (in)	**A (acres)**	**V (acre ft)**	**W (ft)**	**L (ft)**	**w (-)**
Main Sedimentation Basin (May 1988) (Nov. 7, 1996)	 (28) 36	 (2.4) 2.4	 (2.3) 7.2	 (170) 170	 (440) 440	 0.5
Hockey Rink Sedimentation Basin (Nov. 7, 1996)	36	1.2	3.6	120	150	0.5
Outlet Wetland	12	2.4	2.4	230	400	0.5
Wetland 1	12	1	1	50	470	0.8
Wetland 2	12	0.2	0.2	50	100	0.8
Wetland 3	12	0.3	0.3	60	100	0.8
Wetland 4	12	0.3	0.3	70	90	0.5
Wetland 5	12	0.4	0.4	50	180	0.5
Totals		8.2	15.4		2370	

$$H_{ave} = \frac{V}{A} = \frac{15.4}{8.5} = 1.8 \text{ ft}$$

$$W_{ave} = \frac{A}{L} = \frac{8.2x43560}{2370} = 150 \text{ ft}$$

$w_{ave} = 0.5$ or more

Table D-2. Runoff from Precipitation of 2.7 inches in 24 hours; largest observed from March 11, 1995 to November 7, 1995 (period of intensive water quality surveys by the MCES)

	Runoff (acre ft/day)	**Runoff (cfs)**
Site A	26.5	13.25
Site C	10.1	5.05
Site D	9.5	4.75
Site E	14.5	7.25
Site F	1.5	0.75
Site G	27.5	13.75
Average A+G	27	13.5

Baseflow at Site A ~ 0.05 to 0.12 cfs: Q_r=0.1 cfs=0.2 acre-feet/day
Typical non-storm summer flow at Site A in 1995/96: Q_r= 1 acre-ft/day

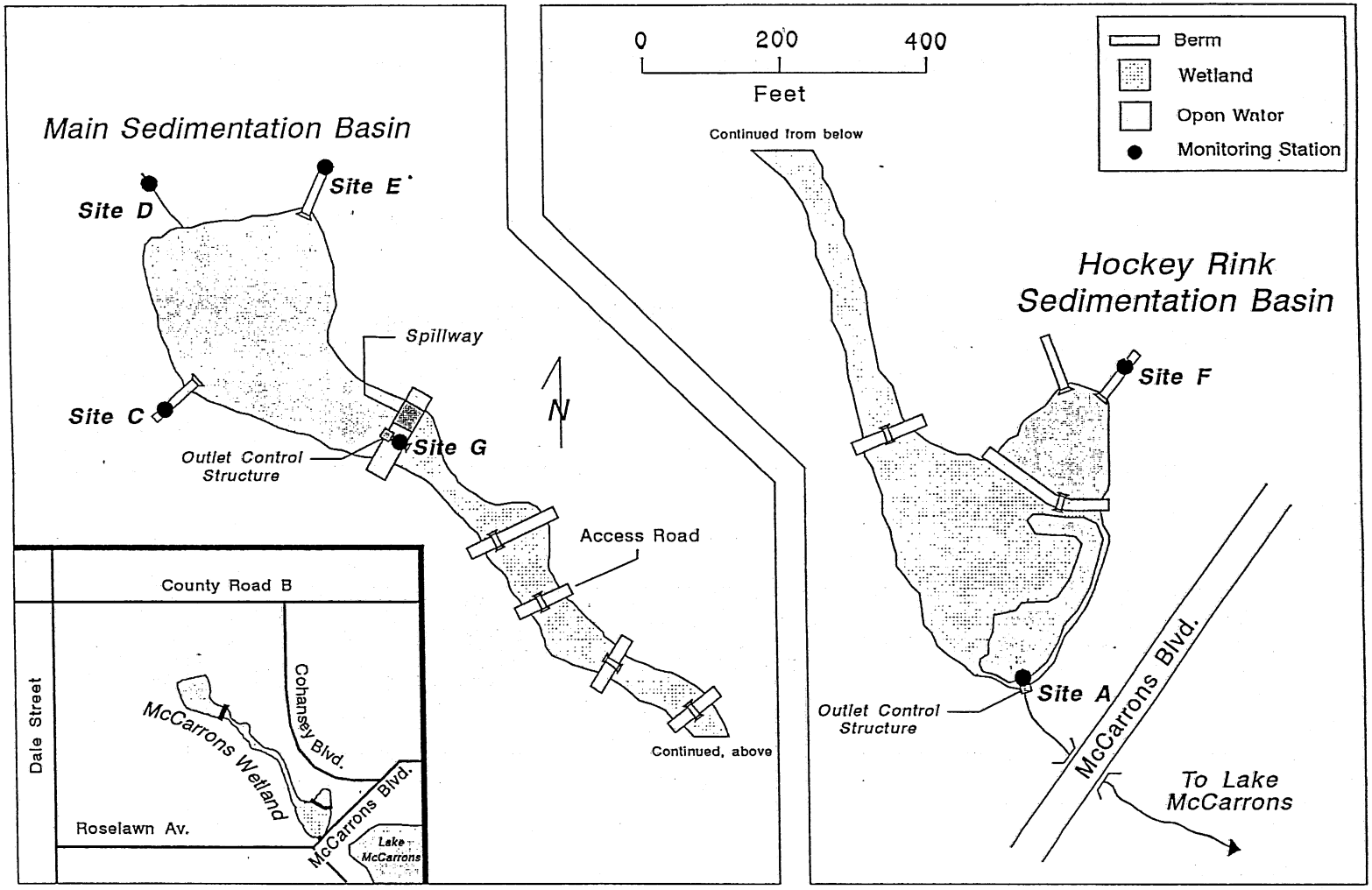

Figure D-1. Layout of McCarrons wetland system and monitoring stadtions (from MCES, 1997).

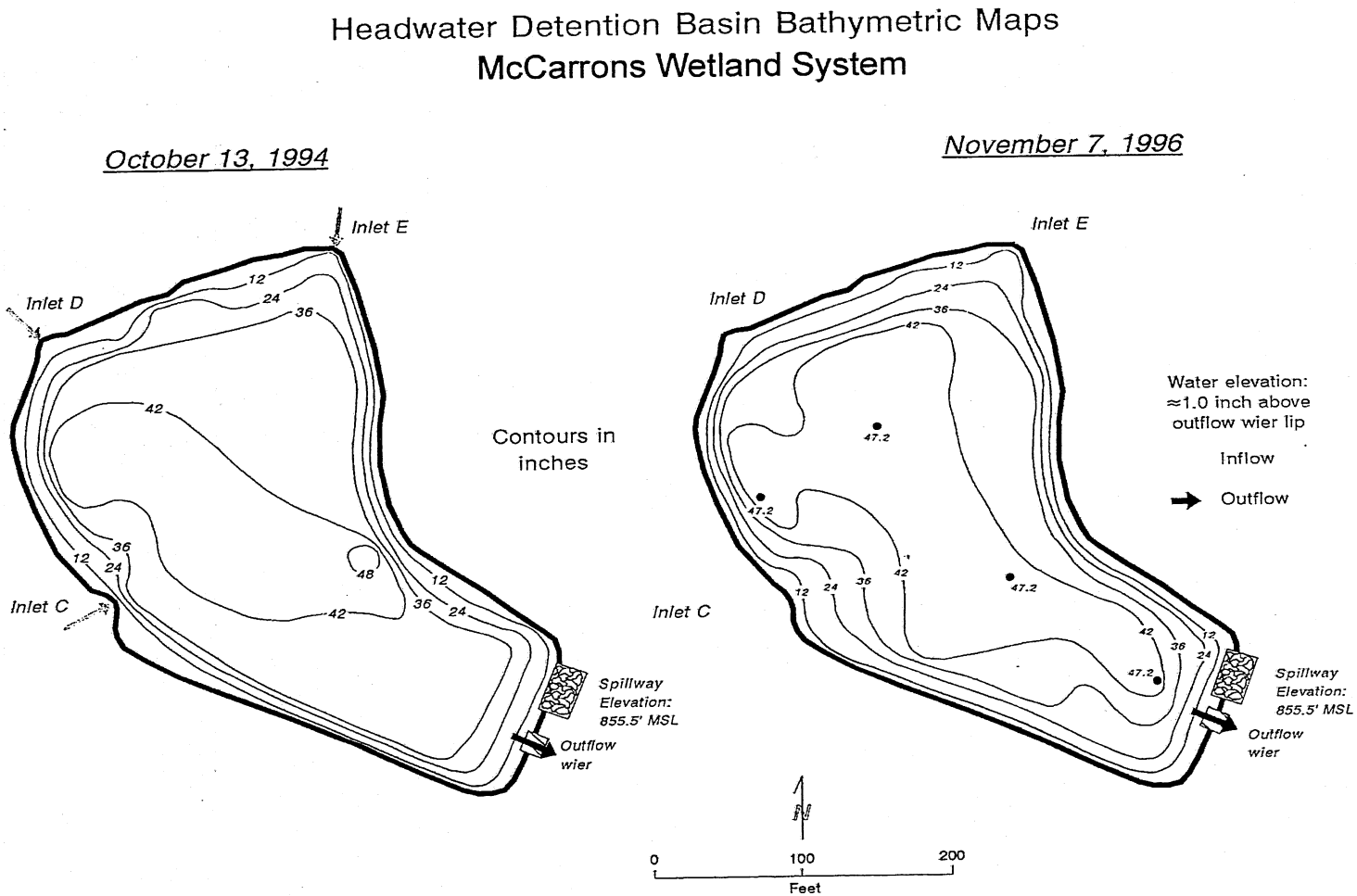

Figure D-3. McCarrons wetland treatment system headwater detection basin bathymetry (from MCES, 1997).

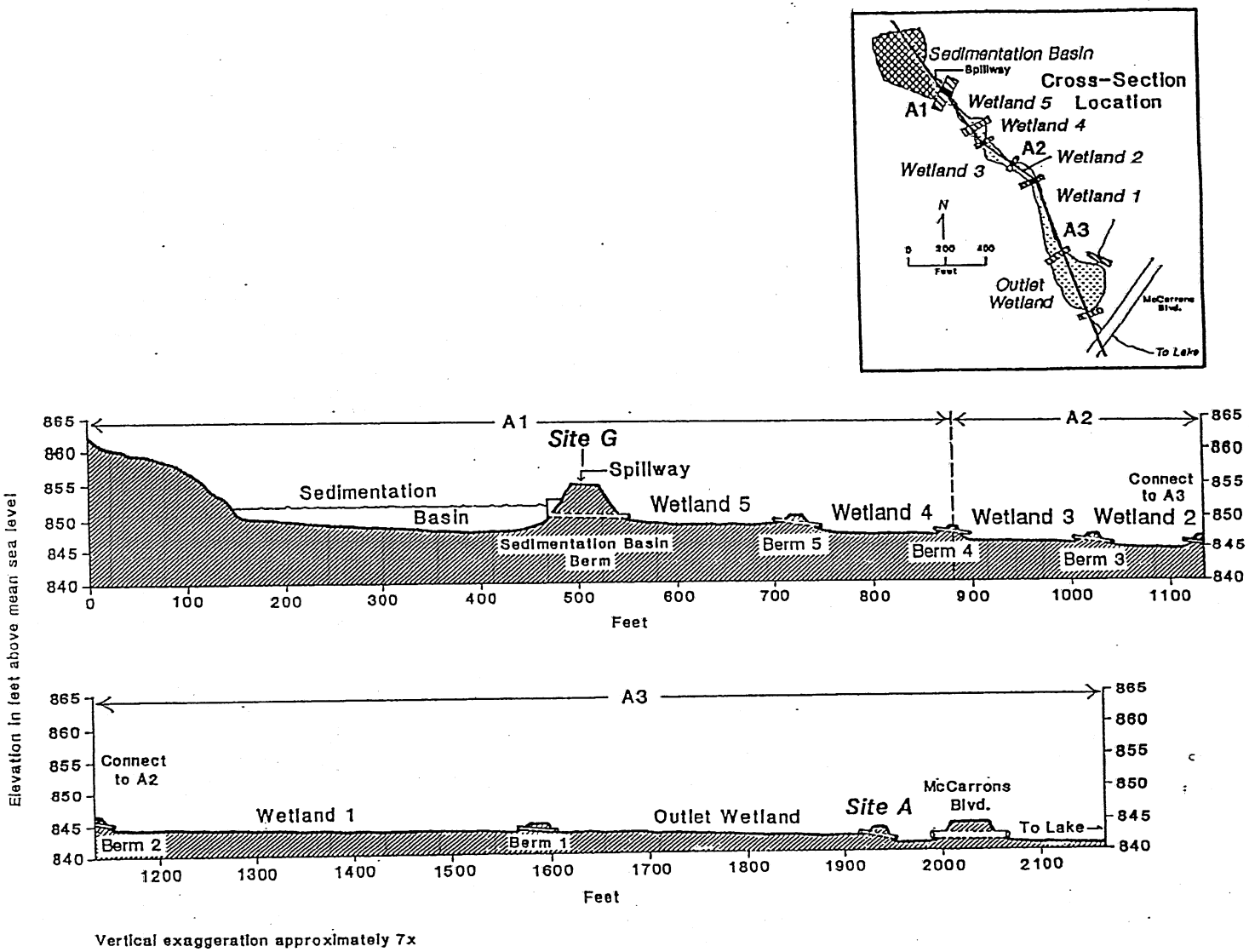

Figure D-2. Longitudinal section through McCarrons wetland system (from MCES, 1997).

Hockey Rink Detention Pond Bathymetric Maps
McCarrons Wetland System

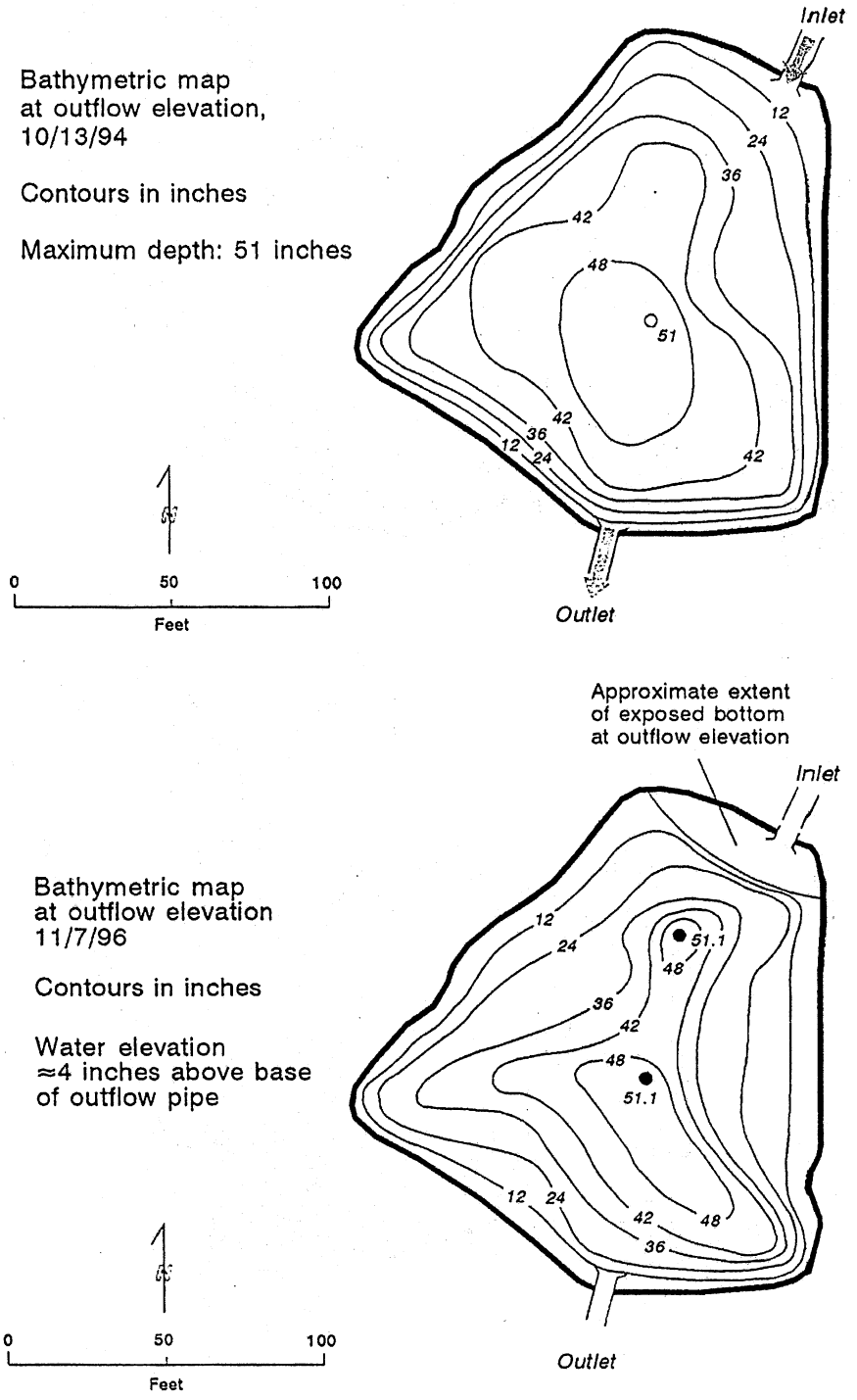

Figure D-4. McCarrons wetland treatment system hockey rink detection pond bathymetry (from MCES, 1997).

Rainfall-Runoff Relationships for Monitored Sites Influenced by Alameda Pond.

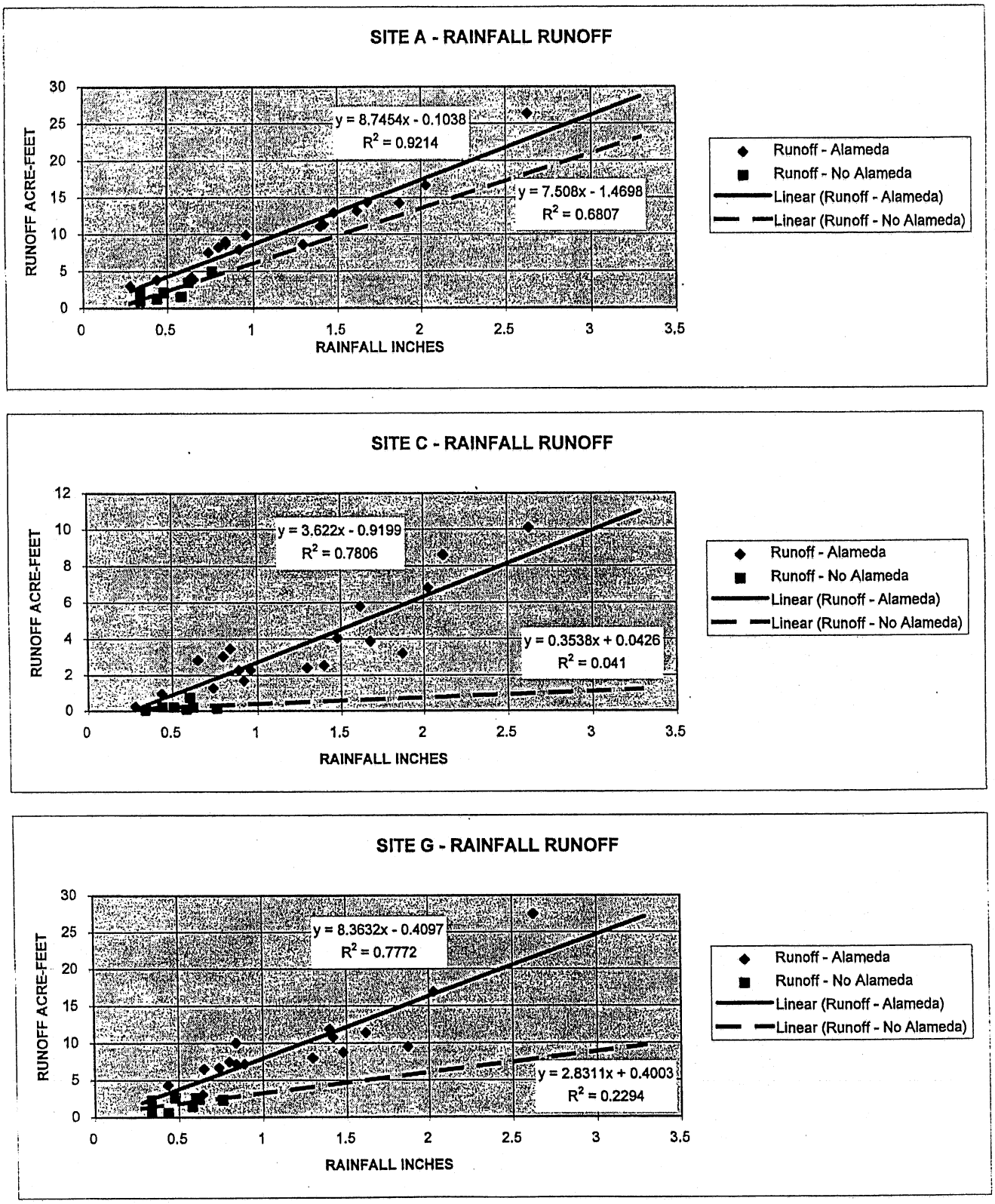

Figure D-5a. Rainfall-runoff relationships for monitored sites (from MCES, 1997)

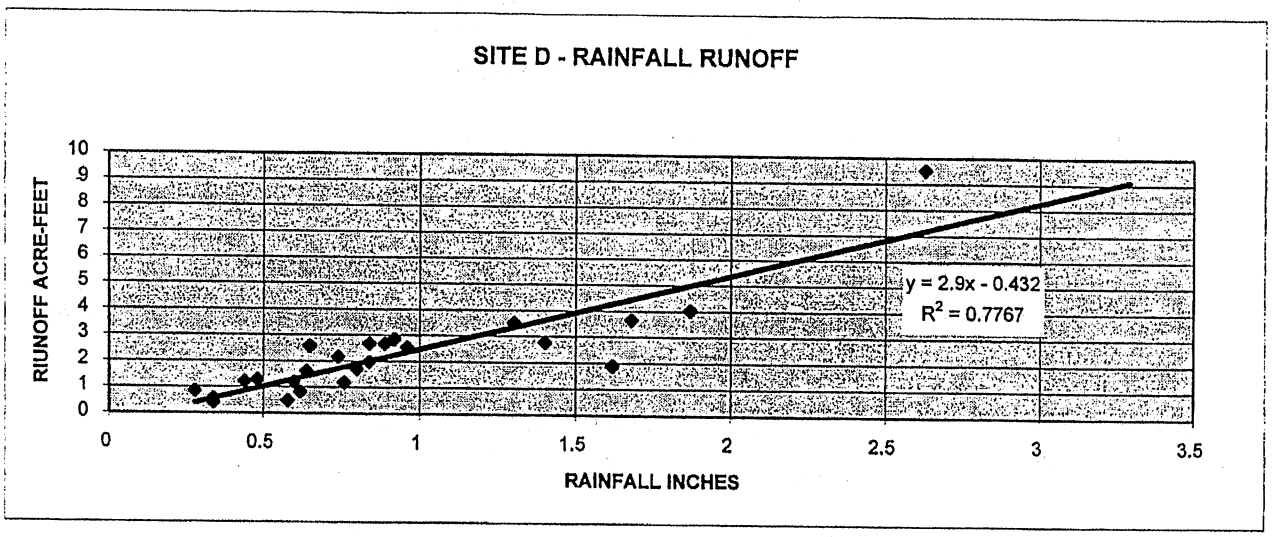

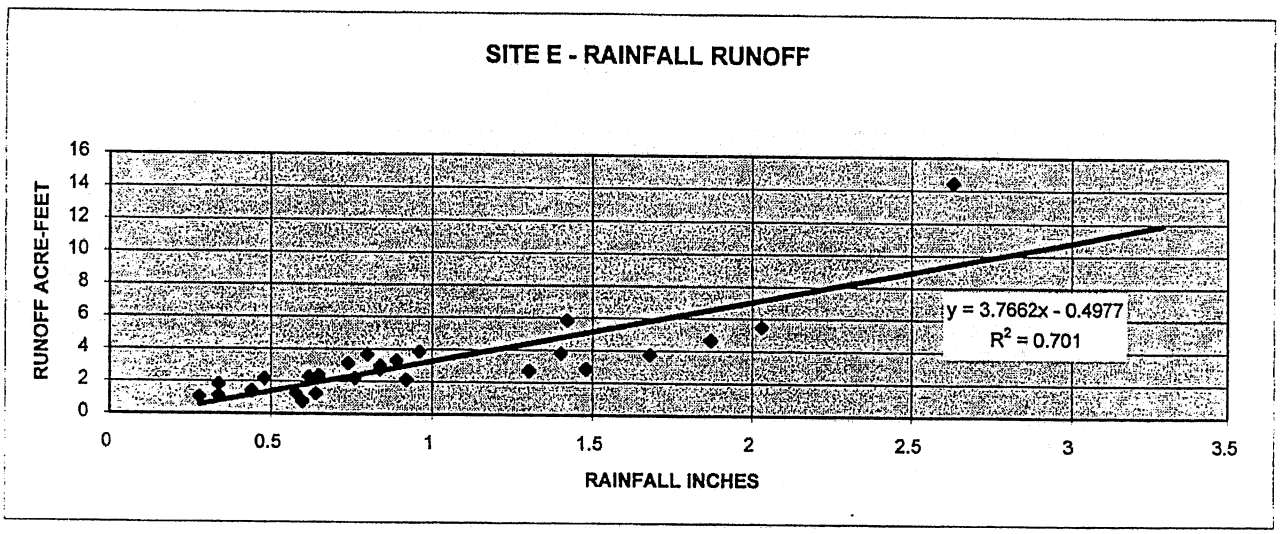

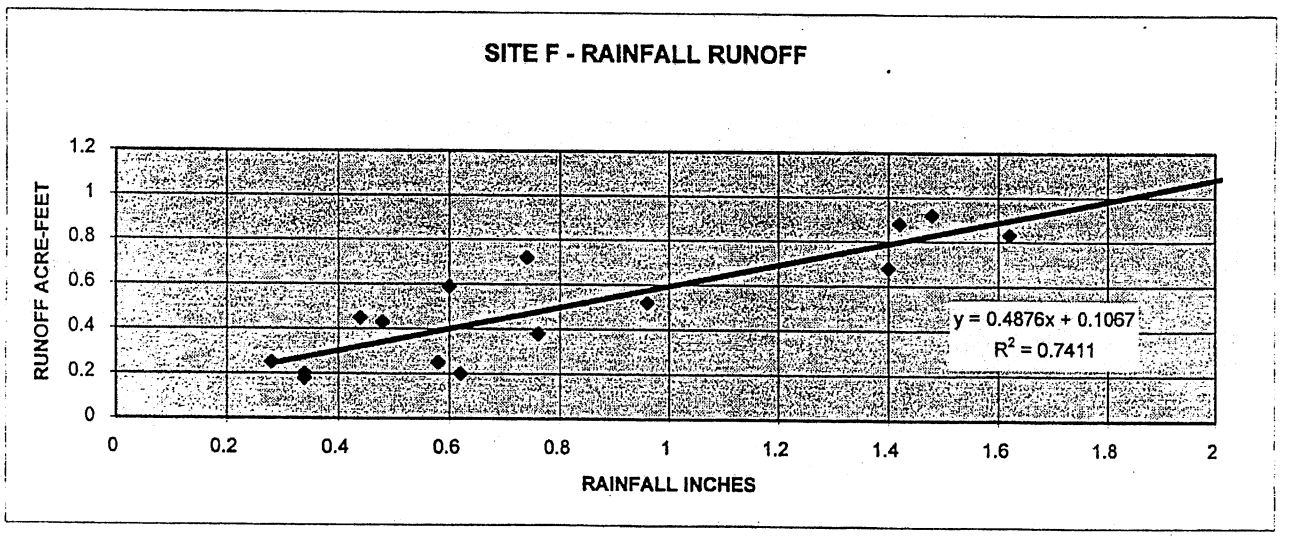

Figure D-5b. Rainfall-runoff relationships for monitored sites (from MCES, 1997).

Figure D-6. Daily flow plots - Sites A and G (from MCES, 1997)

APPENDIX E. DESCRIPTION OF THE MINLAKE98 LAKE WATER QUALITY SIMULATION MODEL

E.1. Phytoplankton (Chlorophyll *a*)

Chlorophyll *a* is used in MINLAKE as an indicator of phytoplankton standing crop (primary productivity) in a lake. Up to three algal groups can be simulated by the MINLAKE model (Riley and Stefan, 1988). A schematic diagram of the phytoplankton cycle is presented in Figure E.1. This cycle is applicable to each algal group. Different coefficients and rates are used to represent a specific group.

Phytoplankton (chlorophyll) growth is simulated by external nutrient limitation using a Michaelis-Menten growth function. Light and phosphorus limitation are simulated. Nitrogen limitation for green algae as well as silica limitation for diatoms is also available. Respiration and mortality are combined in Riley's program but have been separated in MINLAKE98 to allow for differing rates. Respiration removes biomass (chlorophyll) and releases a proportional amount of nutrients directly to the water column. Nonpreditory mortality does not directly release nutrients to the water column but contributes to the detrital mass (BOD). Diffusion of chlorophyll occurs between layers at the same rate as heat (temperature). Loss of chlorophyll *a* due to grazing is treated separately as it is the result of the mobility of zooplankton. Settling results in the removal of chlorophyll from a layer and a contribution to the next layer (or the sediment).

The differential equation representing chlorophyll in the one-dimensional model is given as equation E.1. The losses of phytoplankton (chlorophyll) due to nonpreditory mortality, zooplankton grazing, and respiration are calculated as first order sink terms. Growth is calculated as a zero order source term to maintain stability of the equation.

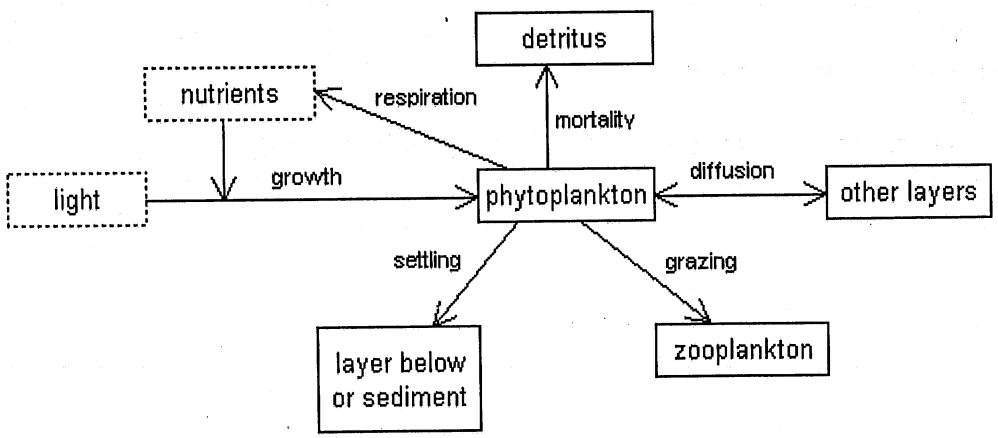

Figure E.1. Processes (arrows) and components (boxes) comprising the phytoplankton (chlorophyll) submodeled in MINLAKE98.

$$\frac{\partial Chla}{\partial t} - \underbrace{\frac{1}{A}\frac{\partial}{\partial z}\left(AK_z\frac{\partial Chla}{\partial z}\right)}_{diffusion} + \underbrace{\frac{V}{A}\frac{\partial(AChla)}{\partial z}}_{advection} + \underbrace{K_m\theta_m^{T-20}Chla}_{mortality} + \underbrace{K_r\theta_r^{T-20}Chla}_{respiration}$$

$$\underbrace{+Gr_{max}\frac{Chla - Chla_{min}}{Chla - Chla_{min} + HSC}\theta_z^{T-20}ZPV_r}_{\substack{zooplankton \\ grazing}}$$

$$\underbrace{-G_{max}f(T)\left[\frac{I\left(1+2\sqrt{K_1/K_2}\right)}{I+K_1+I^2/K_2}:\frac{P}{K_P+P}:\frac{N}{K_N+N}:\frac{Si}{K_{Si}+Si}\right]_{min}Chla}_{growth} = 0 \qquad \text{(E.1)}$$

Individual parameters used in this equation are identified in the list of symbols.

Phytoplankton growth is dependent upon several factors:

- the maximum intrinsic growth rate of the algae ,
- the nutrient half-saturation coefficient,
- the water temperature,
- the solar irradiance,
- the external nutrient concentration, and
- the current chlorophyll concentration.

The **maximum growth rate** of algae varies between classes of algae and even at the species level. A range of values given by several researchers and summarized by EPA (1985) is presented in Table E.1. Most of the maximum growth rates are between 0.9 /d and 2.0 /d. Calibration of the maximum growth rate coefficient, G_{max} , with chlorophyll field data is necessary.

MINLAKE98 is a 'fixed stoichiometry model' where the nutrient composition of the algal cells is assumed to remain constant. The growth of the algae is assumed to be a function of the **external nutrient concentration** using a Michaelis-Menten type relationship. The Michaelis-Menten growth limiting factor, f(S), for a nutrient S is

$$f(S) = \left(\frac{S}{K_S + S}\right) \qquad \text{(E.2)}$$

where

S = concentration of the nutrient in the water (mg/L)
K_S = half-saturation constant for the nutrient (mg/L).

Growth limitation by phosphorus, nitrogen, and/or silica can be simulated by the MINLAKE98 model.

In the Michaelis-Menten growth limiting factor, both the concentration of the nutrient and the half-saturation constant for each nutrient are determining. Each species of phytoplankton has its own half-saturation constant for a given nutrient. Most of the half saturation values for phosphorus are between 0.001 mg/L and 0.02 mg/L with the lower values associated with diatoms. Most of the half saturation values for nitrogen are between 0.03 mg/L and 0.1 mg/L. The half saturation values for silica are between 0.03 mg/L and 0.1 mg/L (only diatoms require substantial amounts of silica).

Table E.1. Phytoplankton Maximum Growth Rates and Half-Saturation Constants for Phosphorus, Nitrogen, and Silica. (EPA, 1985)

Algal Type	Maximum Growth Rate[1] (1/d)	Half Saturation Constant for P[1] (mg/L)	Half Saturation Constant for N[1] (mg/L)	Half Saturation Constant for Si[1](mg/L)
Total Phytoplankton	0.2 - 8.0	0.0005 - 0.08	0.0014 - 0.4	-
Green	0.7 - 9.2	0.002 - 0.475	0.001 - 1.236	-
Blue-green	0.2 - 11.0	0.0025 - 0.06	0.0 - 4.34	-
Diatoms	0.55 - 5.0	0.001 - 0.163	0.003 - 0.923	0.03 - 0.1

[1]Values are from experimental measurements reported in the literature and from documented models.

Water **temperature** affects the growth rate of the phytoplankton substantially. Lehman (1975) provided a function where the maximum yield occurs at an optimal temperature, T_{opt}; the growth rate coefficient decreases both above and below this temperature.

$$x = exp\left(-2.3\left(\frac{T - T_{opt}}{T_{opt} - T_{min}}\right)^2\right) \qquad for\ T < T_{opt}$$

$$x = exp\left(-2.3\left(\frac{T - T_{opt}}{T_{max} - T_{opt}}\right)^2\right) \qquad for\ T > T_{opt} \qquad \text{(E.3)}$$

The "minimum temperature" T_{min} is the low temperature at which phytoplankton growth is reduced 90 percent. Riley's program assumed T_{min} = 0.0 °C. This is a good assumption for some phytoplankton species but not all. MINLAKE98 includes a variable for "minimum temperature" as part of the input to allow for more flexibility in simulating chlorophyll growth temperature limitations. Temperature limitations can vary with algae class as well as at the species level. Table E.2 summarizes literature values reviewed in the CE-QUAL-R1 User's Manual (US Army Corps of Engineers, 1982). The "optimum temperature", T_{opt}, gives the range of temperatures for which growth is occurring near the maximum rate. The "maximum temperature", T_{max}, is the temperature at which growth is reduced 90 percent. The temperatures in Table E.2 are from a literature review in CE-QUAL-R1.

Table E.2. Optimum, Minimum, and Maximum Temperature Values for Phytoplankton. (U.S. Army Corps of Engineers, 1982)

Algal Type	Optimum Temperature[1] (°C)	Maximum Temperature[1] (°C)	Minimum Temperature[1] (°C)
Total Phytoplankton	10 - 40	15 - 42	0 - 18
Green	20 - 40	40 - 42	0 - 7
Blue-green	20 - 29	-	4
Diatoms	20 - 33	30 - 36	0 - 12

[1]Values are from CE-QUAL-R1 model documentation.

The values in Table E.1 suggest that it is important to know the type of algae, at a class level at a minimum, to accurately simulate the chlorophyll growth, respiration, mortality, grazing by zooplankton, and effect of temperature.

In many eutrophic lakes **light** is the limiting growth factor. A Haldane equation (Megard et al., 1984) is used to calculate the light limitation coefficient, L_1. This function describes both light limitation and inhibition.

$$L_I = \frac{I\left(1+2\sqrt{K_1/K_2}\right)}{I+K_1+I^2/K_2} \tag{E.4}$$

In the MINLAKE96 model (Fang et al., 1996), the light limitation and inhibition coefficients, K_1 and K_2 respectively, are calculated using an empirical equation dependent upon the temperature of the water. The light limitation coefficient, K_1, is strongly dependent upon algal species. In MINLAKE98 phytoplanton classes are simulated, and the light limitation and inhibition coefficients are specified by the user as in Riley's model.

Growth is usually limited by either light or phosphorus, depending upon which has the lowest limitation factor. When nitrogen and silica are also modeled the lowest growth limiting factor of light, phosphorus, nitrogen (greens only) and silica (diatoms only) is used to determine the phytoplankton growth rate. Carbon is considered to be available in excess on a daily timescale and is not modeled as a limiting nutrient.

Respiration rates do not appear to vary as greatly as settling rates. The range of respiration rates is presented in Table E.3 (EPA, 1985). Most respiration rates are between 0.02 /d and 0.05 /d. Mortality rates are not as well known, and only values for total phytoplankton and for diatoms are presented in Table E.3. MINLAKE98 differs from Riley's model in that respiration and nonpreditory mortality are treated separately. Respiration contributes immediately to the available phosphorus and dissolved oxygen concentration while mortality contributes with a timelag through detrital decay.

Table E.3. Phytoplankton Settling Velocities, Respiration Rates, Non-Predatory Mortality Rates, and Zooplankton Grazing Rates. (EPA, 1985)

Algal Type	Settling Velocity[1] (m/d)	Respiration Rate[1] (1/d)	Non-Predatory Mortality Rate[1] (1/d)	Zooplankton Grazing Rate[1] (mg Chla/ind. day)
Total Phytoplankton	0.0 - 30.0	0.005 - 0.8	0.003 - 0.17	
Green	0.02 - 0.89	0.01 - 0.46	-	0.0015
Blue-green	0.0 - 0.2	0.03 - 0.92	-	0
Diatoms	0.02 - 17.1	0.03 - 0.59	0.03	

[1]Values are from experimental measurements reported in the literature and from documented models.

Zooplankton grazing rate depends upon the class of algae available. (Zooplankton grazing on phytoplankton is simulated only to represent the dynamics of the algae and not for studying zooplankton dynamics.) A single class of zooplankton is simulated with feeding preference on algae designated by grazing rates. Zooplankton are more likely to feed on green algae than blue-green algae.

Advection is used to describe the settling of the phytoplankton (chlorophyll *a*). The settling velocity for each algal class simulated is set by the user. The settling velocity of algae, varies between classes of algae, and even at the species level. A range of values by EPA (1985) is presented in Table E.3. There is a wide range of values for each of the classes; however, in general the blue-greens exhibiting the lowest rates and the diatoms the highest rates. MINLAKE98 does not simulate the ability of some phytoplankton to float due to buoyancy (vacuoles), but this can be accounted for by adjusting the settling rate. It is necessary to calibrate the settling velocity with available field data.

E.2. Phosphorus

Phosphorus is often the principal chemical affecting phytoplankton (chlorophyll *a*) concentration in lakes. The model simulates only the readily accessible phosphate composed of orthophosphate and polyphosphate ions referred to as soluble reactive phosphorus (SRP). A schematic diagram of the principal SRP flux components is presented in Figure E.2. A schematic diagram of the SRP mass balance for the entire lake is presented in Appendix A Figure A.2. Phytoplankton growth removes SRP from the water at a mass yield ratio of approximately 1.1 mg phosphorus/mg chlorophyll *a*. Respiration releases phosphorus into the water column (Chapra, 1997). Mortality does not directly release phosphorus to the water column but contributes to the detrital mass (BOD); the phosphorus is released from the detrital mass through decay. The SRP is calculated for each layer. Diffusion of phosphorus occurs between layers but phosphorus is also transported indirectly between layers by phytoplankton and detritus settling. In MINLAKE98 there is no atmospheric deposition of phosphorus, as there is for models of Lake Superior (Chapra, 1977). Lake Superior has a considerable atmospheric input because of the large lake surface compared to the watershed area. For lakes modeled by MINLAKE98 the watershed area is usually much larger than the lake surface area. Adjustments for atmospheric input to the surface layer would be required for lakes with

large surface areas. The differential equation representing phosphorus transport is presented as equation E.5. The uptake of SRP due to phytoplankton (chlorophyll *a*) growth is calculated as a zero order sink term. Phosphorus release due to detrital decay and respiration is calculated as a zero order source term. The release of phosphorus from the lake sediment is calculated as a zero order source/sink term depending on the dissolved oxygen concentration in the overlying water.

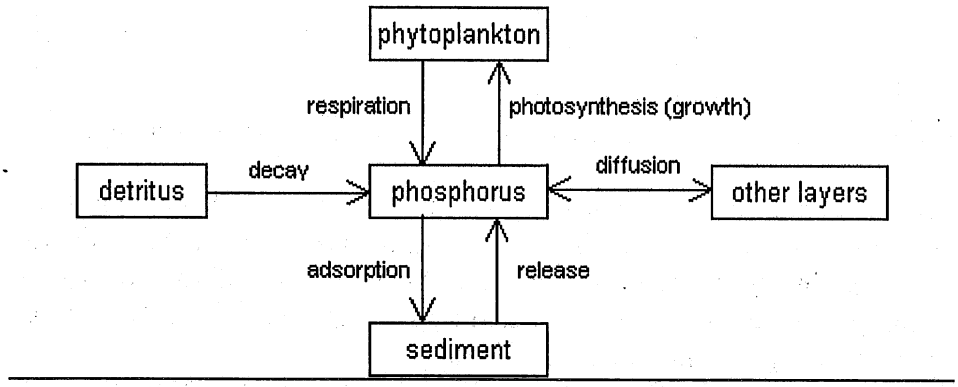

Figure E.2. Processes (arrows) and components (boxes) comprising the soluble reactive phosphorus submodel in MINLAKE98.

$$\underbrace{\frac{\partial P}{\partial t} - \frac{1}{A}\frac{\partial}{\partial z}\left(AK_z\frac{\partial P}{\partial z}\right)}_{diffusion}$$

$$\underbrace{+\sum_{n=1}^{3} G_{max} f(T)\left[\frac{I\left(1+2\sqrt{K_1/K_2}\right)}{I+K_1+I^2/K_2}\cdot\frac{P}{K_P+P}\cdot\frac{N}{K_N+N}\cdot\frac{Si}{K_{Si}+Si}\right]_{min} Y_{PCHLA}Chla_n}_{phytoplankton\ growth\ uptake}$$

$$\underbrace{-K_{BOD}\theta_{BOD}^{T-20}Y_{PBOD}BOD}_{detrital\ decay} \pm \underbrace{\frac{S_p}{A}\frac{\partial A}{\partial z}}_{\substack{sediment\\release}} \underbrace{-\sum_{n=1}^{3} K_{rn}\theta_{rn}^{T-20}Chla_n Y_{PChla}}_{\substack{chlorophyll\\respiration}} = 0 \qquad \text{(E.5)}$$

Individual parameters used in this equation are identified in the list of symbols.

MINLAKE98 differs from Riley's model in that the phosphorus uptake by algae is directly related to phytoplankton growth. Riley's model uses luxury uptake where more phosphorus is consumed than required for growth and saved for future use when phosphorus concentrations in the water are low. (See Section E.1.1 for a more detailed discussion of the effect of phytoplankton photosynthesis on the uptake of phosphorus).

A phosphorus/chlorophyll *a* yield coefficient (Y_{PCHLA}) is used to determine the amount of phosphorus consumed during photosynthesis as well as the amount of phosphorus released during algal respiration. The value of Y_{PCHLA} is the mass yield

coefficient of phosphorus to BOD (Y_{PBOD} = 0.0091 mg P/mg BOD) divided by the mass yield coefficient of chlorophyll to BOD (Y_{CBOD} = 0.0083 mg Chla/mg BOD) [$Y_{PBOD}/Y_{CBOD} = Y_{PCHLA}$]. This value of Y_{PCHLA} = 1.1 mg P/mg Chla is close to that presented by Thomann and Mueller (1987) of 1.0 µg P/µg Chla. (The Y_{PCHLA} was originally in Riley's program but later removed as it is not needed for luxury uptake simulation.) Riley's value was developed from a ratio of carbon to phosphorus [Stumm and Morgan, 1981] and a fixed chlorophyll/carbon ratio.

Point source inputs (such as municipal and industrial effluents) to many lakes in the US have been modified or diverted. This has eliminated large sources of input of phosphorus to the lakes. For many lakes with a history of progressive eutrophication the lake sediments have now become the primary source of phosphorus to the water. If the sediment-water interface is anoxic, phosphate ions go to the water at an increased rate, dependent upon the concentration difference between porewaters and the overlying water (Horne and Goldman, 1994). In many eutrophic lakes the dissolved oxygen concentration in the hypolimnion falls below 1 mg/L during both the summer and late winter (during ice cover). When this happens phosphorus, as well as other ions, are released from the sediment.

Riley uses a constant phosphorus release rate from the sediments, independent of dissolved oxygen concentration. This phosphate flux rate must be calibrated to the hypolimnetic phosphorus profile under anoxic conditions. MINLAKE98 uses a function of dissolved oxygen (DO) concentrations to specify phosphorus release from the sediments instead of a constant release rate. This is based on field data from three lakes in Minnesota were retrieved from EPA's STORET database. The data cover a wide range of years: the Square Lake data and Fish Lake data are from 1972 to 1996 and the Lake Riley data from 1980 to 1995. In all 790 pairs of dissolved oxygen and total phosphorus (TP) points were retrieved. The relationship between these two variables is presented in Figures E.3a, E.3b, and E.3c. As can be seen in Figure E.3a the concentration of total phosphorus remains fairly constant for dissolved oxygen concentrations from 2 to 14 mg/L. Although this is not a comparison of just interstitial waters, it confirms that dissolved oxygen levels below 2 mg/L appear to trigger a release of phosphorus from the sediment. Total phosphorus was plotted instead of SRP because of the limited number of SRP data points available. On average 50 percent of the total phosphorus is SRP. Monthly profiles of total phosphorus and SRP versus depth for several lakes show that total phosphorus and SRP show the same trends (Jensen, 1998). Ishikawa and Nishimura (1989) reviewed phosphate sediment flux rates. They found aerobic rates from -0.006 g/m^2d (sink) to 0.259 g/m^2d (source) and anaerobic rates from 0.060 g/m^2d (source) to 0.336 g/m^2d (source).

In MINLAKE98, dissolved oxygen concentrations of 0.2 mg/L and 1.0 mg/L are used to trigger a change in the sediment dissolved phosphorus release rate. The sediment phosphorus release rate below 0.2 mg/L DO is set by the user. The SRP release rate at DO concentrations between 0.2 mg/L and 1.0 mg/L is set to one half the release rate at DO concentrations less than 0.2 mg/L DO. The release rate for dissolved oxygen concentrations greater than 1.0 m/L is set to 0.0. Because the range in values found by various researchers is very wide, the sediment phosphorus release rate should be calibrated for each lake. The phosphorus release rate is also dependent upon temperature

(CE-QUAL-R1). During ice cover the phosphorus release rate is reduced to 50%. This value needs to be calibrated to the winter hypolimnetic phosphorus profile.

Most available data of phosphorus in lakes give total phosphorus (TP). MINLAKE98 simulates the change in SRP which is the bioavailable form. To compare simulated SRP results with TP field data, total simulated phosphorus is estimated as the sum of the dissolved phosphorus, P, the BOD concentration times the phosphorus/BOD yield coefficient, and the chlorophyll concentration times the phosphorus/chlorophyll *a* yield coefficient.

$$TP = P + BOD \times Y_{PBOD} + Chla \times Y_{PCHLA} \tag{E.6}$$

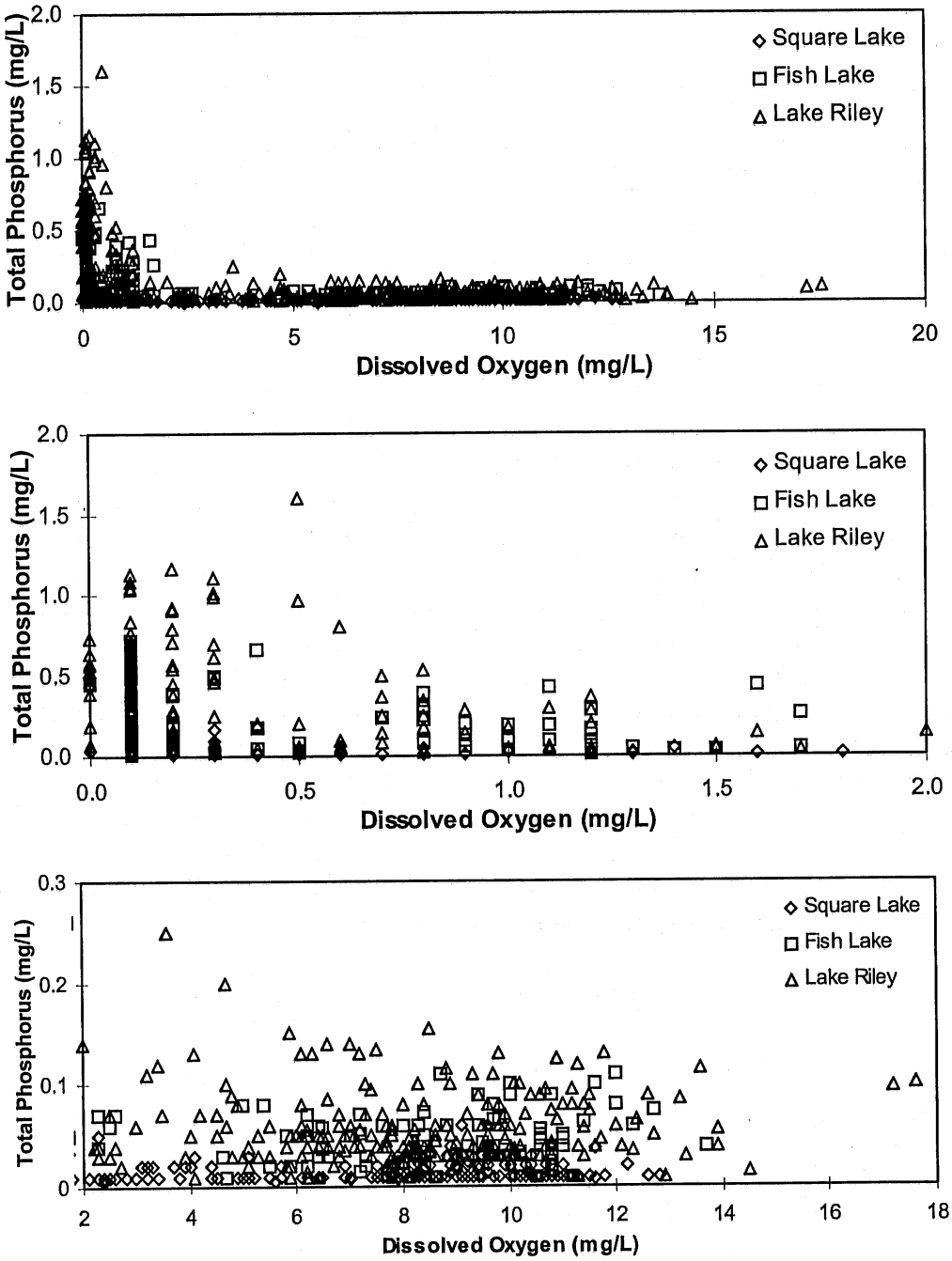

Figure E.3. Total phosphorus versus dissolved oxygen in three lakes in Minnesota (a) for the entire range of dissolved oxygen concentrations, (b) for dissolved oxygen less than 2.0 mg/L, and(c) for dissolved oxygen larger than 2.0 mg/L.

E.3 Dissolved Oxygen

A schematic diagram of dissolved oxygen (DO) fluxes in a lake is presented in Figure E.4. A schematic diagram of the dissolved oxygen mass balance for the entire lake is presented in Appendix A Figure A.6. During the open water season reaeration is a significant source of dissolved oxygen. It is possible for the phytoplankton (chlorophyll *a*) to add dissolved oxygen to the water layer through photosynthesis to the point where water is supersaturated with dissolved oxygen. In this case the dissolved oxygen is released into the atmosphere. These dynamic processes can have time scales of less than one day - the timestep of the simulation. Therefor the simulated dissolved oxygen profiles are an average over the day and not "snapshots" like observed profiles Dissolved oxygen removal from the water layer through respiration is simulated to occur at a constant rate throughout the day while photosynthesis occurs only during day light hours. The sediment oxygen demand is applied to all layers in proportion to the sediment surface area in contact with the water layer. Calibration of the sediment oxygen demand is especially important for simulating DO in the hypolimnion. Diffusion of dissolved oxygen occurs between layers of the hypolimnion. Zooplankton respiration is simulated to occur at the day depth only. Even though the zooplankton migrate during the simulated day to graze on phytoplankton, respiration in other layers is not simulated. The zooplankton spend the largest amount of their time in the day depth layer. Biochemical oxygen demand (BOD) removes oxygen from the water layer through the decay of detrital material. Nitrification removes oxygen from the water layer through the conversion of ammonia or organic nitrogen to nitrate. Nitrification is only simulated if nitrogen is simulated. The differential equation representing the dissolved oxygen transport is presented in equation E.10. Reaeration or release of oxygen at the surface layer is calculated as both a first order source/sink term. Respiration, photosynthesis, zooplankton respiration, sediment oxygen demand, BOD, and nitrification are calculated as a zero order (with regard to oxygen) source/sink terms.

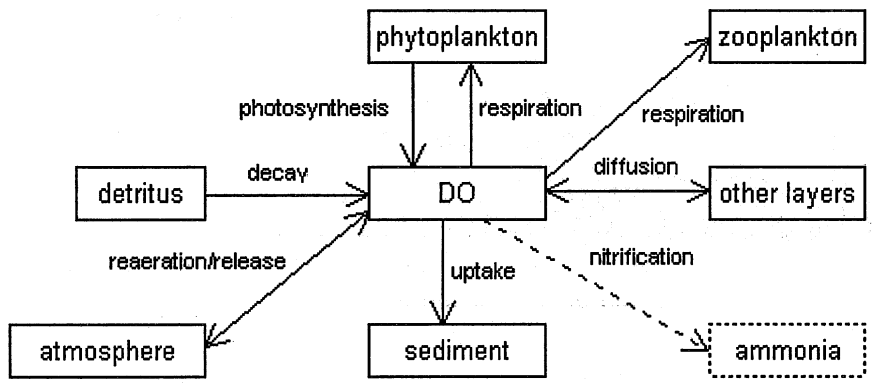

Figure E.4. Processes (arrows) and components (boxes) comprising the dissolved oxygen submodel in MINLAKE98. Nitrificiation is simulated only if nitrogen is simulated.

$$\frac{\partial DO}{\partial t} \underbrace{- \frac{1}{A}\frac{\partial}{\partial z}\left(AK_z \frac{\partial DO}{\partial z}\right)}_{diffusion}$$

$$+\frac{1}{YCHO2}\underbrace{\sum_{n=1}^{3}\left(K_{rn}\theta_{rn}^{T-20} - G_{max}f(T)\left[\frac{I\left(1+2\sqrt{K_1/K_2}\right)}{I+K_1+I^2/K_2}\cdot\frac{P}{K_P+P}\cdot\frac{N}{K_N+N}\cdot\frac{Si}{K_{Si}+Si}\right]_{min}\right)}_{respiration\ and\ photosynthesis} Chla_n$$

$$+\underbrace{K_{BOD}\theta_{BOD}^{T-20}BOD}_{\substack{detrital\\ decay}} + \underbrace{\frac{S_b}{A}\frac{\partial A}{\partial z}\theta_{SOD}^{T-20}}_{\substack{sediment\\ oxygen\\ demand}} + \underbrace{\frac{1}{YNHO2}K_{NH}\theta_{NH}^{T-20}NH}_{nitrification} - \underbrace{k\left(DO_{sat}-DO\right)_{surface}}_{\substack{reaeration\\ (surface\ only)}}$$

$$\underbrace{+0.04167TD\cdot K_{zr}\theta_{zr}^{T-20}ZP\frac{0.001}{V_{iz}}}_{\substack{zooplankton\ respiration\\ (day\ depth\ only)}} = 0 \qquad \text{(E.7)}$$

Individual parameters used in this equation are identified in the list of symbols.

Diffusion of dissolved oxygen between layers occurs similarly to heat. However, the maximum epilimnetic diffusion coefficient is different from that used for heat and is a function of the wind speed (Walters, 1978). The hypolimnetic diffusion coefficient is a function of the density and the surface area of the lake.

Fang increased the sensitivity of the model to light intensity when calculating **photosynthesis**. Riley computed the light distribution over the photoperiod in 8 subsections. The distribution is assumed to be symmetrical about a midday maximum. Fang computes the light distribution over the photoperiod in hourly subsections. The distribution is assumed to be a sine function starting from sunrise.

Fang's model differs from Riley's in that it does not simulate chlorophyll *a*. Instead a seasonal cycle is imposed on a given mean annual chlorophyll concentration. The mean annual value is selected dependent on the trophic state of a lake. Fang simulates photosynthetic oxygen production directly without calculating chlorophyll production. MINLAKE98 simulates both chlorophyll *a* and nutrients. The light intensity is used to calculate the light limitation component of photosynthetic growth (production). DO production is calculated from the biomass (chlorophyll *a*) production using a ratio of mg chlorophyll/mg oxygen released in photosynthesis. The productivity is also used to calculate the uptake of nutrients.

Respiration rates are simulated separately for each algae class (respiration rates are presented Section E.1.1). The respiration rates are also dependent upon temperature. Temperature adjustment coefficients are presented in Table E.4. MINLAKE98 uses a step-wise function to reduce the respiration rate with decreasing DO concentration. The

user defined rate is reduced to half of its value for DO concentrations less than 1.0 mg/L and set to zero for DO concentrations less than 0.2 mg/L.

For the DO simulations in a lake during the winter ice cover period oxygen consumption by plant respiration is assumed to be very small and is not represented as a separate sink term. The reasons are that phytoplankton concentrations are small and water temperatures are low.

Table E.4. Temperature Adjustment Coefficients for Dissolved Oxygen Sources and Sinks.

Source or Sink	**Range**[1]	**MINLAKE98**
Phytoplankton respiration	1.08[2]	1.08
BOD	1.02 - 1.15[3]	1.047
SOD	1.02 - 1.13[3]	1.065
Nitrification	1.0548 - 1.0997[2]	1.08
Zooplankton respiration	-	1.06

[1]Values are from experimental measurements reported in the literature and from documented models.
[2]Ethomann and Mueller, 1987.
[3]EPA, 1985.

Detritus (dead biomass) consumes oxygen as it decays. This is simulated as **biochemical oxygen demand (BOD).** The BOD decay rate, K_{BOD}, is also dependent upon temperature. A range of values is presented in Table E.5 (EPA. 1985). For MINLAKE98, a value of 0.05 d^{-1} is recommended for the open water season. The BOD decay rate is dependent upon the DO concentration the user defined rate is reduced to half of its value for DO concentrations less than 1.0 mg/L and set to zero for DO concentrations less than 0.2 mg/L. During ice cover a value of 0.03 d^{-1} which is independent of temperature is used. The value of 0.03 d^{-1} during ice cover was used successfully by Fang for several studies (Fang 1984b, Fang and Stefan, 1984a, Fang and Stefan 1996.

In MINLAKE98 the temperature adjustment coefficient, θ_{BOD}, is assumed constant. The widely used temperature adjustment coefficient value of 1.047 is used. A range of values given by several researchers and summarized by EPA (1985) is presented in Table E.4. Some researchers have found that this value is only valid for temperatures between 20°C and 30°C and suggest higher values for lower temperatures (Fair *et al.*, 1968). As the BOD concentration in a lake is frequently not measured and simulation can only be grossly calibrated, the temperature adjustment coefficient will be held constant.

Table E.5. Rate Coefficients for Dissolved Oxygen Sources and Sinks. (EPA, 1985)

Source or Sink	Range[1]	MINLAKE98
BOD	0.02 - 3.4 d^{-1}	0.05 d^{-1}
SOD	1.04 - 1.13 g $m^{-2}d^{-1}$	0.5 - 2.0 g $m^{-2}d^{-1}$
Nitrification	0.10 - 9.0 d^{-1}	0.25 d^{-1}
Zooplankton respiration	0.001 - 0.772 d^{-1}	0.002 d^{-1}

[1]Values are from experimental measurements reported in the literature and from documented models.

Sedimentary oxygen demand is treated as a sink term for each layer, since each layer is in contact with sediments. The sediment oxygen demand (SOD) is dependent upon temperature. Temperature adjustment coefficients at temperatures ranging from 10°C to 30°C given by Thomann and Mueller (1987) are presented in Table E.4. A value of 1.065 which is used by several other researchers is also used in MINLAKE98. During ice cover the SOD rate is specified according to trophic state of a lake as well as the presence of a euphotic zone (see Table E.6). The SOD values in Table E.6 are based on field studies summarized by Barica and Mathias (1979) in ice covered temperate zone lakes in Canada. The user also has the option of making the SOD rate dependent upon the presence of the euphotic zone by a user defined coefficient. (A default value of 1.0 is used by MINLAKE98 - i.e. the presence or absence of the euphotic zone does not affect the SOD rate.)

MINLAKE98 uses a step-wise function to reduce the SOD rate with DO concentration similar to that used for the BOD rate. The user defined rate is reduced to half of its value for DO concentrations less than 1.0 mg/L and set to zero for DO concentrations less than 0.2 mg/L.

Table E.6. Sediment Oxygen Demand Rates during Ice Cover.

	Eutrophic	Mesotrophic	Oligotrophic
Secchi depth (m)	$z_s < 1.8$ m	1.8 m $< z_s <$ 4.5 m	>4.5
Euphotic zone (g/m^2 d)	0.23	0.16	0.08
Below euphotic zone (g/m^2 d)	0.30	0.23	0.16

z_s = Secchi depth (m)

The consumption of oxygen through **nitrification** is simulated when nitrogen concentrations are modeled. Nitrification removes oxygen from the water layer through the conversion of ammonia or organic nitrogen to nitrate. MINLAKE98 utilizes an overall oxidation rate of the organic plus ammonia nitrogen instead of individual kinetic reactions. A range of values for the nitrification rate, K_{NH}, determined by several researchers is presented in Table E.5 (EPA, 1985). MINLAKE98 uses a values of 0.25

d^{-1}. The nitrification rate is dependent upon the DO concentration, the user defined rate is reduced to half of its value for DO concentrations less than 1.0 mg/L and set to zero for DO concentrations less than 0.2 mg/L.

Nitrification is also affected by temperature. A range of values given by several researchers and summarized by EPA (1985) is presented in Table E.4. A value of 1.08 is used by MINLAKE98.

The transfer of oxygen between the atmosphere and the surface layer depends upon the saturation value and the actual value of the water. If the water is undersaturated oxygen is transferred from the atmosphere to the water surface layer (**reaeration**). If the water is supersaturated then the oxygen transfers from the water to the atmosphere (**release**). For freshwater dissolved oxygen saturation concentration is dependent upon the temperature and the lake elevation and given by APHA (1985). The oxygen exchange coefficient determined by Wanninkhof et.al. (1990) in the field is used in MINLAKE98. The oxygen exchange coefficient can be written as (Fang and Stefan, 1994b).

$$k_e = 0.02256 \left[0.10656\, e^{(-0.0627T)} + 0.00495\right]^{-0.5} U_{10}^{1.64} \qquad \text{(E.11)}$$

Individual parameters used in this equation are identified in the list of symbols.

The oxygen gas transfer coefficient is affected by both surface water temperature and wind speed. This equation developed by Fang (1994b) is a change from Riley's which is only dependent upon wind speed and not temperature.

For the DO simulations in a lake during the winter ice cover period, Fang made modifications to account for the presence of an ice cover and low temperatures. Reaeration is set to zero because the lake ice cover prevents any significant gas exchange between the atmosphere and the water body.

Zooplankton respiration is simulated for the number of hours of daylight at the day depth only. The day depth identifies the layer in which the zooplankton are seeking refuge during the day as they are responding to predation pressure. The zooplankton tend to remain in the lowest layer of a lake where there is at least 0.5 mg/L of dissolved oxygen. No zooplankton respiration is simulated during non-daylight hours assuming that while migrating the zooplankton do not remain in one layer for enough time to significantly impact the dissolved oxygen concentration in the other layers.

APPENDIX F. LAKE MCCARRONS WINTER 1999 WATER QUALITY FIELD SURVEYS

The purpose of sampling Lake McCarrons during the winter months (January to early April) was to provide more information on the phytoplankton population during the winter, especially during ice cover. The data were included to be used to calibrate a year-round simulation of Lake McCarrons using MINLAKE98.

The sampling station was located in the middle of the lake. The station was sampled four times under ice cover (January 21, February 9, March 5, and March 16) and once a few days after ice out (April 6). The inflow water from the wetland was also sampled on these days. Water temperature and dissolved oxygen (DO) profiles were measured at the lake station. Water samples were collected at three depths: surface, mid-depth (8 m), and bottom (15 m). Water temperature and DO measurements and a water sample were collected at the weir to the outflow of the wetland into the lake. Sampling was conducted by personnel from the University of Minnesota – St. Anthony Falls Laboratory and the Twin Cities Metropolitan Council – Environmental Services. Water samples were analyzed by the Metropolitan Council Environmental Services.

Measurements and sampling

The following steps where taken to collect water temperature and dissolved oxygen profiles and water samples for analysis. This method was used to minimize the disturbance in the water column due to drilling a hole in the ice.

1. A hole for the collection of water was drilled using a power auger. The thickness of the ice was noted.
2. Another hole for the measurement of temperature and dissolved oxygen profiles was drilled approximately 15 ft to 20 ft away. The hole was drilled with the power auger until just the center spike was completely through the ice.
3. The drilled hole was allowed to fill with water.
4. The rest of the hole was chipped out using an ice pick.
5. Temperature and dissolved oxygen measurements were made from the surface down.

Snow depth and ice thickness are presented in Table F-1.

Temperature Measurements

The water temperature was measured using a YSI Model 46 TUC Tele-thermometer with a YSI 400 series probe. The thermistor was calibrated in a water and ice mixture at 0°C. No correction was necessary.

Dissolved Oxygen Measurements

The dissolved oxygen in the water was measured using a YSI Model 50 meter with a YSI 5739 probe. The dissolved oxygen probe was calibrated following the manufacturers recommendation of using moisture saturated air near sample temperature at the beginning of each sampling day.

The water temperature measurements are presented in Table F-2. The water temperature profiles are shown in Figure F-1. The water temperature profiles show an increase in temperature over time. The sediment is shown to be a heat source. After ice out the water temperature through out the profile is fairly homogeneous, within 0.3°C.

The DO measurements are presented in Table F-2. The DO profiles are shown in Figure F-2. The DO profiles show a continuous decrease in DO under ice cover (January through March) with some lower depths reaching anoxic conditions. The DO profile after ice out (April) shows a well mixed water column with a reduction of DO near the bottom due to sediment oxygen demand.

Water sample collection

Water samples were collected at the surface, 8 m depth and 15 m depth for analysis of chlorophyll *a* (Chla), total phosphorus (TP), dissolved phosphorus (TDP), total Kjeldahl nitrogen (TKN), conductivity, and pH. The samples were collected in polyethylene bottles and brought back to the Metropolitan Council laboratory for processing and analysis. The conductivity values are presented in Table F-3. The pH values are presented in Table F-4.

Secchi Depth

The Secchi depth was measured using a Secchi disk placed in the hole drilled for sample collection. This measurement includes some of the effect of ice and snow cover on light in the lake and gives an indication of the clarity of the water underneath (this is not a standard secchi depth measurement). The Secchi depth measurements are presented in Table F-5.

Table F-1. Snow depth and ice cover on Lake McCarrons – Winter 1999.

	1/21/99	2/9/99	3/5/99	3/16/99	4/6/99
Snow depth (in)	6	0	0	1	0
Ice thickness (in)	16	16.5	12	16	0

Table F-2. Water measurements for Lake McCarrons – January 21, 1999.

Depth (m)	Temperature (°C)	DO (mg/L)	TP (mg/L)	TDP (mg/L)	TKN (mg/L)	Chla (mg/L)
0	0	9.75	0.20	0.18	2.4	0.006
0.1	0.4	9.69	-	-	-	-
0.2	0.7	9.60	-	-	-	-
0.3	0.9	-	-	-	-	-
0.7	1.5	9.36	-	-	-	-
1.2	1.7	9.28	-	-	-	-
2.2	1.8	9.09	-	-	-	-
3.2	2.0	8.97	-	-	-	-
4.2	2.2	8.70	-	-	-	-
5.2	2.3	8.52	-	-	-	-
6.2	2.3	8.41	-	-	-	-
7.2	2.3	8.39	-	-	-	-
8.2	2.3	8.17	0.25	0.18	2.7	-
9.2	2.4	7.60	-	-	-	-
10.2	2.4	7.11	-	-	-	-
11.2	2.3	7.18	-	-	-	-
12.2	2.4	6.46	-	-	-	-
13.2	2.7	3.30	-	-	-	-
14.2	3.2	0.23	-	-	-	-
14.7	3.1	0.08	1.00	0.22	-	-
Inflow	0	5.2	0.12	0.03	0.006	-

Table F-2 (cont.). Water measurements for Lake McCarrons – February 9, 1999.

Depth (m)	Temperature (°C)	DO (mg/L)	TP (mg/L)	TDP (mg/L)	TKN (mg/L)	Cha (mg/L)
0	0	7.8	0.21	0.18	2.1	0.002
0.1	0.7	7.6	-	-	-	-
0.2	1.1	-	-	-	-	-
0.6	1.8	7.1	-	-	-	-
1.1	2.0	6.8	-	-	-	-
2.1	2.2	6.6	-	-	-	-
3.1	2.3	6.4	-	-	-	-
4.1	2.4	5.7	-	-	-	-
5.1	2.4	5.4	-	-	-	-
6.1	2.4	5.3	-	-	-	-
7.1	2.4	5.2		-	-	-
8.1	2.5	4.8	0.20	0.19	-	-
9.1	2.5	4.4	-	-	-	-
10.1	2.4	4.6	-	-	-	-
11.1	2.4	4.4	-	-	-	-
12.1	2.4	4.4	-	-	-	-
13.1	2.5	2.4	-	-	-	-
14.1	2.8	0.8	-	-	-	-
14.6	3.2	0.0	0.20	0.19	-	-
Inflow	0.2	8.2	0.19	0.14	2.2	-

Table F-2 (cont.). Water measurements for Lake McCarrons – March 5, 1999.

Depth (m)	Temperature (°C)	DO (mg/L)	TP (mg/L)	TDP (mg/L)	TKN (mg/L)	Chla (mg/L)
0	0	4.75	0.21	0.16	2.0	0.002
0.1	1.0	4.72	-	-	-	-
0.2	1.9	4.61	-	-	-	-
0.3	3.0	-	-	-	-	-
0.7	3.5	3.95	-	-	-	-
1.2	3.6	3.78	-	-	-	-
2.2	3.6	3.74	-	-	-	-
3.2	3.6	3.68	-	-	-	-
4.2	3.5	3.65	-	-	-	-
5.2	3.5	3.66	-	-	-	-
6.2	3.5	3.66	-	-	-	-
7.2	3.5	3.58	-	-	-	-
8.2	3.1	3.30	0.16	0.16	-	-
9.2	3.1	2.27	-	-	-	-
10.2	2.8	1.34	-	-	-	-
11.2	2.8	1.39	-	-	-	-
12.2	2.7	0.60	-	-	-	-
13.2	2.8	0.52	-	-	-	-
14.2	3.0	0.11	-	-	-	-
14.7	3.0	0.05	0.21	0.20	-	-
Inflow	0	8.15	0.05	0.03	1.7	0.016

Table F-2 (cont.). Water measurements for Lake McCarrons – March 16, 1999.

Depth (m)	Temperature (°C)	DO (mg/L)	TP (mg/L)	TDP (mg/L)	TKN (mg/L)	Chla (mg/L)
0	1.1	7.51	0.16	0.16	1.1	0.023
0.1	2.0	6.24	-	-	-	-
0.2	2.4	-	-	-	-	-
0.6	3.7	3.48	-	-	-	-
1.1	3.8	3.34	-	-	-	-
2.1	3.8	3.29	-	-	-	-
3.1	3.8	2.90	-	-	-	-
4.1	3.7	2.68	-	-	-	-
5.1	3.4	1.61	-	-	-	-
6.1	3.4	1.79	-	-	-	-
7.1	3.4	2.25	-	-	-	-
8.1	3.4	0.88	0.19	0.18	-	-
9.1	3.5	1.77	-	-	-	-
10.1	3.4	1.65	-	-	-	-
11.1	3.4	1.79	-	-	-	-
12.1	3.3	1.04	-	-	-	-
13.1	3.1	0.46	-	-	-	-
14.1	3.1	0.32	-	-	-	-
14.6	3.2	0.51	0.20	0.20	-	-
Inflow	1.1	11.8	0.34	0.20	1.8	-

Table F-2 (cont.). Water measurements for Lake McCarrons – April 6, 1999.

Depth (m)	Temperature (°C)	DO (mg/L)	TP (mg/L)	TDP (mg/L)	TKN (mg/L)	Chla (mg/L)
0	6.5	13.95	0.16	0.02	1.2	0.088
0.1	6.6	14.01	-	-	-	-
0.2	6.6	14.04	-	-	-	-
0.3	6.8	14.08	-	-	-	-
0.4	6.8	14.32	-	-	-	-
0.5	6.8	14.31	-	-	-	-
1.0	6.8	14.35	-	-	-	-
1.5	6.8	14.37	-	-	-	-
2.5	6.8	14.41	-	-	-	-
3.5	6.8	14.43	-	-	-	-
4.5	6.8	14.40	-	-	-	-
5.5	6.8	14.41	-	-	-	-
6.5	6.8	14.36	-	-	-	-
7.5	6.7	14.31	0.15	0.02	-	-
8.5	6.7	14.29	-	-	-	-
9.5	6.8	14.35	-	-	-	-
10.5	6.8	14.40	-	-	-	-
11.5	6.8	14.42	-	-	-	-
12.5	6.8	13.75	-	-	-	-
13.5	6.7	11.50	0.57	0.24	-	-
Inflow	9.9	-	0.12	0.05	1.0	0.033

Table F-3. Conductivity (µmho/cm) in Lake McCarrons – Winter 1999.

	1/21/99	2/9/99	3/5/99	3/16/99	4/6/99
Surface	525	500	586	546	512
8 m	526	517	606	558	491
15 m	570	572	650	614	594
Inflow	1015	1664	1398	812	534

Table F-4. pH in Lake McCarrons – Winter 1999.

	1/21/99	2/9/99	3/5/99	3/16/99	4/6/99
Surface	7.66	9.72	8.7	7.36	8.09
5 m	7.67	8.18	8.1	7.28	8.04
15 m	7.57	7.77	7.6	7.29	7.12
Inlet	7.34	7.66	7.5	7.36	7.45

Table F-5. Secchi depth for Lake McCarrons – Winter 1999.

	1/21/99	2/9/99	3/5/99	3/16/99	4/6/99
Secchi depth (m)	(under ice) 2.8	(under ice) 4	(under ice) 4.5	(under ice) 2	0.75

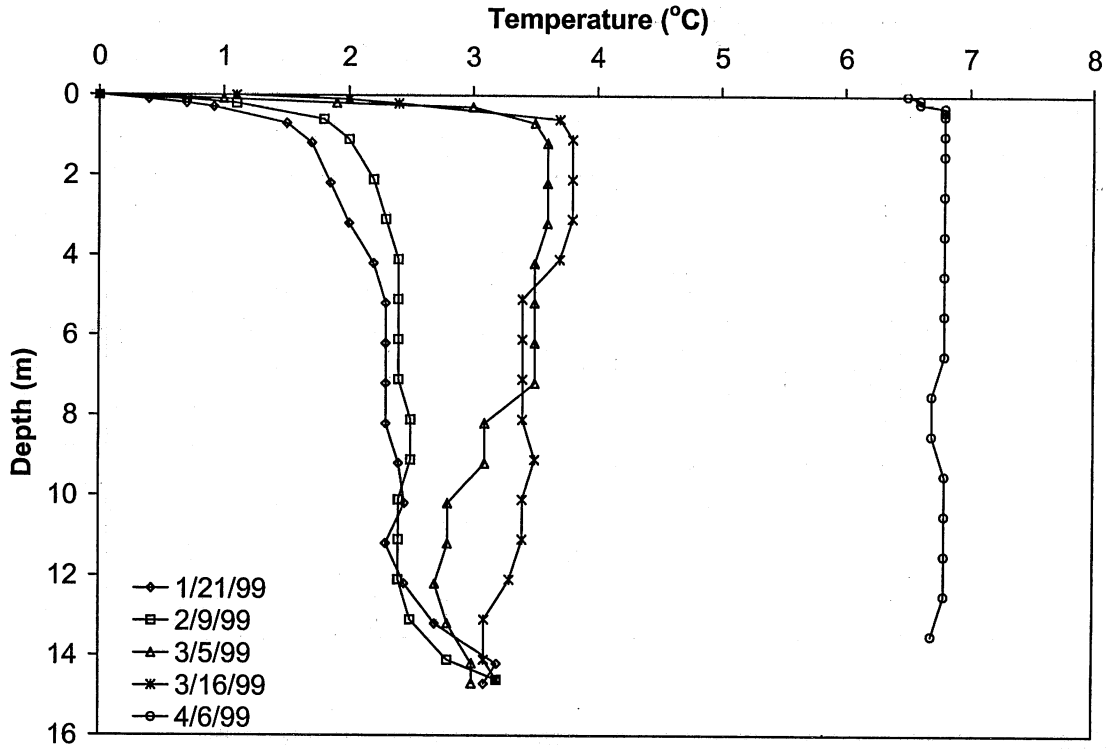

Figure F-1. Water temperature profiles for Lake McCarrons – Winter 1999.

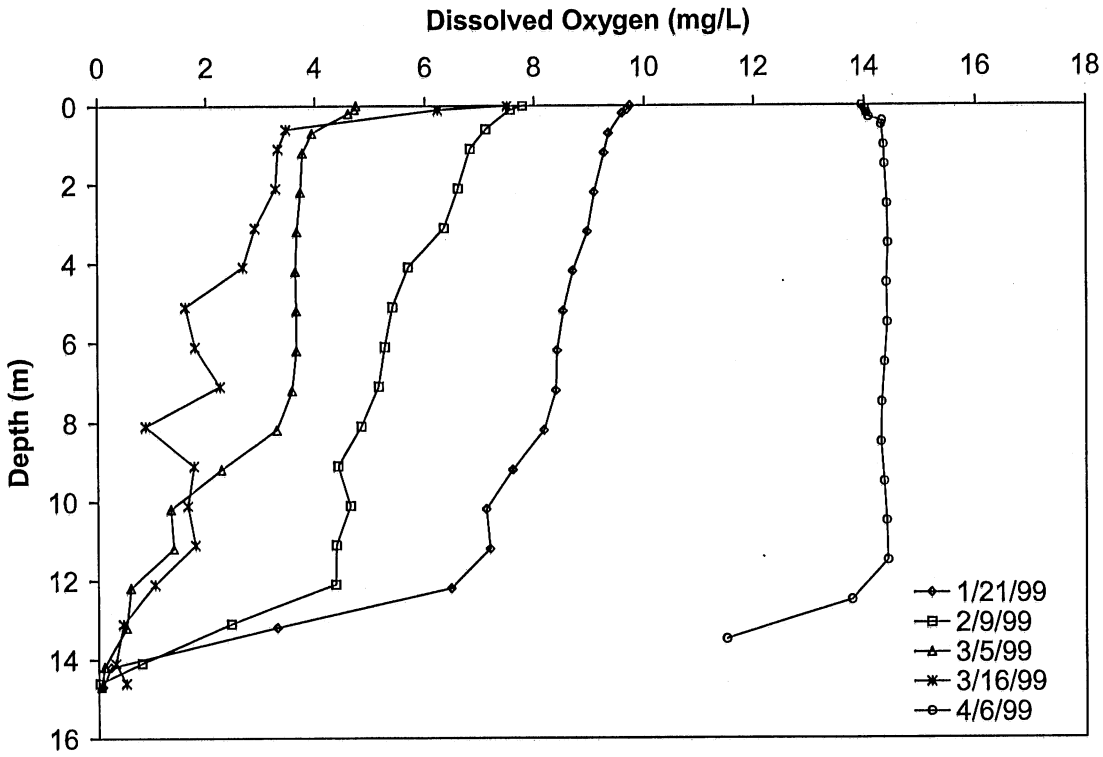

Figure F-2. Dissolved oxygen profiles for Lake McCarrons – Winter 1999.